Study of behavioral and neuronal maturation during development on Danionella cerebrum and comparative study with Danio rerio

Julie Lafaye

THÈSE DE DOCTORAT

de Sorbonne Université

Spécialité : Physique

École doctorale n°564: Physique en Île-de-France

réalisée

au Laboratoire Jean Perrin

sous la direction de Georges DEBRÉGEAS et Filippo DEL BENE

présentée par

Julie LAFAYE

Sujet de la thèse :

Study of behavioral and neuronal maturation during development on *Danionella cerebrum* and comparative study with *Danio rerio*

soutenue le 26 septembre 2022

devant le jury composé de :

M.	Lambert Regis,	Président du jury
M.	Neri Peter,	Rapporteur
M.	Orger Michael,	Rapporteur
Mme.	Hong Elim,	Examinatrice
M.	Randlett Owen,	Examinateur
M.	Debrégeas Georges,	Directeur de thèse
M.	Del Bene Filippo,	Co-directeur de thèse

Abstract

Locomotion is essential for motile animal to adapt to their environment. This ability to navigate is modulated by the sensory information animals are continuously integrating from their environment. Locomotion and information integration are part of the sensorimotor program that is controlling animal exploratory behavior. In this thesis, we explored how stereotyped stimuli are integrated and influence locomotion. We also investigate how the underlying neuronal circuit of locomotion change through animal development. We used larvae zebrafish to answer the first question. Our involvement in developing a new vertebrate model *Danionella cerebrum* (*DC*), allowed us to initiate the exploration of the second question.

Sensorimotor program requires the integration of multisensory stimulation that necessitates processing time. To study this, we combined two reflexes already described independently in larvae zebrafish, the optomotor response and the acoustic startle response. We confirmed that larvae are delaying their first movement when exposed to a visual stimulus. We showed that this information did not bias the escape direction triggered by an acoustic signal.

Our laboratory was involved in developing a new vertebrate model for neuroscience, the miniature fish *DC* . With its small size and its optical transparency, this fish is suitable for whole-brain functional imaging with a single cell resolution at different developmental stages. We created a specific fish facility and we established raising and feeding protocols.

During a collaborative study, we took benefits of the phylogenetic proximity between zebrafish and *DC* to propose a comparative study. We focused on the spontaneous locomotion and long-term exploration of the larvae. We showed that despite their different swimming patterns, both species have similar long-term exploration. We defined simple models to describe their trajectories. We are also interested in understanding how light affects the locomotor program.

In parallel, neuronal calcium activity was recorded with light-sheet microscope in larvae to determine neuron populations that are correlated with swimming activity. It has been published that both species have in common brain region that are recruited during swimming behaviors. Thanks to its different locomotion, we highlighted neurons in *DC* that are firing when the fish is not swimming. We also demonstrated that it is possible to record whole-brain calcium activity in juveniles *DC* with the same protocol and setup used for larvae.

This thesis work is part of a global effort to establish *DC* as an interesting model for neuroscience. Further studies in our laboratory will aim at comparing the simple exploration models defined for zebrafish and *DC* larvae to have an insight on the evolution strategies which create divergent behaviors in close species. We will also follow modification on the simple model developed for larvae *DC* and on the locomotor neuronal circuit, in juvenile fish to reveal some mechanisms involved in maturation through development.

Keywords : neurosciences · aquatic models · zebrafish · *Danionella cerebrum* · light-sheet microscopy · calcium imaging · behavior · locomotion

Résumé

Se déplacer est essentiel pour que les animaux puissent s'adapter à leur environnement. Cette capacité est modulée par les informations sensorielles environnementales intégrées en permanence par les animaux. Dans cette thèse, nous avons exploré comment les stimuli stéréotypés sont intégrés et influencent la locomotion. Nous avons également étudié comment le circuit neuronal sous-jacent de la locomotion évolue au cours du développement animal. Nous avons utilisé des larves de poisson zèbre pour répondre à la première question. Notre implication dans le développement d'un nouveau modèle vertébré, *Danionella cerebrum* (*DC*), nous a permis de commencer l'étude de la seconde question.

L'intégration de stimulations multisensorielles est un processus qui nécessite un temps de traitement des informations. Pour l'étudier, nous avons combiné deux réflexes déjà décrits indépendamment chez la larve de poisson zèbre: la réponse optomotrice et la réponse de fuite à une stimulation acoustique. Nous avons confirmé que les larves retardent leur premier mouvement lorsqu'elles sont exposées à un stimulus visuel, et nous avons montré que cette information visuelle n'influence pas la direction de fuite déclenchée par un signal acoustique.

Notre laboratoire participe au développement d'un nouveau modèle vertébré, le poisson *DC* . Par sa petite taille et sa transparence optique, il est adapté pour l'imagerie fonctionnelle du cerveau en entier avec une résolution cellulaire et à différents stades du développement. Nous avons créé une installation et des protocoles d'élevage spécifiques à cette espèce.

Lors d'une collaboration, nous nous sommes intéressés à comparer la locomotion spontanée et l'exploration à long terme chez les larves de poisson zèbre et de *DC* . Nous avons montré que malgré leurs différents modes de nage, les deux espèces ont une exploration à long terme similaire. Pour mieux décrire ce phénomène, nous avons modélisé les trajectoires avec des modèles mathématiques simples.

En parallèle, l'activité calcique neuronale a été enregistrée avec un microscope à nappe laser afin de déterminer les populations de neurones impliquées dans la nage. Nous avons montré que les deux espèces ont en commun des régions du cerveau recrutées pendant la nage. Chez les larves de *DC* , nous avons mis en évidence des populations neuronales qui sont activées lorsque le poisson ne nage pas. Nous avons aussi démontré qu'il est possible d'enregistrer l'activité calcique du cerveau entier chez des *DC* juvéniles avec les mêmes protocoles que pour les larves.

Ce travail de thèse fait partie d'un effort global pour établir *Danionella cerebrum* comme modèle animal en neurosciences. Les futures études dans notre laboratoire viseront à comparer les modèles d'exploration définis pour les larves de poisson zèbre et de *DC* afin d'avoir un aperçu des stratégies d'évolution créant des divergences de comportement. Nous comparerons aussi les évolutions du modèle et du circuit neuronal locomoteur chez *DC* à différents âges pour révéler les mécanismes impliqués dans la maturation au cours du développement.

Mots-clés : neurosciences · modèle aquatique · poisson zèbre · *Danionella cerebrum* · microscope à nappe laser · imagerie calcique · comportement de navigation

Résumé détaillé en langue française

La capacité de se déplacer est essentielle pour la survie des êtres mobiles tels que les animaux. Afin de naviguer au mieux dans leur environnement, les animaux échantillonnent en permanence les informations sensorielles environnementales qu'ils perçoivent leurs permettant de s'orienter vers des zones favorables en nourriture, en partenaires et d'éviter les prédateurs. Cette faculté d'adaptation est présente tout au long du développement des animaux. Ainsi, les stratégies de navigation d'un animal sont modifiées par les signaux sensoriels et lors de leur développement. Comprendre comment ces transformations se font à l'échelle comportementale et au niveau des circuits neuronaux correspondants, est une problématique centrale en neurosciences.

Introduction générale

Dans le premier chapitre introductif (chap.1), je propose une description globale du domaine des neurosciences ainsi que l'apport de certains modèles animaux tels que les poissons.

Les neurosciences regroupent l'ensemble des disciplines scientifiques qui ont pour objectif commun de comprendre comment fonctionne le cerveau et le système nerveux. Cette vaste problématique est étudiée à différentes échelles macroscopiques et/ou microscopiques en fonction des axes de recherches choisis. Au laboratoire, la thématique de recherche privilégiée est celle des neurosciences comportementales qui visent à déterminer les circuits neuronaux impliqués dans certains comportements stéréotypés grâce à des organismes modèles. Ceux-ci permettent d'étudier en parallèle des comportements pertinents ainsi que les circuits neuronaux sous-jacents.

Les organismes modèles en neurosciences ont permis de nombreuses avancées dans ce domaine. Parmi les vertébrés utilisés, les poissons et notamment le poisson domestique *Danio rerio* ou poisson zèbre, présentent de nombreux avantages. La larve de poisson zèbre est un organisme modèle bien établi dans les neurosciences depuis les années 1970. Sa transparence optique à ce stade de développement et la possibilité de le modifier génétiquement en font un organisme approprié pour les neurosciences. En combinant les études comportementales et l'imagerie cérébrale, il a permis de mieux comprendre le fonctionnement du cerveau et les circuits neuronaux impliqués dans certains comportements. Néanmoins, ces études ne sont pas possibles à des stades de développement plus avancés, limitant les comportements étudiés. Les poissons miniatures sont une solution envisageable pour pallier ce problème, comme le montre ce travail de thèse.

Chapitre 2 : Intégration sensorielle chez la larve de poisson zèbre

Dans le second chapitre (chap.2), je présente le projet développé pour explorer les processus d'intégration de l'information et leurs impacts sur les comportements de navigation en cas de fuite déclenchée par un stimulus sensoriel. Dans une première section, je décris les comportements utilisés pour ce projet : le réflexe opto-moteur qui se traduit par une réorientation du corps du poisson dans la direction d'une stimulation visuelle et le comportement de fuite suite à une stimulation acoustique. Ces deux comportements ont des temps d'intégration des informations sensorielles perçues différents.

En utilisant le réflexe opto-moteur comme marqueur de l'influence de l'environnement sur le comportement de nage, l'étude a pour but de déterminer si cette influence est prise en compte lors d'une fuite, comportement nécessitant un court temps de réflexion. Après avoir expliqué les différents protocoles expérimentaux et d'analyses mis en place, les résultats montrent que le comportement de fuite déclenché par un signal acoustique ne tient pas compte du réflexe opto-moteur le précédent. Néanmoins, un délai dans le déclenchement du premier mouvement de nage est observé lorsque la stimulation visuelle est présentée pour le réflexe opto-moteur. Cela suggère l'existence d'un temps de traitement de l'information par la larve de poisson avant de prendre une décision sur la direction du mouvement suivant.

Chapitre 3 : un nouveau modèle animal en neuroscience : *Danionella cerebrum*

Dans le troisième chapitre (chap.3), je propose un aperçu des connaissances sur le genre des poissons miniatures *Danionella* dont l'espèce *Danionella cerebrum* est particulièrement intéressante comme organisme modèle pour les neurosciences. Les différentes étapes nécessaires à l'établissement d'une animalerie aquatique spécifique à cette espèce sont décrites, ainsi que les protocoles d'élevage et de nourrissage que j'ai développés. Des observations réalisées lors des moments passés à l'animalerie et par une expérience montée dans l'animalerie sont aussi présentées.

Le *Danionella cerebrum* est un modèle émergent pour les neurosciences en raison de sa petite taille (moins de 15 mm au stade adulte) et de sa transparence optique du stade larvaire au stade adulte. Cette espèce présente également un riche répertoire comportemental qui, combiné avec les caractéristiques précédentes, offre une lecture directe des circuits neuronaux sous-jacents grâce à des techniques d'imagerie fonctionnelle du cerveau en entier in-vivo.

Ce poisson d'eau douce a des conditions de vie et d'élevage assez similaire au poisson zèbre, dont il est phylogénétiquement proche. Cependant, il existe encore peu de données sur ce poisson sauvage qui demande plus de soins lors de l'élevage, notamment des larves. Ce chapitre regroupe les observations faites lors de l'établissement des différents protocoles

d'élevages, lors des soins apportés aux poissons, mais aussi par une expérience montée dans l'animalerie pour suivre le développement des poissons en conditions non biaisées. Ce chapitre peut servir de support technique pour l'élevage de ces poissons prometteurs pour les études en neurosciences.

Chapitre 4 : Navigation spontanée et préférence lumineuse chez les larves de poisson

Dans le quatrième chapitre (chap.4), je présente les résultats de deux collaborations sur des études de comportements. Je commence par résumer les conclusions obtenues lors de l'étude sur les divergences de comportements chez deux espèces proches phylogénétiquement : les larves de *Danionella cerebrum* et celles du poisson zèbre. Je décris ensuite les différentes stratégies utilisées par les larves de poisson zèbre pour se diriger vers les zones lumineuses, ainsi que le modèle mathématique proposé pour décrire l'influence de la luminosité sur la navigation spontanée.

En plus de leur proximité phylogénétique, les larves de ces deux espèces ont un milieu de vie similaire et des similitudes morphologiques qui favorisent une étude comparative. Malgré ces rapprochements, le comportement de nage diffère avec une nage saccadée pour les larves de poisson zèbre, et une navigation continue pour celles de *Danionella cerebrum*. Je résume dans un premier temps le modèle mathématique proposé par le laboratoire pour décrire les trajectoires spontanées des larves de poisson zèbre, basé sur une double chaine de Markov. Ensuite, je résume les observations faites sur les différences des nages entre les deux espèces. Suite à ces collaborations, la problématique de recherche de ma thèse s'est orientée vers la détermination d'un modèle mathématique le plus simple possible décrivant les trajectoires des larves de *Danionella cerebrum*. Je décris les analyses utilisées pour définir ce modèle, reposant sur un processus de Poisson.

Avec l'objectif de poursuivre la comparaison entre les comportements des deux espèces étudiées, je présente les travaux réalisés sur l'influence de la luminosité sur la trajectoire des larves de poisson zèbre au laboratoire. Il a été montré que les larves de poisson zèbre nagent préférentiellement vers des zones lumineuses. Ce comportement a été caractérisé par des expériences de réalité virtuelle qui ont mis en évidence que les larves tournent davantage lorsqu'elles nagent vers une zone sombre. La lumière a donc un effet sur la navigation spontanée des larves, influençant aussi le modèle mathématique. Ces expériences sont en cours d'adaptation pour les larves de *Danionella cerebrum* qui ont un comportement opposé au poisson zèbre, en préférant naviguer vers des zones sombres.

L'objectif de cette comparaison est de mieux comprendre la divergence évolutive au niveau du comportement, puis des circuits neuronaux.

Chapitre 5 : Etude du circuit neuronal de la locomotion chez la larve de *Danionella cerebrum*

Dans le cinquième chapitre (chap.5), je décris les expériences mises en place pour déterminer les circuits neuronaux impliqués dans les comportements de navigation chez les larves de poisson zèbre et de *Danionella cerebrum*. Grâce à leur transparence optique naturelle et à leur petite taille au stade larvaire, des lignées transgéniques ont été développées pour les espèces de *Danionella cerebrum* et de poisson zèbre afin d'enregistrer leur activité calcique cérébrale à l'échelle neuronale. Il est ainsi possible de compléter l'étude comparative comportementale par l'identification des circuits neuronaux impliqués dans leurs différents modes de nage. C'est aussi l'occasion d'explorer comment ces circuits neuronaux ont divergé.

Je commence par un rappel sur l'imagerie calcique et la microscopie à feuille de lumière, les principaux outils que j'ai utilisés pour enregistrer l'activité des neurones du cerveau entier. J'expose ensuite les expériences et les analyses des données que j'ai modifiées par rapport aux analyses utilisées pour les larves de poisson zèbre. Puis je présente trois grandes populations de neurones impliquées dans la nage chez les larves de *Danionella cerebrum*. Une première population est active lorsque les poissons battent de la queue. Grâce aux phases de nage et de pause plus longues chez les larves de *Danionella cerebrum*, une deuxième population anti-corrélée aux phases de battements, donc active lorsque que le poisson ne nage pas, a pu être mise en évidence. Ces temps longs d'activité sont aussi favorables à la détection de neurones actifs lors des transitions entre la nage et le repos, la troisième population de neurones que j'ai détectée.

En parallèle de ce projet principal, j'ai effectué des expériences préliminaires pour valider la faisabilité de projets futurs. Ainsi, j'ai montré qu'il était possible d'imager le cerveau des larves de *Danionella cerebrum* au microscope à nappe laser avec un laser 2 photons, permettant l'étude des circuits neuronaux impliqués lors de stimulations visuelles. J'ai aussi imagé le cerveau en entier de *Danionella cerebrum* à différents stades de développement, prouvant ainsi qu'il est possible de suivre l'évolution des circuits neuronaux au cours du développement d'un individu, du stade larvaire au stage juvénile voir adulte, favorisant les études de maturation et de vieillisemment. Grâce à sa nage continue et ses rythmes compatibles avec les temps caractéristiques de l'imagerie fluorescente calcique, les larves de *Danionella cerebrum* offrent de nouvelles opportunités d'étude des circuits neuronaux sous-jacents de la nage.

Conclusion

Dans le chapitre de conclusion (chap.6), je résume les travaux présentés dans ce manuscrit de thèse. Je commence par revenir sur les expériences menées pour comprendre l'intégration de stimulations sensorielles lors de la prise de décision chez la larve de poisson zèbre. Les hypothèses espérées n'ont pas été vérifiées et je propose des explications et d'autres expériences réalisables pour aller plus loin.

Le travail principal de cette thèse a été la mise en avant du poisson miniature et transparent *Danionella cerebrum* pour les neurosciences. Je reprends les résultats marquants de ce travail, le modèle basé sur un processus de Poisson pour la description des trajectoires des larves de *Danionella cerebrum*, la population de neurones corrélée aux phases de nage, celle anti-corrélée et active lors des périodes de pause et la possibilité de déterminer des neurones actifs lors des changements de rythmes. Je rappelle les avantages de ce modèle et les axes de recherches futures ouverts par ce poisson.

Acknowledgements

Merci à Georges de m'avoir accompagnée et conseillée lors de cette thèse. Tu fais énormément confiance à tes étudiants et c'est un vrai plaisir d'avoir pu grandir scientifiquement et humainement à tes côtés.

Merci à Filippo pour ton regard complémentaire sur cette thèse. Je suis ravie d'avoir pu partager ma passion sur les poissons avec toi.

Merci à tous les membres du laboratoire Jean Perrin, anciens et actuels, qui m'ont accompagnée lors de ces quatre années. Je remercie particulièrement l'équipe poisson de son soutien et des bons moments partagés. Je remercie Sophia, Geoffrey et Guillaume (alias le Clutch). Je remercie Natalia, Thomas, Hugo, Benjamin, Hippolyte, Sharbat, Tom, Mattéo, Alexandre, Antoine, Marcus. Je remercie Monica et Leonardo. Je remercie Ghislaine et Raphaël. Je remercie Volker.

En dehors de l'équipe poisson, je remercie l'ensemble des étudiants d'hier et d'aujourd'hui dont Nicolas, Guillaume S., Darka, Wafa, Nidia, Nabil, Pierre, Florence, Anis, Jean-Baptiste, Amaury, Manon et tous les autres. Je remercie Laetitia d'avoir été ma marraine de thèse. Je remercie tous les permanents avec qui j'ai pu échanger.

Un gros merci à Malika, Anissa et Marie-Nicole qui accompagnent nos travaux de recherches.

Un merci à Didier et ses encouragements.

Merci aux animaliers de la plateforme aquatique de l'IBPS qui permettent à la recherche d'avancer. Merci Karim, Alex, Marco, Edouard, Jérémy, Stéphane, Sylvie.

Merci à l'IBPS.

Merci à l'équipe de FDB de m'avoir accueillie lors de vos réunions. Merci Karine pour le soutien et les poissons. Merci Gokul, Fanny, Giulia, Elena, Marion, Shahad, Malo, Jonathan.

Merci à German d'avoir fait partie de mon comité de suivi de thèse.

Merci à Peter Neri et Michael Orger d'avoir lu et apprécié mon manuscrit de thèse.

Merci aux membres de mon jury de thèse, Elim Hong, Regis Lambert et Owen Randlett, d'avoir évalué mon travail.

Merci Maria Barbi pour le plaisir que j'ai eu à enseigner à tes côtés.

Merci à l'ensemble des personnes ayant travaillé avec moi à l'Aquarium tropical du Palais de la Porte Dorée.

Un énorme merci à ma famille. Maman, de toujours nous soutenir dans nos projets et d'être toujours là quand on a besoin; Pauline pour aller prendre un thé et se vider la tête; Titi, pour se rebooster. Un merci à mes grands-parents et particulièrement à mes grands-mères: mamie Gigi et mamie Claude (Jojo).

Je remercie tous mes amis qui ont d'une manière ou d'une autre participé à ma thèse par des encouragements, des sorties, des jeux, des papotages, des danses, des rires, bref de très bons moments. Je pense particulièrement aux amis de lycée, prépa (LLG for ever !), PC, la danse, la plongée, les voyages, les amis d'amis devenus des amis, et toutes les personnes qui se sentiront concernées.

Enfin, un énorme merci à mon Thibault, qui a vécu au plus près de moi les montagnes russes de ma thèse. On forme une très bonne équipe.

Merci à tous !

Contents

Preamble

Notes

Abbreviations :

- *DC* : *Danionella cerebrum*
- dpf : day(s) post-fertilization
- fps : frame(s) per second
- LLC : long latency C-bend
- MLMNs : mesencephalic locomotion maintenance neurons
- MLR: mesencephalic locomotor region
- MSD : mean square component
- OMR : opto-motor response
- pdf : probability density function
- ROI : region of interest
- RS : reticulospinal (neurons)
- SEM : standard error of the mean
- SLC : short latency C-bend
- WT : wild type
- ZF : zebrafish

Chapter 1

Introduction

1.1 What are neurosciences?

1.1.1 General definition

Neuroscience is the scientific study of the brain and the nervous system. This simple definition conceals a more complex reality. Indeed, neuroscience is a multidisciplinary research which combines behavioral observation, anatomy, physiology, cellular and molecular biology, developmental biology, genetics, chemistry, physics, computer sciences, mathematical modelling and other scientific domains. All those scientific disciplines are needed in order to understand how the brain works, or in other words, how behaviors arise from neuronal circuits. One may represent the animal body as a "black" box which receives sensory inputs and produces actions. From the antiquity, humans have tried to localize the exact position of this "thinking" black box. It was first thought that the heart was the seat of the decision but with the first dissections and medical progress, the brain was established as the main decision center. With the improvement of imaging and genetics, researchers' interest for exploring brain organization and function grew to a point where neuroscience is now recognized as a distinct research topic which regroups different branches [1].

Nervous systems can be described at diverse scales, from molecular with neurotransmitter pathways that activate or inhibit neuronal action potentials, to neuronal circuits with neuron interactions and connections in different brain regions, to simple or more complex behaviors studied by cognitive sciences. Each study scale requires numerous concepts of anatomy, cellular and molecular biology among others. The complexity of the interactions between those units partially explains the numerous knowledge gaps that still exist. The entanglements of those various biological problems also illustrate the difficulties encountered by the scientific community in this domain but also motivate the enthusiasm that neuroscience creates.

Within neuroscience, behavioral neuroscience aims at exploring how behaviors are gen-

erated and modulated. At Laboratoire Jean Perrin, we are mainly focused on deciphering neuronal circuits that modulate the locomotor circuit with single or multisensory stimulation.

1.1.2 Neuronal circuits

Analogy in sciences is used to approach complex problems with techniques already used in the analogous field. This approach allows one to better visualize a problem and to approach it with a different angle. The brain is often compared to a "black box" or a computer. This box receives information, mostly environmental sensory stimulation, that are processed with an electronic-like circuit, the neuronal circuit, to generate outputs, behaviors and decisions. The main objective is to establish the transfer function of the black box and how it is wired.

It is common to start this investigative work by reducing the problem complexity, either by reducing the number of inputs by making the other parameters invariant in order to characterize what are their impacts on the output, or by addressing the same problem on a simpler model. For example, some studies focus on the effect of a specific neurotransmitter or receptor on a particular action (role of G-Protein-Coupled Receptors on *C.elegans* locomotion [2], or its role on sensorimotor decision-making on larvae fish [3]), or at a higher level, on the impact of one sensory stimulation on a specific behavior (impact of the light level on mice nocturnal activity [4], impact of temperature on larvae fish locomotion [5]). This offers insights of the possible interaction between the basic units, neuron, and their connections at a more global scale.

With the improvement of functional imaging techniques and genetic manipulations, it is possible to have a readout of the "black box" unit components, neurons, and to validate the connection and role inferred before. Fluorescent microscopy and dedicated genetic calcium probes offer a unique view at the neuronal scale on neuronal global dynamics (see section 5.1). Those techniques allow delving into the mechanisms of the brain. But connections are still unknown and can be determined by removing (ablation) or activating (drugs, optogenetics) some sepcific regions.

Even with those two methods, a black box as complex as the human brain is still hard to describe. It possesses tens of billions of neurons, which makes it difficult to decipher at the neuronal scale. To address this problem, simpler organisms (with fewer neurons and "simple" behaviors) are used to discover basic principles of neuronal function, that are conserved in most invertebrates and vertebrates.

1.2 Animal models in neurosciences

1.2.1 Animal models

Main progresses on brain knowledge during the 20th century, have resulted from data from animal models. Most of those models have been developed in parallel of breakthrough in imaging techniques and genetic manipulation. Models are chosen for their anatomic, physiologic or genetic features compatible with those improvements.

Across vertebrate, the nervous system and the main brain area organization are conserved and similar in their basic arrangement. Even if some brains areas have changed a lot over time, essential behaviors that appeared early in evolution and that are shared, such as locomotion, involve similar structures despite some variations (hindbrain [6], spinal cord [7] ...). Thus, not only studying a wide range of species favors comparative studies, but early traits can also be integrated into more complex networks during evolution.

To perform comparative study, it is important to make the distinction between homology and homoplasy. The first concept, homology, refers to structures or behavior that have the same origins but that have diverged over time. It is this notion that is commonly used to identify similar brain regions on animal model brains and human brain (which are also confirmed with other techniques) [8]. On the contrary, homoplasy is the process by which distinct traits are evolving to reach comparable shape and/or function.

Both vertebrates and invertebrates are used for exploring brain functions. Fruit flies, *Drosophila melanogaster*, are easy to genetically modify, which make them interesting for genetic research. The nematode *Caenorhabditis elegans*, or *C.elegans*, is transparent and it is the only organisms that have its full connectome (neuronal wiring diagram) described [9]. Indeed, this invertebrate is remarkable for its invariant development, as it always contains the same number of cells with 302 neurons for the hermaphrodite form [10]. But despite its connectome and its 302 neurons, the neuronal circuit controlling its locomotion is still incomplete. Both species are easy to genetically manipulate and have a brain small enough to allow *in vivo* whole brain imaging. Thus, exploration of neuronal circuits in their entirety, from the stimulus perception to the processing and final decision-making or motor output can be performed on those species.

Even if invertebrates offer unique features to explore the brain, they are phylogenetically far from human. Thus, vertebrates and mammals models are favored for homology studies. Rodents, mostly mice and rats, are the most used animal models in neuroscience [11], mostly due to the numerous genetic tools developed for those models. However, more and more researchers argue in favor of animal model diversity in neuroscience, to avoid over-interpreting and drawing general conclusion based on few animal models. Analysis of neuronal circuit (and other studies) across species is important to uncover the general strategies for adaptive

behavioral responses.

In terms of diversity, fish are among the vertebrates that offer a wide range of physiologic, anatomic, behavioral and ecological specializations. Around 27 000 species have been described [12], which represents almost one third of the total vertebrate species. Among them, *Danio rerio* is now a well-established model in neurosciences.

1.2.2 Small fish in neurosciences

1.2.2.1 *Danio rerio* or Zebrafish

Danio rerio or zebrafish (ZF) is a freshwater teleost fish species from India. It became popular as ornamental fish before being established as a major model for research by Georges Streisinger in the 1980s for the study of genetics and neuronal system development [13]. ZF have been particularly used for genetic and embryonic developmental studies due to the high number of eggs laid and their external and fast development. Indeed, an adult couple can spawn a clutch containing more than hundreds of eggs per week. ZF larvae hatch between 48 and 72 hours post-fertilization and their yolk sac is emptied around 5 days post-fertilization (dpf), pressuring them to swim and hunt. At 3 month, they have reached their sexual maturity and are considered as adults. They can live up to 3 to 4 years in captivity. Larva stage corresponds to the developmental period between 3 and 30 dpf i.e. before the first metamorphosis and the appearance of adult traits. Over this period, ZF larvae continuously grow and acquire more complex behaviors such as socialization around three weeks [14]. Their brains expand from 100 000 neurons up to $\approx$ 10 000 000 neurons at the adult stage.

In addition to their advantages for genetics and development biology, ZF larvae have gained popularity over the last two decades in neurosciences, especially to study brain function and neuronal circuit identification [15]. ZF larvae morphologic and anatomic specificities are highly valuable for *in vivo* whole brain optical recording. Larvae are small, with a brain size of $\approx 1 * 0.3 * 0.5$ mm, optically transparent, with a few neurons, that are still enough to generate interesting behaviors, and their oxygenation is provided by gas diffusion through their skin, allowing to immobilize them in hydrogels, without the need for anesthesia. Moreover, ZF larvae at 5 dpf already display a wide behavioral repertoire (see section 2.1.1, [16, 17]) which is an important asset for their use in behavioral neuroscience.

With their amenability to genetic manipulation, diverse ZF lines have been developed for whole brain imaging. Despite their relative optical transparency, ZF larvae have melanophores all along their spinal cord and on the top of their skull (fig.1.1.A, top). Those pigments partially absorb the different photons used for imaging. The *nacre* mutation [18] affects the *mifta* gene involved in melanocyte production which leads to non-pigmented ZF, giving access to deeper brain regions (fig.1.1.A, middle). Another decisive breakthrough for *in vivo* imaging of ZF larvae brain was the development of the genetically encoded calcium indicator (GECIs,

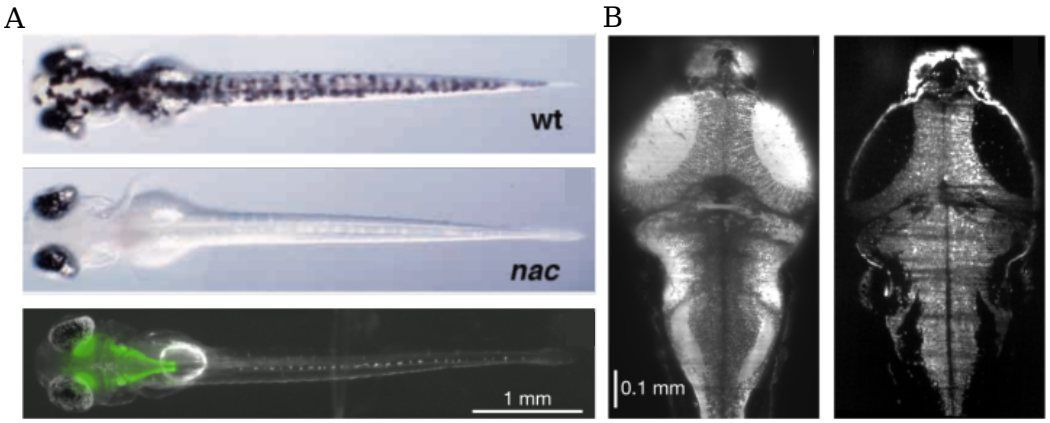

Fig. 1.1 ***Common zebrafish line for imaging.*** ***A*** *Zebrafish transgenic lines. Top: WT, middle: nacre (from [18]), bottom: GCaMP5 expressing in neurons in ZF larvae illuminated by a light-sheet.* ***B*** *Brain layer of ZF larvae expressing GCaMP in neuron cytoplasm (left) and nucleus (right) imaged with a light-sheet microscope. From [19].*

see section 5.1.2, fig.1.1.A, bottom), that can be expressed on targeted cells and localization, such as neuron cytoplasm (fig.1.1.B, left) or nucleus (fig.1.1.B, right) for neuronal recording. The main GECIs family used in neuroscience is the GCaMP which has been reported to have an optimal expression in ZF larvae. By combining those lines and whole-brain single-cell resolution calcium imaging, those methods together allowed neuronal activity recording in thousands of neurons for the first time in vertebrate brain [20, 21]. The relative simplicity and accessibility of neuronal connectivity in zebrafish offer a unique opportunity to monitor the dynamics of neuronal circuits, a feat that is not yet possible in mammals brain wide.

Despite their numerous qualities for neuroscience research, ZF brains are only available for whole brain imaging at larval stages, which limits the behavior repertoire to reflex and simple behaviors compared to the one exhibited at adult stage (socialization, learning, mating...). As mentioned in the previous section, it is also essential to diversify the species used for brain studies to explore neuronal wiring adaptation and the evolution strategies that led to such brain diversity.

1.2.2.2 Other small fish

Other small fish species are used in neurosciences. They are mostly freshwater fish because they are easier to maintain and reproduce in captivity than seawater species. Medaka, *Oryzias latipes* (fig.1.2.A), have been used in research for more than a century. They mainly contributed to research on endocrinology, organogenesis and genetics. They contributed to understand sex differentiation, as they possess defined sex characteristics, contrary to ZF

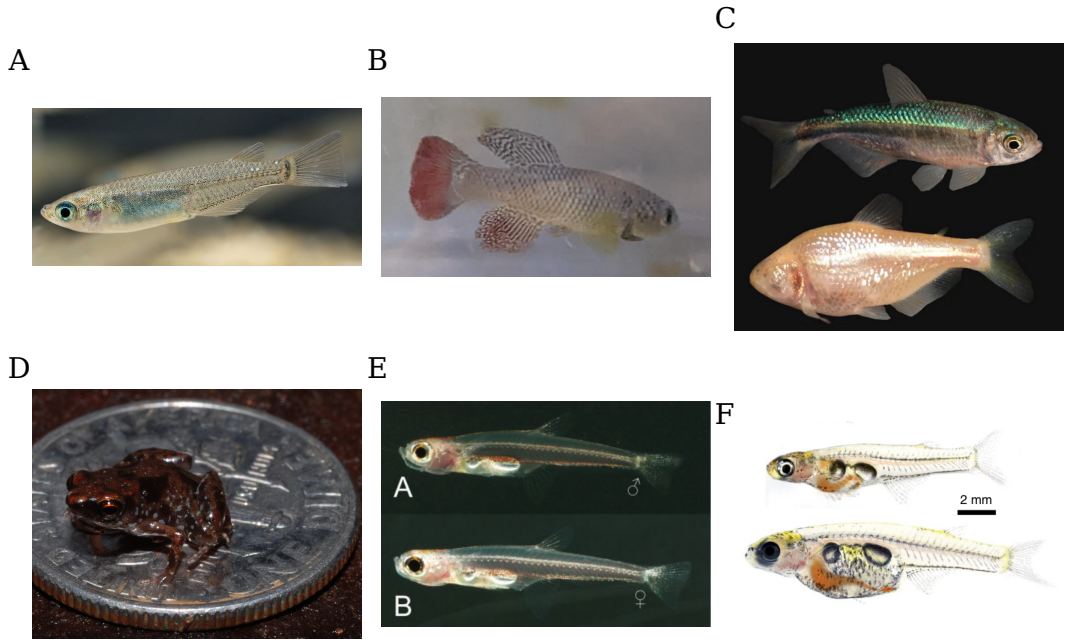

Fig. 1.2 ***Common fish models and smallest vertebrates.*** ***A*** *Medaka [26].* ***B*** *Killifish with red tail.* ***C*** *Astyanax mexicanus surface form (top) and cave form (bottom) (Credit: Daniel Castranova, NICHD/NIH (CC BY-NC-ND 2.0), from [27]).* ***D*** *Paedophpryne amauensis [28].* ***E*** *Paedocypris [29].* ***F*** *Danionella cerebrum [30].*

[22].

Among killifish, the African turquoise species *Nothobranchius furzeri* (fig.1.2.B) has emerged as a vertebrate model for aging processes. Indeed, those fish have a lifespan of 6 to 8 months with a sexual maturity reached at 3-4 weeks after fertilization. This is due to their environmental condition with a short wet season during which eggs have to develop faster to allow reproduction before the dry season [23]. Embryonic development can also be paused during a diapause state in which eggs can survive several months in dry condition, waiting for the wet season to come back. Despite its short lifespan, killifish have many molecular, cellular and physiological aging phenotypes that are shared among vertebrates, which make them suitable for studying those processes in a restrained time.

Mexican tetra, *Astyanax mexicanus*, is widely studied due to its two distinct forms, the surface one and the cave one (fig.1.2.C), that have evolved in parallel within a short timescale for evolution (20 000 years ago) [24]. Cave form is an interesting case of high phenotypical adaptability in fish, which can be investigated to explore the genetic and evolution basis of these modifications. Most of the studies have focused on the optic system evolution because of the eye degeneration or even loss in some cave phenotypes [25].

Other species are often used as animal models, such as the goldfish (*Carassius auratus*),

trout, salmon, seawater species, focusing on behavior, toxicology and ecological studies.

Among all those fish, few allow whole brain recording as easily as in ZF larvae. Until now, no other vertebrate, mammalian or non-mammalian, have proved accessible to whole-brain activity recording at a single-cell resolution. Suitable vertebrates should be small enough to enable imaging of deeper brain regions with optical techniques and to be recorded in its entirety. They should also be easy to raise and to maintain in captivity. Another important characteristic is the possibility to genetically modify them. All those constraints restrain the choice among the smallest known vertebrate. Among them, it is possible to cite the frog *Paedophpryne amauensis* described in 2012, and which measures 7.7 mm [28] (fig.1.2.D), the fish genus *Paedocypris* which lives in highly acid water in Southeast Asia (8 mm long for mature female [31]) (fig.1.2.E) and the *Danionella* fish genus, including *Danionella cerebrum* which is a particularly promising candidate as it is also fully transparent [32, 33] (see chapter 3, (fig.1.2.F)).

1.3 Thesis work

A PhD work is not a perfectly linear project for which the initial subject is explored as it was firstly designed. Experiments, results, readings, discussions and collaboration are supports to mature the project that can be redefined accordingly.

I started my PhD project with the objective to work on multisensory integration on zebrafish larvae. This well established model in neuroscience allows whole-brain recording at single-cell resolution, which make them suitable for determining neuronal circuit modulating simple behaviors. Some of those circuits were already determined for unique sensory stimulation (visual, thermal, mechanical, acoustic, balance...) and the main idea was to add complexity to the neuronal circuit by adding a second sensory stimulation. In chapter 2, I am presenting the results I obtained by stimulating ZF larvae with visual stimulation leading to body orientation (opto-motor response) and an acoustic stimulus which trigger escape behavior. The hypothesis was to determine if the escape direction would be biased with the integration of environmental information. This paradigm was also the occasion to study information integration.

In parallel to this project, I collaborated with Gokul Rajan, PhD student supervised by Filippo Del Bene, on *Danionella cerebrum* (abbreviated *DC*) for a published work [34]. I learn about this emerging model for neuroscience and with the support of my laboratory, I decided to dedicate most of my PhD to settle a specific fish facility and to be part of the global effort to promote *DC* for neuroscience (see chapter 3).

With their similar morphology at larval stage, a comparative work between ZF and *DC* between 5 and 7 dpf is straightforward. This work is part of the diversification of species model to explore the evolution strategy basis. In particular, despite their body similarities, both

species have diverging swimming patterns [34]. I started to detail the locomotor pattern and statistics used by *DC* to explore their environment. With a strong experience on phototaxis, I also decided to investigate their light preference in order to propose a simple model to ease the determination of the neuronal circuit involved. Those preliminary results on behavior comparison and model are developed in chapter 4.

Finally, one of the main advantage of *DC* is their natural optical transparency. Their close relationship with ZF allowed to use genetic tools already developed to create new *DC* transgenic lines for calcium imaging. Thus, I performed whole-brain imaging at single-cell resolution of *DC* larvae with the objective to decipher the neuronal circuit involved in their locomotion. I found a neuronal population that has not been yet reported and that seemed to play an important role during non-swimming phase. I also succeeded to record brain activity on older *DC* juvenile, which is opening new horizon for studying neuronal circuit maturation at different developmental stage, while it is not possible on other vertebrate models. Those findings are discussed in chapter 5.

My PhD work switched from multisensory integration to the development of a new vertebrate model for behavioral and neuronal circuit studies. *Danionella cerebrum* development will hopefully contribute to the diversification of the animal models used in neuroscience to better understand the principle of evolution mechanism in closely related species. Moreover, *DC* also offers a unique opportunity to disentangle the developmental and aging process all along lifespan, at behavioral but also neuronal scale, which is not possible with other species.

Chapter 2

Information integration study in larval zebrafish

Larva zebrafish (ZF) is a well-established model from 1970's. Its optical transparency at this developmental stage and the easiness to genetically modify it, makes it a suitable organism for neuroscience. By combining behavioral studies and brain imaging, it has allowed a better understanding of brain functions.

In this chapter, I explain the project I developed to explore the information integration processes and their impact on reflex behaviors. I start by describing the behaviors I used for this project. I then describe the paradigm I utilized and the results I obtained. I finish with a discussion on this project.

Personal contribution. I designed and implemented all the experiments described in this chapter. I performed the experiments and the analysis.

2.1 Review

2.1.1 Larval zebrafish behavior repertoire

One of the advantages that led to establish ZF larva as an important vertebrate model for neurosciences is its wide and rich behavioral repertoire [16, 17]. ZF larvae start swimming after the inflation of their first swim bladder, around 4 days post fertilization (dpf). They swim with discrete motions, called burst and glide movements or bouts, that can be classified according to their orientation (forward swim, routine turn [35, 36]), speed (burst swim, short or long latency escape [37]), induced body shape (J-turn [38], O-bend [36]) or goal (hunting [39], struggling when embedded). This list is still being updated with the use of machine learning to refine the categories [40].

Most of those swimming patterns are stable between 5 and 7 dpf. At those stages, larvae are relatively similar in their development within the same batch. This period corresponds to the end of the yolk sac which was ensuring autonomous nourishment, and thus, a uniform development for all larvae. This time also triggers more complex behaviors with the need to forage for food. At 5 dpf, ZF larvae are able to hunt unicellular organisms [39], and to explore their environment for food. Thus, ZF larvae are able to respond to sensory information perceived in their environment. It has been shown that ZF are responding to light [35, 41, 36, 42], temperature [5, 43], chemicals [44], and water current [45]. If larvae navigate in order to find food, they also have to avoid predators. They possess a huge variety of escape behaviors that can be elicited by touch on the tail [46], looming [47], acoustic (see section 2.1.3), vibration stimuli [37, 3], dark light flash [36] and others.

Visual information is the main sensory stimulation that ZF are exposed too. It is linked to different reflex behaviors such as optomotor response which allows fish to maintain their position [48] (see section 2.1.2), optokinetic response [49] and opto-vestibular response [50], suggesting that ZF larvae vestibular system is functional [51].

In the following section, I am giving more details on two of those behaviors: the optomotor response (see section 2.1.2) and the acoustic startle response (see section 2.1.3).

2.1.2 Opto-Motor Response

Optomotor response (OMR) is the reflex of body reorientation and orientation maintenance in response to a whole-field visual motion. It is found on many species such as insects (flies [52] among others [53]), fishes [54, 55] and mice [56]. This reflex allows animal stabilizing their positions in a moving environment. It is used as a behavioral control test to screen for visual defective mutants [56, 57] or drug screening effect [58] but also to dissect the neuronal circuit involved in processing sensory stimulation into motor output [55, 59]. OMR is usually evoked with a pattern in which black and white stripes are alternating and moving in one direction, presenting either from below or from the side.

From an ecological point of view, OMR can be related to the relative motion of the bottom of the river when fish drift with the water current. Thus, fish reorientation in the visual stimulation direction is similar than swimming against water current, in order to maintain their relative position [60].

In zebrafish, OMR is already present at larval stage. It has been demonstrated that this behavior is mediated by the red and green cones in the retina [55] that are related to a "luminance channel" suggesting that OMR is colorblind. To respond to this stimulation, fish are both sensitive to first-order signals, i.e. the motion created by the luminosity variations, but also to second-order motion, for which motion is created with texture or contrast changing, but not by light-intensity [61].

This reflex is widely used to investigate neuronal circuit modulation as fish response is influenced by visual stimulation features. For example, fish angle reorientation is dependent on the angle from the initial fish orientation and global direction of the visual stimulation [48]. Speed grating also impact fish swimming kinematics: fish tend to adjust their swimming velocity, bout duration, tail-beat frequency and interbout interval to match the speed stimulation [62].

2.1.3 Acoustic startle escape

Escape motions are an important part of ZF larvae behavioral repertoire. Flight behaviors are essential for motile animals to survive, even at early life stages. In fish, these are already observable at 24 hours post-fertilization, when embryos are reacting to touch stimuli [63]. ZF larvae respond with fast escape swimming to diverse sensory stimulation: touch, light drop [36], looming [47] and acoustic, vibration stimulation [37, 3].

In ZF larvae, acoustic stimulation triggers a C-bend escape pattern, which refers to the fish body shape to initiate the flight. C-bend kinematics are modulated with the stimulus intensity. At high intensity, ZF react with a delay shorter than 10 ms, called short latency C-bend (SLC) response, whereas larvae are taking more time to react to weak stimulation, i.e. more than $\approx$ 20 ms after the signal firing. This latter behavior is named long latency C-bend (LLC) response [37, 3]. In addition to having different latency times, these two movements also have different kinematics. LLC initial angle, angular velocity and latency vary with the stimulation intensity, whereas only the percentage of SLC responses increase with it. This suggests that LLC involves a sensory integration mechanism, and that LLC and SLC are not generated from the same neuronal circuit than SLC responses.

In most escape behaviors, Mauthner cells play a central role within the dedicated neuronal circuit. Those bilateral giant reticulo-spinal (RS) cells are located in the hindbrain, and are well known for their implication on initiating fast start response [46]. They receive information from both sensory hair cells of the lateral line and from the otic vesicle in the inner ear. It has been demonstrated that SLC responses are Mauthner cell dependent whereas ablation of those cells do not impact LLC responses [37]. Thus, SLC and LLC responses are not modulated behaviors from a same neuronal circuit but they engage distinct pathways.

SLC responses are believed to be of all-or-nothing events, i.e. they do not integrate environmental information when activated. In contrast, the fact that LLC kinematics are modulated by the stimulation intensity suggests that those responses are sensitive to environmental stimulation and might integrate other information, an hypothesis that has not yet been demonstrated.

2.1.4 Information integration, decision-making

In the environment, animals are surrounded by diverse sensory information that overlap and are obscured by noise. Multisensory integration requires decoding and analyzing capacity to extract from these multiple signals the relevant information that will lead to the adequate action. Thus, reacting in a good way to sensory stimulation suggests an ability to accumulate and integrate enough environmental clues in a short time, especially when facing a threat. This sensory evidence accumulation over periods of few milliseconds to seconds has been reported in various organisms such as flies [64], rodents [65], primates [66] and humans [67].

During the last few years, evidence accumulation for decision-making behavior has been explored in larval zebrafish [68, 69]. Both studies adapted a well-established experiment to test evidence accumulation on primates: the random dot motion [66]. In monkeys, this task consists on showing multiple dots, of which a certain percentage is moving coherently in a same direction. Depending on the study, animals need to turn their head in the moving direction, either when they have determined the direction, to extract the accumulative time threshold, either after a certain time, to test their persistency. Both studies in fish adapted this paradigm to ZF larvae. They demonstrated that freely swimming and restrained fish are able to integrate motion coherence and to modulate their behavior accordingly. Thus, ZF larvae are able to accumulate environmental information before reacting in consequence.

2.2 Is it possible to bias acoustic escape with visual cues in larval zebrafish?

One of the objectives of my project was to explore the possible influence of information accumulation by disrupting this process just before the animal response. I chose to use the OMR reflex as the behavior which requires information integration. To perturb it, I selected an acoustic stimulation which triggers escapes. I then recorded the escape direction to see whether or not it is influenced by the visual stimulation. Moreover, long latency escape responses can be elicited by the acoustic stimulation. Thus, it was also an opportunity to verify the possible multisensory integration mechanism of those LLC response.

2.2.1 Experimental setup

2.2.1.1 First trials

Before ending with the final experimental setup I used, I tested diverse electronic compounds and ideas. The main experiment design was to record ZF larvae on a petri dish put on a screen, on which a visual stimulation was displayed with a projector. This setup was already in use, the only missing part was the acoustic, vibrational stimulation.

First trial. Taking inspiration from the thesis of a former PhD student of the laboratory, Raphaël Olive [70], I decided to use waterproof piezoelectric speakers controlled with a function generator. As those speakers were used for individual embedded larvae, I decided to put three speakers on a plexiglass ring. I tested different frequency and amplitude, but even at the maximum amplitude allowed by the function generator (20 V peak to peak), no fish were escaping. So I decided to change the way to create an escape response.

Second trial. Taking into account that acoustic stimulation is also a mechanical stimulation, I decided to use coin vibrating motors, that are used in e.g. mobile phones and were available in the laboratory. I glued the coin directly on the petri dish and I was able to elicit robust escape behaviors from the larvae. To control the motor trigger and vibration amplitude, I used an Arduino and a digital potentiometer. I tested diverse parameters to optimize the setup with this coin vibrating motor controlled by Arduino. For many reasons, I had to move to another setup. Indeed, the motor needed hundreds of milliseconds to start vibrating due to inertia. Moreover, the shorter mechanical stimulation I could obtain was $\approx$ 120 ms, which is too long to distinguish SLC from LLC. Moreover, I did not manage to find a good way to have a fast communication between Arduino and Matlab, making it difficult to trigger the visual stimulation and the mechanical stimulation with a precise timing.

For all those reasons, I decided to move to another implementation of an acoustic stimulation. With a vibrating pot, an amplifier and a function generator, I succeeded to establish a suitable experimental setup.

2.2.1.2 Final experimental setup and protocols

Experimental setup. The experimental setup was installed in a light-tight box. The temperature inside was maintained between 26 °C and 28 °C using "The Cube" (Life Imaging Service). The arena consisted of 8.5 cm in diameter Petri dish containing few millimeters high of E3 medium, salted water in which zebrafish embryos are growing. The Petri dish was drilled to fix a screw connected to a vibrating pot (mini shaker type 4810, Brüel & Kjær). This vibrating pot was connected to an amplifier (Power Amplifier Type 2718, Brüel & Kjær), which received a sinusoidal signal of 3 ms at 1000 Hz with 3 V peak to peak amplitude generated with a function generator (HP 33120A). The arena was placed on a screen illuminated from below by a projector (ViewSonic M1). A camera (FLIR Chameleon3 CM3-U3-13Y3M-CS) with an adjustable macro lens (Navitar, Zoom 700) equipped with an IR filter recorded the fish behavior from above the tank, which was also illuminated by an IR LED panel (fig.2.1.A). Behaviors were recorded at 150 fps, the maximum framerate allowed for full field of view with no pixel binning, with this camera. Individual pgm (portable gray map) frame were saved. Only data within an 8 cm diameter area (called ROI for region of interest) were analyzed. Behavior recording, visual and acoustic stimulation were controlled

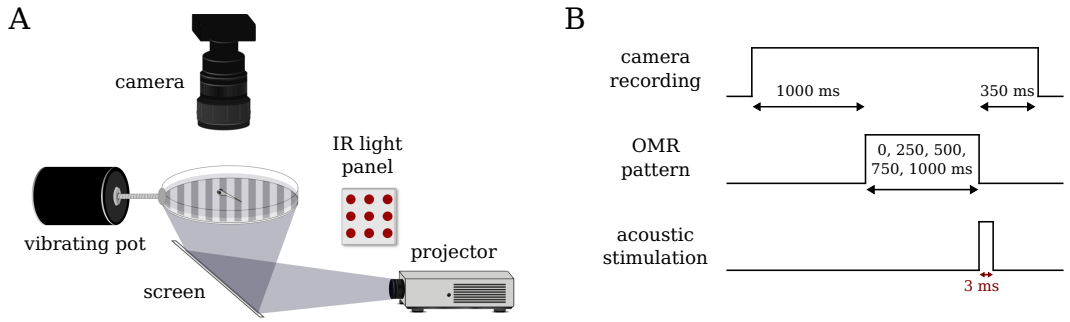

Fig. 2.1 ***Experimental setup and protocol for visual and acoustic stimulation.*** ***A*** *Schema of the experimental setup.* ***B*** *Schema describing the protocol structure of the visual and acoustic stimuli.*

with a custom-written software in Matlab (The MathWorks). The visual stimulation was created using the PsychToolBox (PTB) version 3.0.14 add-on. The camera and acoustic stimulation were triggered with a DAQ card system.

Protocols. Here, I described the four protocols I used for the experiments and the controls. All experiments were performed with ZF WT AB line, with larvae between 5 and 7 dpf. They were fed every morning of experimental days with paramecia, one hour before the experiment. Experiments were done between 10 am and 6 pm. Larvae were accustomed to their environment during 10 to 15 minutes before starting the assay, with the higher light intensity of the projector. The visual pattern consisted of 5 mm alternating black and white stripes that moved at 20 mm/s. I chose those parameters based on [62].

Bias acoustic escape direction with a moving visual stimulation. The structure of the protocol consisted in recording 1 second of spontaneous behavior, then the moving visual pattern started for different durations (0, 250, 500, 750, 1000 ms) before the acoustic signal generation. The acoustic signal consisted of a short pulse of 3 ms at 1000 Hz, with a voltage set at 3 volt peak to peak. After the acoustic signal, the fish behavior was recorded for 350 ms. This protocol is schematized in fig.2.1.B. Ten runs were recorded for each visual stimulation duration.

Spontaneous. To have baseline swimming parameters of ZF larvae, I recorded for 5 seconds, three times, the spontaneous swimming of ZF larvae under the same illumination conditions than for habituation, so with the higher light intensity of the projector. Those experiments were used as control.

OMR. I recorded ZF larval response to moving patterns appearing 1 second after the beginning of the recording, for 5 seconds. The experiment was repeated 10 times, with at least 5 minutes break in between.

Visual pattern appearance. To check if visual pattern appearance could trigger an

escape, I let the ZF larvae adapt for 10 to 15 min with an immobile visual pattern. Then, I used the same protocol as before, for which fish movements were registered for 1 second with a fixed visual pattern, then for 5 seconds with the pattern moving, for 10 times, with at least 5 minutes break in between.

2.2.2 Analysis and Results

2.2.2.1 Analysis

Tracking. Fish tracking was performed offline using a program developed by a former PhD student of the laboratory, Benjamin Gallois, which is called FastTrack [71]. The program allows tracking of multiple objects. For each movie, I first defined a background with a Matlab code. I used the adaptive threshold function of Matlab (adaptthresh) with sensitivity set at 0.67, on a random frame of the movie. I then added a mask to only keep the ROI in which I wanted to observe fish behaviors. This background was used in FastTrack to ease fish detection. FastTrack parameters used for tracking are in Annex.A.2. An example of fish trajectories obtained with FastTrack is shown on fig.2.2.C.

Characterization of the escape response after acoustic stimulation. For all the experiments, burst and glide motions and orientations were detected with custom-written coded in Matlab used in a previous study [35]. Reorientation angles were defined according to the visual pattern direction, if it was displayed, or according to the horizontal axis otherwise. I only considered fishes that were in the ROI from the beginning of the visual stimulation until the movie end. For the visual and acoustic stimulation, I defined a score for each escape according to its direction. ZF larva first escape angles are between $\pm\frac{\pi}{2}$ and $\pm\pi$. Thus, it is possible to determine if the larva was escaping toward or against the visual stimulation direction. According to the sign of the fish orientation angle before the escape, comprised in $[-\pi, +\pi]$, and the sign of the escape direction, I assigned a score of +1 for escape in the direction of the visual stimulation, and a score of -1 it is in the opposite direction (fig.2.2.A). By averaging all the scores, it is possible to determine if larval escapes were random (mean around 0), biased in the OMR direction (positive sum) or in the opposite direction (negative sum).

First bout latency. I determined for OMR movies the latency between the visual stimulation beginning and the first bout. The probability density function (pdf) of this latency distribution was compared to the one of the latency between each time step and each first fish bout during spontaneous measuring.

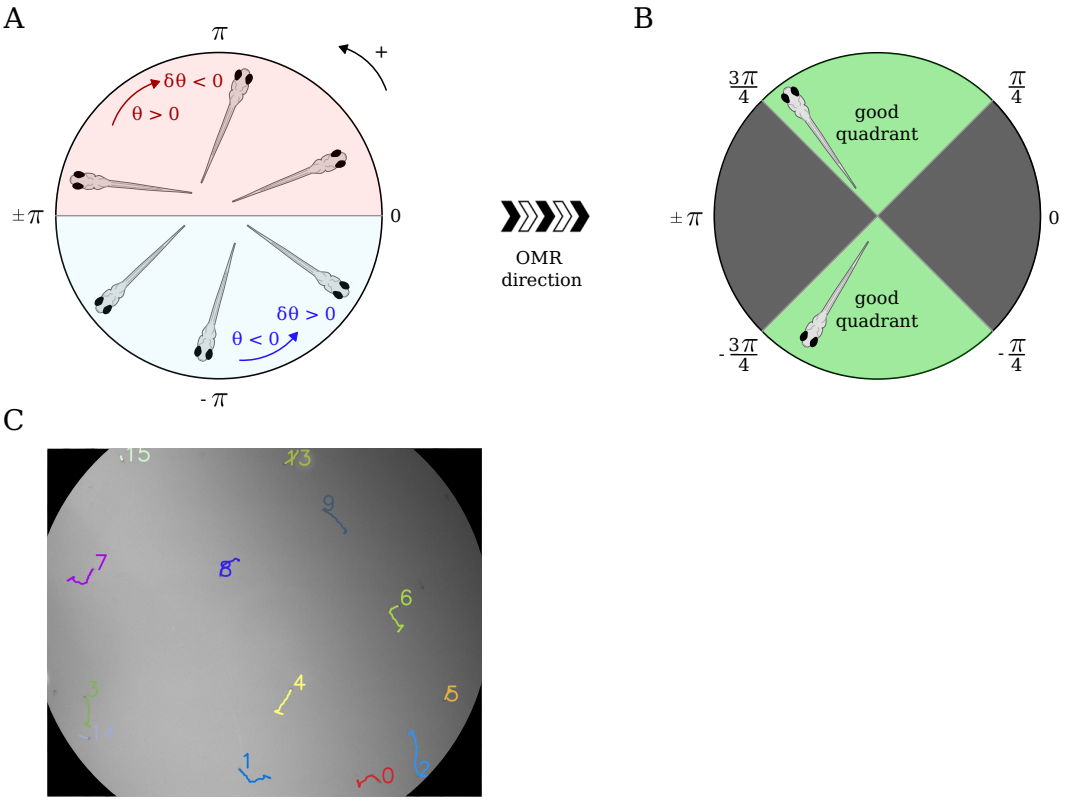

Fig. 2.2 ***Visual and acoustic experiment analysis.*** ***A*** *Schema for explaining the link between the sign of body orientation before escape (θ) and the reorientation sign (δθ).* ***B*** *Schema for explaining the "good quadrant" orientation selection.* ***C*** *Trajectories obtained with FastTrack.*

Statistics. I used the one sample Student t-test to compare the escape score distribution of the visual and acoustic stimulation experiments, from a random distribution of +1 and -1. To confirm the significant difference between the first bout latency between spontaneous and OMR distributions, I employed a two sample t-test. As the spontaneous distribution contains more samples (91 252 time steps) than other distributions (652 time steps for the red curve, 329 for the blue one), I created a sub-distributions by selecting 600 time steps of the spontaneous distribution at random. I used the two sample t-test to compare the spontaneous sub-distribution and the two OMR distributions.

For angular uniformity, I used the Rayleigh test from the CircStat toolbox for Matlab [72].

2.2.2.2 Results

ZF larvae are delaying their first bout when OMR starts. To integrate a sensory stimulation, it is necessary to accumulate evidence and information about this stimulus. After

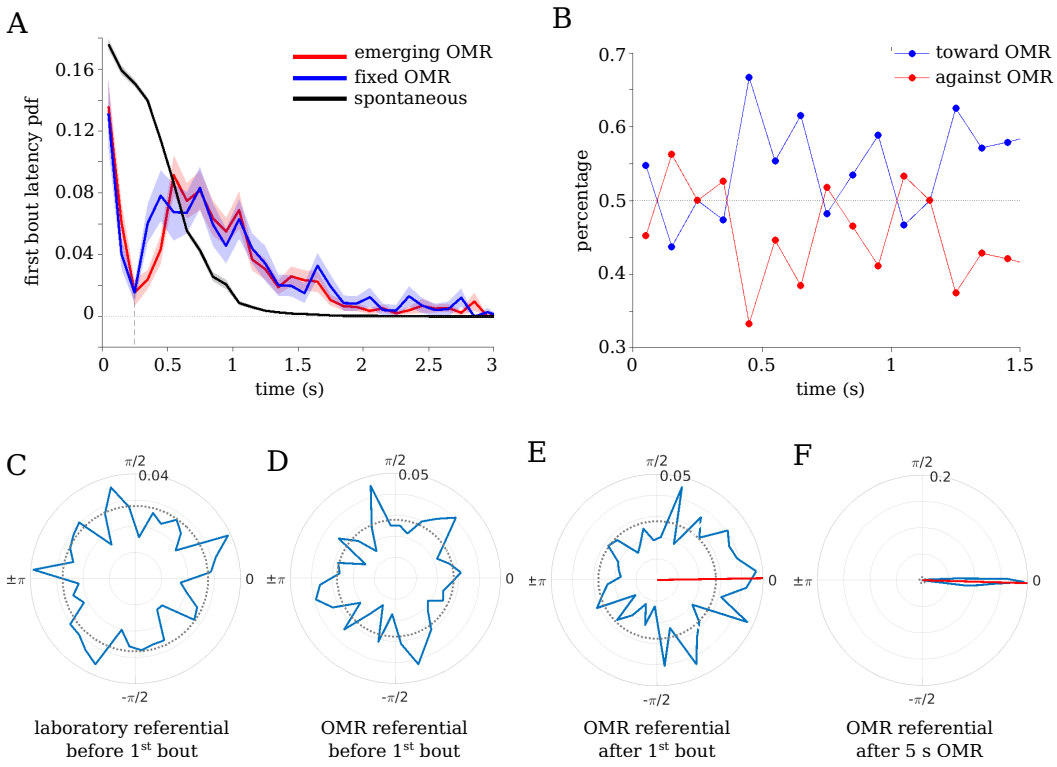

Fig. 2.3 ***OMR analysis.*** ***A*** *Probability density function of the latency between OMR moving beginning and fish first bout. Red curve: the OMR pattern was displayed only at the beginning of the visual stimulation. Blue curve: fish were adapted with the OMR pattern, which started to move at the beginning of the stimulation. Black curve: Probability density function (pdf) of the latency between each time step and the next first bout. Thick line: mean. Light color: SEM.* ***B*** *Percentage of 1^{st} bout toward (blue) or against (red) OMR, in function of time.* ***C*** *Polar pdf of fish orientation before 1^{st} bout in the laboratory referential (Rayleigh test $p > 0.05$).* ***D*** *Polar pdf of fish orientation before 1^{st} bout in the OMR direction referential (0 : OMR direction, Rayleigh test $p > 0.05$).* ***E*** *Polar pdf of fish orientation after 1^{st} bout in the OMR direction referential (0 : OMR direction, Rayleigh test $p < 0.001$). Red line: mean angle.* ***F*** *Polar pdf of fish orientation at the end of the experiment (5 seconds OMR) in the OMR direction referential (0 : OMR direction, Rayleigh test $p < 0.001$). Red line: mean angle.*

a certain accumulation time, neuronal circuit have acquired enough information to process it and to act accordingly. I was interested in understanding what was the ZF larvae strategy in response to OMR. For this, I examined the latency between the beginning of the visual stimulation and the initiation of the first bout, then plotted its pdf (fig.2.3.A red and blue curves). In order to have a reference curve, I also traced the equivalent pdf for spontaneous swimming (fig.2.3.A black curve).

I found that the appearance of the visual pattern had no effect on the bout initiation, leading to the conclusion that the OMR pattern emergence was not triggering an escape response. Indeed, first bout latency to visual stimulation beginning distribution, with (fig.2.3.A red curve) and without appearance of the pattern (fig.2.3.A blue curve), are significantly comparable (two samples t-test: $p > 0.05$). However, those two distributions are significantly different from the spontaneous one (fig.2.3.A black curve) (two samples t-test: $p < 0.001$). Indeed, it is clearly visible that the OMR onset seems to initially inhibit tail bout execution as there is an important decrease in the pdf around 0.2 second. Then, the pdf increases again with a maximum reached around 0.5 second after the stimulation beginning, and which decreases again.

When I compared the proportion of first bout initiated after the visual stimulation onset, I noticed that those bouts tend to be oriented towards the OMR direction, only after 0.5 second (fig.2.3.B). This suggests that this delay is necessary to integrate visual information in order to bias the bout orientation in the appropriate direction. This is confirmed with the angular distribution of fish orientation before the first bout (fig.2.3.D), which is homogenous, whereas after the bout, fish are mainly heading toward the OMR direction (fig.2.3.E).

Those experiments were done in the same petri dish as the OMR and acoustic stimulation, meaning that ZF larvae had a visual clue, the screw. By looking at the movie and the body orientation of the fish before the first bout, in the laboratory referential, which is uniform (fig.2.3.C), I concluded that the screw was not inducing any bias.

OMR stimulation does not bias acoustic startle response in ZF larvae. Another objective of this study was to determine if visual sensory stimulation was taken into account when the fish was exposed to an acoustic stimulation triggering an escape behavior. For this, I used the OMR reflex which requires visual information integration. I was assuming that the more the fish would be exposed to the OMR pattern, the more its escape should be biased by the stimulation direction. I plotted the average of the escape score (+1 if the escape was in the visual stimulation direction, -1 if it was against) as a function of OMR duration, and I observed that no significant bias was noticeable, except for 500 ms and 750 ms of OMR (fig.2.4.A). In these intervals, a small bias is observed, created by the visual pattern was against the OMR direction. It is possible to understand this preferential direction as escaping with the water current, increases the fish velocity. Visual bias strength is not

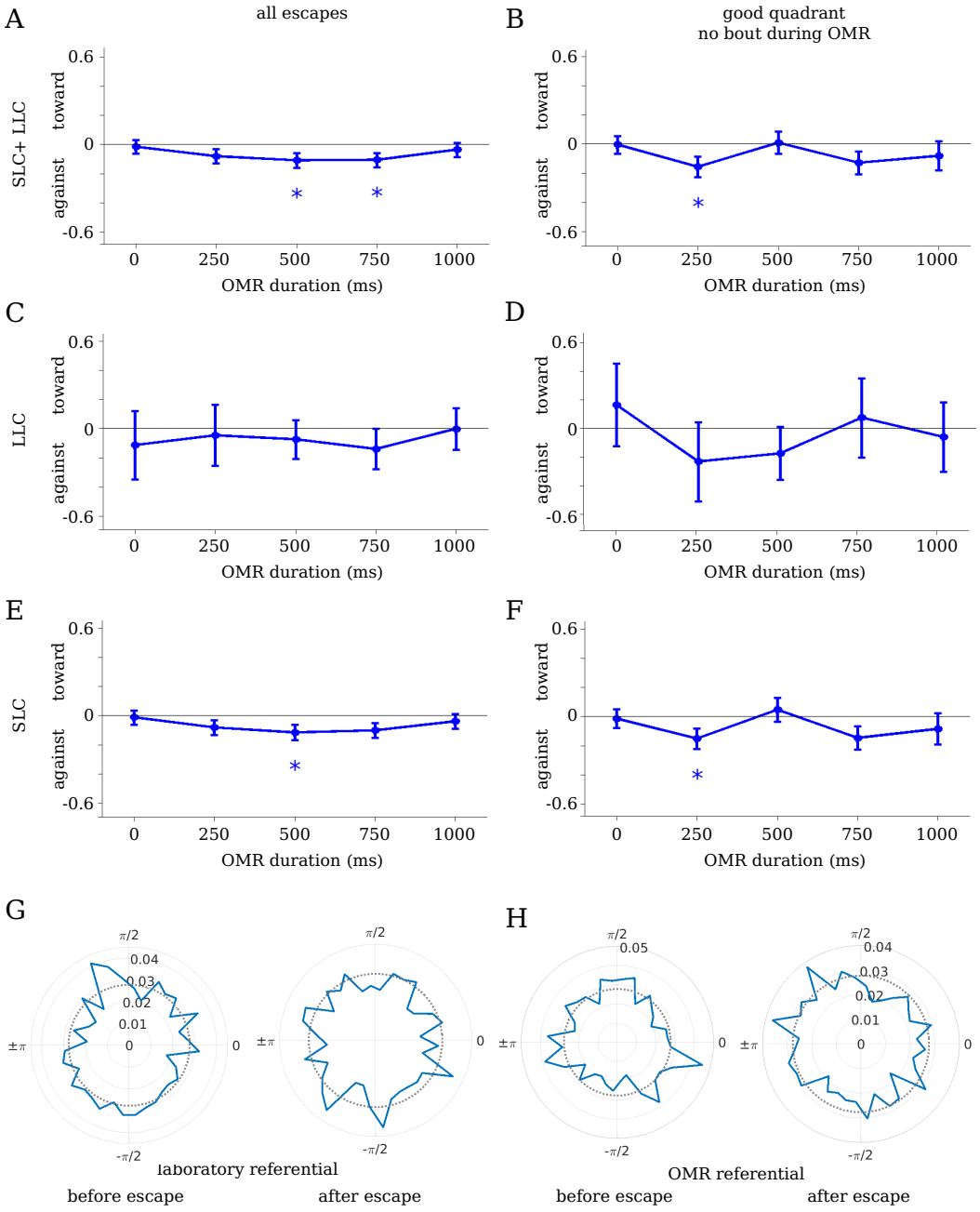

Fig. 2.4 ***Results of the OMR and acoustic stimulation experiments. All escapes.*** ***A*** *Escape vector average in function of OMR duration.* ***B*** *Escape vector average for fish which had a body orientation in the good quadrants (fig2.2.B), and did not move during OMR stimulation (no bout during OMR).* ***LLC escapes.*** ***C*** *All fish.* ***D*** *Fish in good quadrants, with no bout during OMR stimulation.* ***SLC escapes.*** ***E*** *All fish.* ***F*** *Fish in good quadrants, with no bout during OMR stimulation.* ***G*** *Polar distribution of fish orientation before acoustic stimulation (left) and after (right) in the laboratory referential (Rayleigh test $p > 0.05$ for both) and* ***H*** *in the OMR direction referential (0 : OMR direction, Rayleigh test $p > 0.05$ for both). All fish numbers are summarized in annex.A.1 table.*

increasing with the OMR duration, even decreasing.

For long OMR durations, some larvae could have already reacted to OMR and performed a bout in the OMR direction. Thus, fish are already oriented in the OMR direction which would lead to a random escape direction. Moreover, ZF larvae response to OMR pattern is higher when the OMR direction is orthogonal to the fish. For those two reasons, I decided to refine the escape selection by only considering fish that did not swim between the OMR beginning and the acoustic stimulation, and that had a body orientation in $[\pm\frac{\pi}{4}, \frac{3\pi}{4}]$ interval (fig.2.2.B). With those conditions, I obtained a visual bias on the escape direction null (fig.2.4.B). ZF larvae acoustic startle response direction is not influenced by visual stimulation.

There are two kinds of acoustic escape response: the SLC and LLC (see section 2.1.3). I assumed that only LLC responses would involve an integration mechanism. I categorized the fish escape into those two categories, with a time threshold set at 20 ms and I plotted the same graphics as before, by considering all fish, and then only fish in the good interval and that did not move before the acoustic stimulation. I found that for both escape types, SLC (fig.2.4.C,D) and LLC (fig.2.4.E,F), the visual stimulation had no effect on the escape direction.

To verify that the acoustic stimulation elicited an anisotropic response, I plotted the body orientation before and after escape, in the laboratory referential (fig.2.4.G). Both distribution were uniform which implied that ZF larvae were not escaping on a specific direction influenced by the acoustic stimulation and visible screw. By plotting the same orientations on the OMR direction referential, I confirmed that fish escape directions were not biased by any stimulation (fig.2.4.H). All fish numbers for the various conditions are summarized ina table in the annex section (annex.A.1).

2.3 Discussion

ZF larvae first bout latency to OMR stimulation. The experiments showed that the probability to trigger a bout is depleted in the first 0.5 s after the OMR onset, which is consistent with the results found by Severi et al. [62]. In this study, they demonstrated that the first bout initiation latency was decreasing with OMR speed between 0 and 20 mm/s and to be around 500 ms at this last speed. It could be interesting to reproduce my experiment with a lower OMR velocity to verify if a shift in the probability maximum toward higher time would be observable. They also showed that ZF larvae bouts can be clustered into *slow* and *fast* swimming [62]. Slow bouts are more used with slow OMR speed, up to 10 mm/s whereas higher OMR speeds are correlated with fast motions.

If I had time to do more experiments, I would probably use a smaller OMR velocity (less than 10 mm/s), in order to test if ZF larvae being in a slow state would respond with more LLC escapes to the acoustic stimulation, and would be biased by the OMR direction. When

I designed my experiment, I was looking for a fast reaction to OMR pattern, expecting that above this latency time, ZF larvae would always be biased, which is apparently not the case.

For this study, I was interested in understanding how fish accumulates sensory information in order to respond to this stimulation with the adequate behavior. My problem was to determine when ZF larvae have accumulated enough information to reach a threshold for responding correctly to OMR stimulation. Is it the latency between the OMR starting and the first bout initiation? Or is it the first bout allowing the fish to reorient itself toward OMR? In most case, the first bout reorientation after the OMR onset is oriented towards the direction of the visual stimulation (fig.2.3.B,E). However, all fish do not respond this way, which make it difficult to assume that the first bout can be used as an indication that the fish have integrated visual stimulation. In other words, the first bout is not always performed in response to information integration. The question on how to determine behaviorally this threshold on fish in OMR is still open.

Nevertheless, the delay in first bout initiation when exposed to OMR pattern, suggests that fish are indeed waiting for evidence accumulation before moving, either toward the OMR direction, either randomly, depending on other internal states. To better understand the evidence accumulation strategy for OMR, one may perform the same experiments by varying stripe sizes with a fix speed, to understand if the accumulation is based on spatial clues (the number of stripes that have to pass beneath or in front of the fish), or if it is related to temporal integration (independent of the number of stripes). From the results of Severi et al. [62], it seems that for low speed grating, under 10 mm/s, the latency is decreasing linearly or exponentially, assuming that spatial and temporal accumulation are linked. Then, there is a latency plateau for pattern velocity between 10 and 33 mm/s, suggesting that the accumulation is more temporal than spatial. This has to be explored further, also to better understand the underlying neuronal circuits.

OMR visual stimulation does not affect acoustic startle response direction. As fish were adapted in high light intensity, OMR pattern emergence led to a global decrease in luminosity, whose amplitude was not important enough to trigger escape response. Indeed, the blue and red latency probability curves plotted on figure 2.3 are similar, which confirmed that the pattern appearance did not initiate flight behaviors.

From these graphics, I could show that the time threshold needed to accumulate information with these OMR features was around half a second. Then, one may have expected a bias in the acoustic escape direction after 500 ms OMR exposure. When all escape types are taken into account, there is indeed a bias for 500 ms and 750 ms of OMR displaying, against its direction, which can be interpreted as a flight in the water current direction, to increase fish velocity (fig.2.4.A). But this bias is no more visible at 1000 ms. When there is no OMR displayed, fish were escaping in random directions (mean around 0).

Then, I wanted to discriminate between SLC and LLC escapes, in order to discover if LLC responses could integrate other sensory stimulation. This hypothesis was not conclusive. Indeed, LLC escapes were not biased against nor toward OMR direction (fig.2.4.C). For SLS response, surprisingly, they were influenced only for 500 ms OMR (fig.2.4.E). The fact that the LLC distribution were not biased can be explained by the fact that the acoustic stimulation was too intense and triggered more SLC than LLC responses A.1. Even with this low number of LLC escapes, no strong bias can be observed, even after refining the escape selection (fig.2.4.D,F). It is interesting to notice that the LLC proportion increases with the OMR duration (tab.A.1). This might be indicative of an ongoing processing (for OMR reflex) which favors a longer delay for escape.

This experiment was not conclusive. I think the way I designed the protocol was not optimal. To trigger more LLC response, I should have used a lower acoustic signals, even if it is at the expense of global escape number. Moreover, a slower OMR pattern would have required for more integration from the ZF larvae, which could have allowed me to better investigate the information accumulation.

With those experiments, I demonstrated that it is possible to study information accumulation with the well-known reflex OMR in ZF larvae. Moreover, I learned that trials and errors strategy is an important part of designing protocols and defining projects. The first objective was to bias acoustic startle direction with visual stimulation to simulate a multisensory integration on escape behavior. I chose acoustic startle responses because of the LLC responses that are modulated by the trigger stimulation, and that were a good candidate for integrating sensory information. Nevertheless, the signal used was probably too intense to elicit mostly LLC, which had a direct impact on my statistics. Moreover, by selecting larvae that should have been more sensitive to the visual stimulation, I lost the bias I observed when I took into account all escapes, even the one that might create noise. Those results are puzzling.

Scientific projects are not always a success with smooth experimental process and results easy to interpret. With this project, I learned that it is important to push ideas, but also to move to other projects, especially when the opportunity to develop and work on a new vertebrate model is offered.

Chapter 3

A new model in neuroscience: *Danionella cerebrum*

In this chapter, I describe the different steps I did to develop a fish facility for *Danionella cerebrum*. I detail the different protocols I developed to raise and feed this species. I also mention some observations I did while taking care of this fish.

Personal contribution The fish facility creation was a joint effort from different persons, in which I had a major contribution. I was mainly involved in stabilizing the *DC* colony and taking care of the fish. I designed and wrote the feeding and raising protocols in discussion with Ghislaine Morvan-Dubois and fish facility members. I mainly report the observations I did while I was taking care of the fish.

Raphael Candelier developed and collected data from MonitoRack. He also performed all the analysis. We discussed together the results.

3.1 Review

3.1.1 *Danionella* fish

Danionella is a genus of bony fish that is part of the *Cyprinidae* family. Danionella fish belong to the subfamily group *Danioninae* or danionin, which includes also the common *Danio rerio*, zebrafish (fig.3.1.A). Until recently, four species were considered part of the *Danionella* genus: *Danionella translucida*, first described in 1986 by Roberts [32], *Danionella mirifica* [73], *Danionella dracula* [74] and *Danionella priapus* [75]. However, in 2021, a new *Danionella* species was described, called *Danionella cerebrum*, which had been confounded for a long time with *Danionella translucida* [33].

Danionella species are fresh water fish and are found in shallow, slow flowing streams of Myanmar and northeastern India. They are among the smallest fish and vertebrates with a

maximum adult size between 11 and 17 mm. Those miniature fish are an extreme case of vertebrate progenesis, an evolutionary process that leads to sexually mature organism with larval and juvenile features [76, 77]. At the skeleton level, *Danionella* adults are missing the skull roof, implying that their brain is merely covered by skin [33] (fig.3.1.E,F). Moreover, *Danionella* possesses very few melanophores, which are mainly located on the ventral side, on the swim bladders and at the back of their head. This pigment pattern leads to fish that can be considered as transparent (fig.3.1A,C,D). They do not possess scales. Even if *Danionella* adults look like juvenile fish, they display complex behaviors such as shoaling, schooling, social behaviors and most surprisingly, acoustic communication (for *Danionella dracula, translucida and cerebrum.* Males are able to produce click-like sounds that are mainly used during male-male aggressive interactions but not for courtship [30, 78].

All those characteristics, small brain, no ossified skull, optical transparency, complex adult behaviors, have pushed researchers to develop both larval and adult *Danionella* into a vertebrate model organism for neuroscience with the opportunity to perform deep imaging of their brain [30, 79, 80, 34, 81]. Among those five species, *Danionella cerebrum* (abbreviated *DC*) is the one that has been selected for neuroscience studies.

3.1.2 Developing *Danionella translucida/cerebrum* for neuroscience

Danionella cerebrum is a new species that has been confounded for many years with *Danionella translucida* [33]. Most of the studies published before 2021 working with *Danionella translucida* were in fact working with *DC* . For the sake of simplicity, I will use *DC* to refer to both species.

In 2018, two teams published independently their first studies on *DC* to set this fish as an emerging model for neuroscience [79, 30]. They argued that the commonly used larval ZF behavioral repertoire lacks complex behaviors such as socialization or courtship. Socialization appears around 3 weeks in ZF [14], their brains are harder to image due to their relative large size, pigments, scales and ossified skulls that are scattering light. In contrary, *DC* adults lack of such light-scattering features and do not require invasive surgery to image their brain. Due to their close phylogeny, genetic tools developed for ZF can be used to express transgenes in *DC* and to create new transgenic lines. Schulze et al. [30] used the CRISPR-Cas9 genome editing technique to target the *tyr* gene in *DC* to create a mutant deprived of pigmentation. They also used the Tol2-mediated transgenesis technique to create a stable transgenic line. Genetic modification of *DC* genome will be eased in the future thanks to the work of Kadobianskyi et al. [82] who published an assembled and annotated sequence of *DC* .

The first calcium imaging of *DC* adult brain was obtained by Schulze et al. as a proof of concept. They used two-photon microscopy to record neuronal calcium activity on 3-6

months old sedated *DC* [30]. They succeeded to image individual neuron at a depth of 300 μm in the brain, as they tested the fluorescence responsiveness of auditory neurons by using acoustic stimulation mimicking the male sounds. They observed auditory-evoked responses in some neurons, demonstrating that is it possible to record brain activity on *DC* adult.

In parallel, those studies highlighted some interesting behavior of *DC* adult. Schulze et al. reported on the shoaling and schooling behaviors [30]. They also showed that only males are vocalizing, mostly during the morning and that this communication can be recorded when several males are in a same tank. Another study demonstrated that click-like sounds are mostly associated with aggressive interaction but not with courtship [78] for *Danionella dracula*. This communication suggests a learning capacity in *DC* in order to memorize the pattern associated to diverse situations. Penalva et al. shown that *DC* adults are capable of socially reinforced learning [79].

3.1.3 *Danionella cerebrum* project

In our team, and in collaboration with FDB team, we decided to contribute to the *DC* development as a new vertebrate model for neuroscience.

Thanks to its optical transparency and small size even at adulthood, *DC* offers unique research opportunities. In our team, we decided to leverage those assets in order to study how swimming patterns are maturing through fish life, from the larval stage to adulthood, from both the behavioral and the neuronal circuit viewpoint. Ontogeny of neuronal circuit organization is challenging to follow over different developmental stages of vertebrates. Part of the circuits can be studied separately but it is complex to monitor change on the overall circuit. With its small size, lack of pigment and evolving behaviors along its life span, *DC* is optimal for studying behavioral ontogeny, as well as for aging processes, developmental biology, development of pathology and other applications linked to its transparency at adult stage. *DC* 's phylogenetic and anatomical proximity with ZF is facilitating the development of *DC* transgenic lines. It is also possible to use already existing experimental setup and the abundant literature of ZF larvae for *DC* . This close connection between ZF and *DC* also allows cross-species comparison to help identify general principles of evolution, especially for neuronal circuits [34].

In collaboration with other researchers, we developed a project focusing on neuronal circuit maturation and evolution. As a first step, our objective was to identify and record the neuronal circuit dynamics involved in spontaneous locomotion on *DC* from 6 days post fertilization (dpf) up to 1-month-old. In parallel to this work, a behavioral and neuronal comparative study between *DC* and ZF larvae is carried out in order to better understand the evolution process.

Behavioral study of the spontaneous locomotion and phototaxis of *DC* and ZF is explored

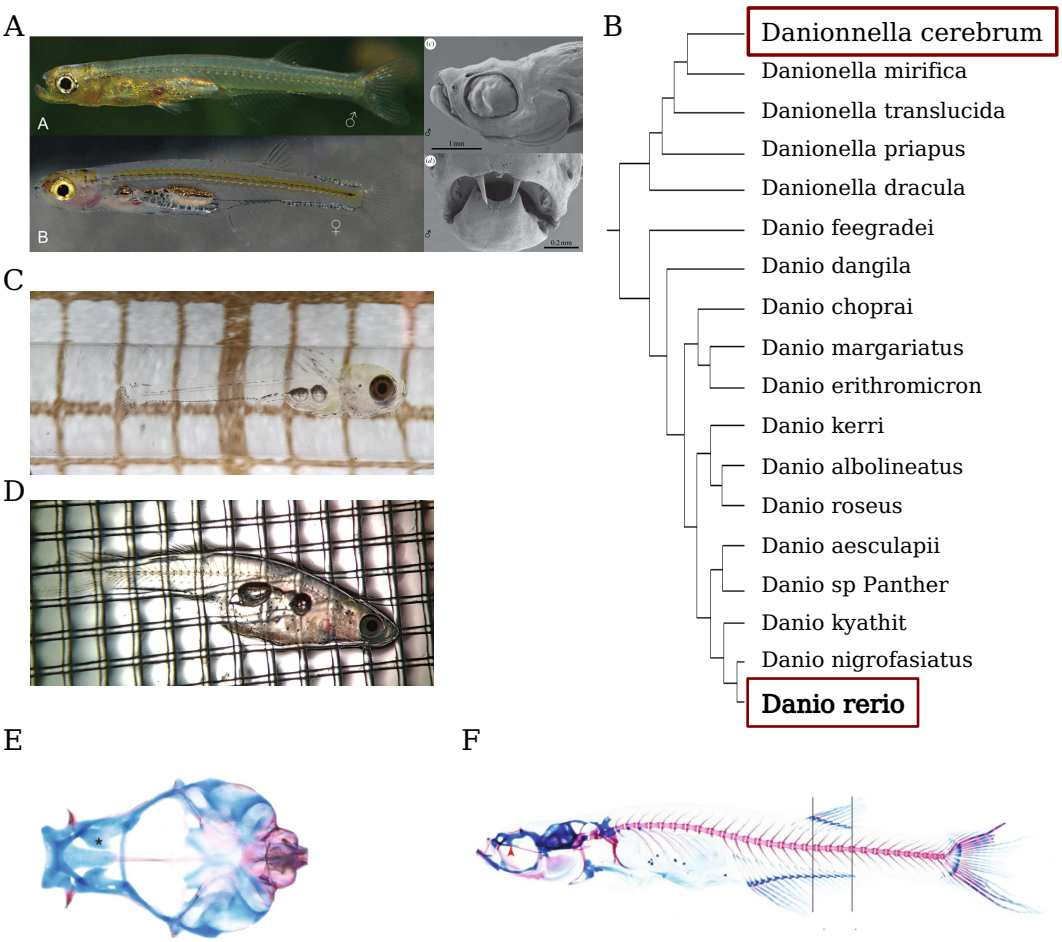

Fig. 3.1 ***Danionella genus.*** ***A*** *Danionella dracula. Left panels: photography of male (top) and female (bottom). Adapted from [77]. Right panels: scanning electron micrograph: side view (top), anterior view (bottom). Male teeth are visible. Adapted from [74].* ***B*** *Simplified phylogenitic tree of Danioninae subfamily showing the close relation between Danionella cerebrum and Danio rerio.* ***C*** *and* ***D****: optical transparency of DC at 15 dpf (C) and adult stage (female, D, photography from Ghislaine Morvan-Dubois). Mesh grid size is 1 mm.* ***E*** *and* ***F****: DC female stained skeleton. Blue: cartilage, purple: ossified bones. No skull roof is visible. Adapted from [33].*

on chapter 4 and results on the locomotor neuronal circuit identification are presented on chapter 5.

3.2 *Danionella cerebrum* facility

3.2.1 Timeline

The project of creating a fish facility at Jussieu for *Danionella cerebrum* emerged at the end of 2019. With the help of the aquatic facility members, we obtained a room in February 2020 in which it was possible to install a rack for *DC* . Most of the painting work and cleaning was done by RC and GMD. The rack installation and starting the water flow to create biological filters were done by the aquatic staff. Those steps were done just before the first lockdown, which delayed the fish installation. In the meantime, *DC* WT and transgenic lines were housed at Institut Curie by the team of FDB. Fish were usually fed two to three times per day but during the first lockdown, the feeding rate was reduced to once time a day. After this lockdown, the feeding rate went back to normal but the egg production took several months to come back to normal. We obtained our first WT eggs end of June 2020 and the first transgenic eggs only in September (4-5 clutch) then we had to wait for another month to obtain more transgenic eggs.

With GMD, we spent between two and five hours per day from June 2020 to July 2021 raising the fish, feeding them, cleaning tanks, changing mechanical filters, defining raising and feeding protocols. We had a hard time in September and October 2020 for raising the transgenic *DC* we had from Karine Duroure because the transgenic adults were not laying many eggs and *DC* larvae are fragile until 15 days. We managed to grow 20 of them.

We obtained our first *DC* WT eggs on September 2020 and our first transgenic eggs on December 2020. For 2 to 4 months, we kept most of the eggs to increase our colony and to improve our raising conditions and protocols. I could start to image my first *DC* larvae on March 2021. My first results were used for an ANR grant that we obtained. In September and October 2021, two PhD students (Leonardo Demarchi and Monica Coraggioso) joined the team to pursue my work on *DC* .

3.2.2 Fish facility installation

The *DC* facility is part of the Aquatic animal facility of IBPS. In addition to *DC* , the platform is growing different aquatic animal models used for developmental biology, evolution, neuroscience and pathophysiology. The facility is raising and keeping two amphibian species, *Xenopus laevis* ($\approx$ 2 000) and *Xenopus tropicalis* ($\approx$ 700), and one fish species, *Danio rerio* also known as zebrafish ($\approx$ 24 000, one of the biggest fish facility in Paris). Since June 2019, the aquatic facility is welcoming a new fish species: *Danionella cerebrum*.

After two years of hard work on *DC* facility, almost 500 adults are part of the colony, which includes around 350 WT fish and 150 *Tg(elavl3:H2B-GCaMP6s)*. It is planned to create new transgenic lines.

Rack installation. *DC* adults are raised in the Techniplast Xenoplus Stand Alone system with 12 emplacements (fig.3.2.A). This system integrates a mechanical filter, carbon filtration, UV disinfection and a pre-filter (fig.3.2.B). Physical and chemical parameters such as water temperature, pH and conductivity as well as the water renewal rate are automatically controlled by the electronic system included. This system is designed for 16 L tank but it can be adapted for 3L tank with additional pipes for water flowing.

As this system is designed for Xenopus, it has to be adapted for *DC* which are smaller. To avoid the fish to go through the overflow water system, specific filters were designed for the bottom and the top of the overflow pipe (fig.3.2.D).

Light, temperature, air. The room light is set with a day/night cycle of 14/10 hours, with the light on between 8 am and 10 pm. The aquatic facility has an air handling unit, and each species room is equipped with a temperature control terminal. For *DC* room, the temperature is set between 26 and 28 °C. The ventilation control system ensures a renewal of 5 volumes of air per hour, which is essential for an aquatic facility to guarantee the absence of saturation of the ambient air with humidity and condensation phenomena. Moreover, to avoid temperature variation in winter, additional heaters can be used in the *DC* room.

Water parameters. Water parameters are defined according to the protocol used at Institut Curie and detailed in this book chapter [83]. The water temperature can vary from 25 to 27 °C. The pH is adjusted around 7.3. The conductivity is maintained in the range of 250-400 $\mu S/cm$. The water renewal is fixed at 10 % per day. All those parameters are controlled and adjusted automatically by the rack electronic system. Water and air temperature, water conductivity and pH are recorded everyday. Moreover, pH and ammonium (NH_4^+), nitrate (NO_3^-), nitrite (NO_2^-) are controlled manually weekly.

Sanitary status. A sanitary checkup is done regularly to ensure the absence of pathogens for the species raised in the facility.

3.2.3 Raising and feeding protocols

Raising and feeding protocols can vary from a facility to another depending on the kind of food available, the setup used and the facility general management. To define the protocols used in ours, I took inspiration from the protocols used at Institut Curie [83] and the larvae ZF feeding protocols used at the IBPS aquatic facility.

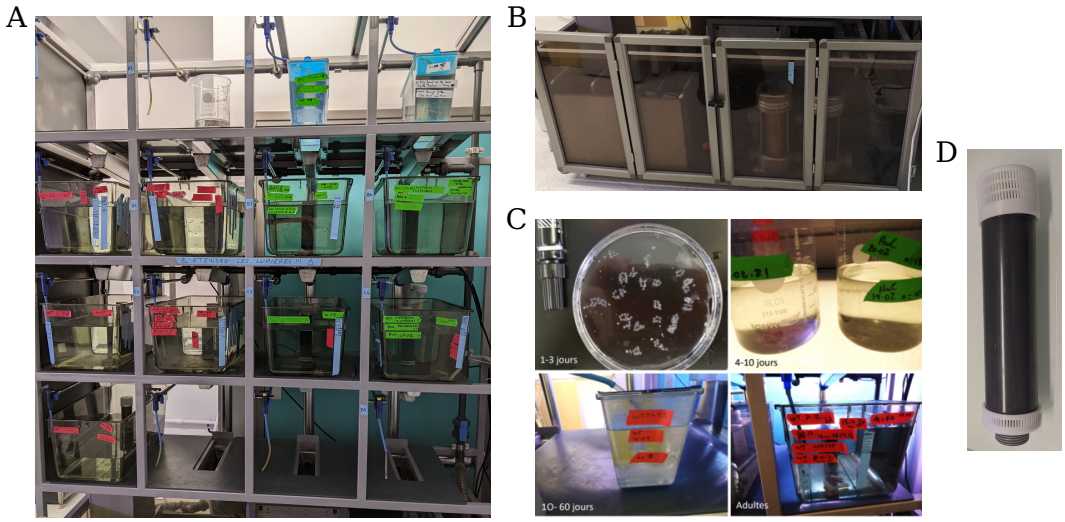

Fig. 3.2 ***DC facility.*** ***A*** *DC rack for adults (16L) and juveniles (3 L).* ***B*** *Mechanical filters included in the system.* ***C*** *The different containers used for DC . Larvae are kept on petri dish, then moved to 1 L beaker from 2 dpf to 15 dpf. Juveniles are then transferred into 3 L tank and at 1 month-old, they are moved to the final 16 L tank.* ***D*** *Top and bottom customized filters to add to the overflow water pipe.*

Raising protocol. Eggs are collected with a long Pasteur pipette (23 mL, 30 cm long) cut at its end. Five egg clutches are put in each petri dish (fig.3.2.C), which is then filled with E3 water (common medium to raise ZF embryos). Petri dish are kept in an incubator at 28 °C for two days. Everyday, dead eggs are removed and the E3 water is changed.

At 2 dpf, *DC* larvae hatch. They are transferred to 1 L beaker that contain 100 mL of E3 and 100 mL of system water (fig.3.2.C). Each beaker can accommodate a maximum of 40 embryos. Until 5 dpf, they are not fed. To compensate for water evaporation, 30 mL of system water is added to the beaker 2 times a day during weekday and 1 time a day during weekend. After 5 dpf, larvae are fed according to the dedicated protocol, with rotifers. Everyday, dead embryos are removed.

At 15 dpf, larvae are moved to 3 L tank (fig.3.2.C). The tank is filled with 1 L of system water. The larvae are carefully transferred with a cut pipette pasteur into the 3 L tank. They are numbered. The 3 L tank is then placed onto the rack and a water flow of few drops per second is maintained until 1-month-old. They are fed with the protocol for juveniles and adults. A total of 40 fishes can be put in a 3L tank.

At 1-month-old, *DC* juveniles are moved to 16 L tank (fig.3.2.C). They are numbered and the higher density is set at 80 fish and the minimal at 20 fish. Several 3 L tanks can be pooled together to create a 16 L tank. They are fed with the same protocols used for juveniles. Some transparent plastic tubes (5-10 cm long, 1 cm diameter) are added to favor the fish reproduction (3 to 5 per 16 L tank). Tanks are cleaned once every 2 months on

average. When eggs are collected, the clutch number is recorded to have a better knowledge regarding possible seasonal variation in *DC* reproduction.

Feeding protocols. I tried multiple variations without quantitative controls. Finally, I selected two protocols, one for larvae and another one for juveniles and adults. They are detailed in Annex section. Dried foods are mostly used (Gemma Micro 150 powder) as well as frozen blood worms, and rotifers (raised in the facility). The blood worms are used for food enrichment and to increase eggs production. When there are problems with the rotifer culture, artemia can be used or paramecia.

3.2.4 Transparent fish

Our first *DC* eggs came from the Institut Curie facility, from the team of Filippo Del Bene. They had three lines of *DC* : the wildtype (WT), the *Tg(elavl3:H2B-GCaMP6s)* that they developed [34] and a *Tyr-/-* which lead to more transparent fish. At some point, both transgenic lines were pulled together. When we got the transgenic eggs, we probably had a mix of those lines because we succeeded in raising three transparent females (fig.3.4.C).

Surprisingly, transparent larvae are also found in WT clutches (fig.3.4.B). With the help of an intern, different protocols were tested to raise those transparent larvae which are more fragile than the other larvae. To determine if this mutation is a spontaneous one or comes from the *Tyr-/-* lines, protocols to genotype both *DC* larvae and adults were tried, but they were not conclusive.

Transparent *DC* do not possess pigments neither on their swim bladders, non-on their body. Moreover, at larval stage, they are barely visible as pigment eyes are missing. To date, no protocol was found to raise efficiently these transparent fish.

3.3 Development of *Danionella cerebrum*

Little is known about *DC* embryonic development, juvenile and adult metamorphosis. In this section, I am presenting anatomical and behavioral observations I made during the time I spent raising *DC* fish. Those observations were made jointly with Ghislaine Morvan-Dubois. They are not quantitative neither highly precise but they offer a first glance at *DC* 's behavior.

3.3.1 Larval stage

DC spawn eggs in clutches. It is important not to separate the individual eggs otherwise they do not develop correctly. *DC* embryonic development (from an external anatomical point of view) is similar but faster than ZF embryonic development. GMD took pictures of *DC* embryos at different stages to create a developmental table similar to the one existing

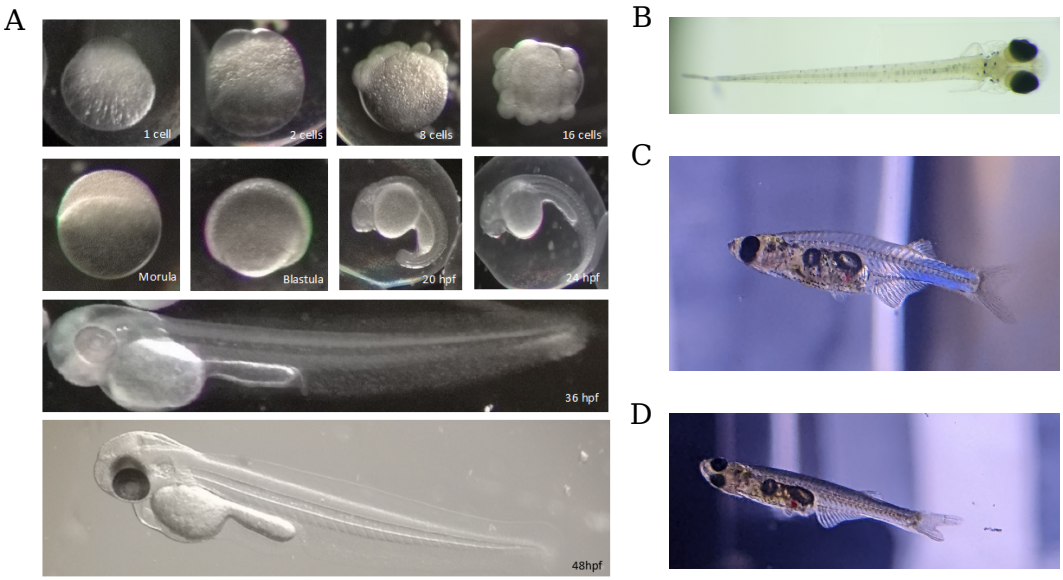

Fig. 3.3 ***DC developmental stage.*** ***A*** *Embryonic development table for DC . Created with Ghislaine Morvan-Dubois.* ***B*** *DC larva at 6 dpf (4 mm).* ***C*** *DC female adult.* ***D*** *DC male adult.*

for ZF [84]. It is possible to identify the first divisions (from 1 cell to 16 cells), the morula and blastula periods (fig.3.3.A). Around 1 dpf, embryos already display a larval shape that makes it possible to distinguish between clutch from one day (egg shape) or from the day before (moving larval shape). *DC* larvae tend to hatch around 2 dpf, which is sooner than ZF larvae (around 3 dpf) and show spontaneous coiling motions, evidences of nervous system development. Larvae are transferred into 1 L beaker at 2 dpf to provide a bigger volume for development. Sometimes, larvae at 3-4 dpf go to the water surface and group together to form *raft* (fig.3.4.D). Those rafts can count between 3 and 10 larvae. Larvae can also go to the surface without joining a raft. They begin to swim continuously at 5 dpf. At this stage, the yolk has almost disappeared (fig.3.3.B), so *DC* larvae start to actively feed. I feed them with living rotifers which are hunted by the larvae. This implies that at 5 dpf, the mouth is opened. Moreover, it seems that *DC* larvae have teeth (fig.3.4.A).

Since little is known on how to raise *DC* larvae, the surviving rate between 5 and 15 dpf is highly variable and is often below 50%. It is necessary to remove dirt and dead animals everyday to avoid any contamination and to ensure a clean environment for living larvae.

The first swim bladder of *DC* larvae, inflates between 10 and 15 dpf, a result that has been reported in Rajan et al. paper [34]. The second swim bladder inflation seems to occur between 25 and 40 dpf.

3.3.2 Juvenile period

The transition between larval and juvenile stages is considered as a first metamorphosis in teleost fish. Multiple changes occur during this period such as external, internal and hormonal modifications [85]. I only describe behavioral changes I observed in the 3 L tank (end of the larval period and beginning of the juvenile one) and in the 16L tank (before they start to lay eggs) are reported. From 15 dpf to 1-month-old (the period spent in the 3L tank), first adult traits are appearing such as fins and ray formation. Moreover, juveniles swim in a more discrete manner than larvae revealing a modification in swimming pattern (see section 4.1.4). These switch in locomotion is followed by the acquisition of shoaling and schooling behaviors that can be observed in the 16 L tank.

3.3.3 Adulthood

Reproduction. *DC* fish are laying eggs in the form of clutches whereas ZF are spawning individual eggs. Each *DC* clutch contains between 5 and 15 eggs. In our fish facility, *DC* lay eggs for the first time around 2 months and half old ($\approx$ 10 weeks). At 2 months-old, three to five silicon tubes ($\approx$ 5 cm long) are added to the 16 L tank to assist spawning, as *DC* in natural environment use crevices to lay eggs (fig.3.4.E). *DC* are communal breeders. The fish tank should count at least 20 individuals to favor reproduction and they do not feed on their eggs. Food has an impact on eggs production. I observed that I collect more clutches after the first feeding than before. A higher number of clutches are spawn after two days of extra-feeding with blood worms, suggesting that food, and food diversification are stimulating mating. A cleaned tank also favors reproduction. *DC* mating is sensitive to any environmental variations which can pause the spawning for few days up to few weeks. One important example was the first lockdown. *DC* were fed two to three times per day at Institut Curie, which fell to one time a day from March to mid-June 2019, and the *DC* transgenic line started to lay again in September 2019.

Although *DC* and ZF are raised at constant temperature and light cycle, year seasons influence the eggs quantity laid for ZF. To determine if seasons can modulate the *DC* clutch production, the clutch number for each tank is annotated at each collection. With only one year of data, it is not yet possible to establish any correlation between spawning and season for *DC* , even if a peak is visible during spring. More years will be necessary to establish seasonal rhythm in spawning.

Sometimes, females are restraining their spawning which leads to eggs decomposition in their abdomen (fig.3.4.F). This egg retention is also observed on ZF when females are too old or do no lay eggs often.

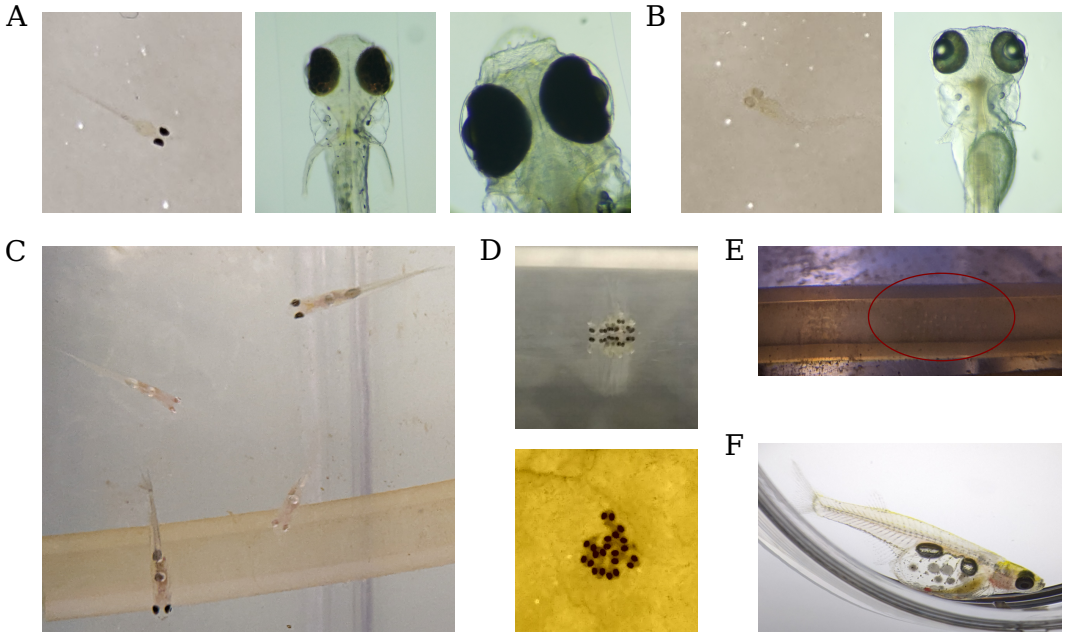

Fig. 3.4 ***Transparent DC and behaviors.*** ***A*** *Pigmented DC larva. Left panel: in petri dish (3 dpf). Middle panel: head top view (5 dpf). Right panel: larva teeth (5 dpf).* ***B*** *Transparent DC larva. Left panel: in petri dish (3 dpf). Right panel: head top view (5 dpf). Development of non pigmented DC larvae is slower (mouth not opened yet).* ***C*** *DC adults with and without pigments.* ***D*** *Raft formed spontaneously by some larvae around 3-4 dpf. Top panel: side view. Bottom panel: top view.* ***E*** *Egg clutch laid in a silicon tube.* ***F*** *DC female adult which has eggs retained in her abdomen.*

Life span. *DC* have now been raised for two years in our fish facility. I noticed a decrease in fecundity around 1 year and half which also corresponded to a reduction in the group around 15 fish. For now, little is known on how long *DC* can be kept in captivity. At Institut Curie, there were fish aged of 2 years and half. In our facility, fish of almost 2 years are still living.

Behaviors. *DC* are social fish that live in community. They are shoaling and also schooling [30]. The main remarkable behavior of *DC* is their ability to vocalize. Indeed, they produce sounds that resemble cicada. Only males are able to make sounds mostly during male-male aggression [30, 78], that I observed and heard. They do not vocalize every day at specific hours. It is possible to hear them even over the pump and other electronic noises when they all sing. A collective drive might occur when one tank starts to produce noise, as it seems that the other males are triggered.

Robustness. Some problems occurred in the facility which allowed to test *DC* robustness to pH and conductivity. One heater broke which lead to a pH increase from 7.2 up to 8.2 for few hours. All the fish survived but they did not lay eggs for almost 10 days. An increase in conductivity from 300 $\mu S/cm$ to 1200 $\mu S/cm$ happened over a weekend. No fish died but the egg production was null for a week. *DC* adults fish are robust to pH and conductivity variations, as well as temperature, which has fluctuated between 23 and 28 °C in our facility.

3.3.4 MonitoRack

The creation of the *DC* fish facility was the opportunity to create a new behavioral setup. Under Raphaël Candelier's leading, MonitoRack was build, installed and used directly in the fishroom. The setup was designed to be used on the *DC* rack to record the behavior of several clutches growing in a tank for a few minutes every hour, every day for 3 months. The main advantage of this setup is to follow the maturation of the swimming patterns directly in the fish facility, where fish have a behavior unperturbed by preparation, protocol and handling biases.

This unique experiment allows following the evolution of the individual and collective dynamics of *DC* through development but also to explore their circadian rhythm and the behavioral difference between day and night.

MonitoRack setup and protocol. MonitoRack consists of a large field-of-view camera attached above the fish tank. The camera was installed on a frame resting on the upper raw of the rack, allowing a large working distance and a wide field of view. IR lights were installed to dissociate imaging from day/night cycle and the camera was adapted with an IR filter (fig.3.5.A). Recording was controlled by a computer with a custom-written program (fig. 3.5.B). The optic was adapted to the tank used for the fish (see section 3.2.3): from 5 dpf to 15 dpf, *DC* larvae were kept in 1 L beaker, then from 20 dpf to 2 months, juvenile and young adults were in a 3 L tank (fig. 3.5.E) and finally, adults were raised in a 16 L aquarium. To increase the contrast, all containers were customized with black plastic sheets glued on the bottom. When the fish were transferred into the 16 L tank, some tubes were added to favor the reproduction behavior and a hydrophone (fig.3.5.C) was added to record the sound emitted by the *DC* males. The hydrophone was triggered simultaneously with the camera. All movies were recorded at 25 fps. The feeding times were indicated in a notebook. The recordings took place from 5 dpf to 3 months (91 dpf) and consisted of 200 seconds movies every hour. The experiment started with 35 larvae. At 15 dpf, I changed the fish container for a 3L tank and counted 22 juveniles. At 1 month-old (31 dpf), I put juveniles fish in the 16L tank. There were only 10 fish left that all grown up to 3 months-old.

Due to technical issues, a few movies were lost. There are nevertheless around 2 000 movies, which represents 3.5 To of data to process and analyze.

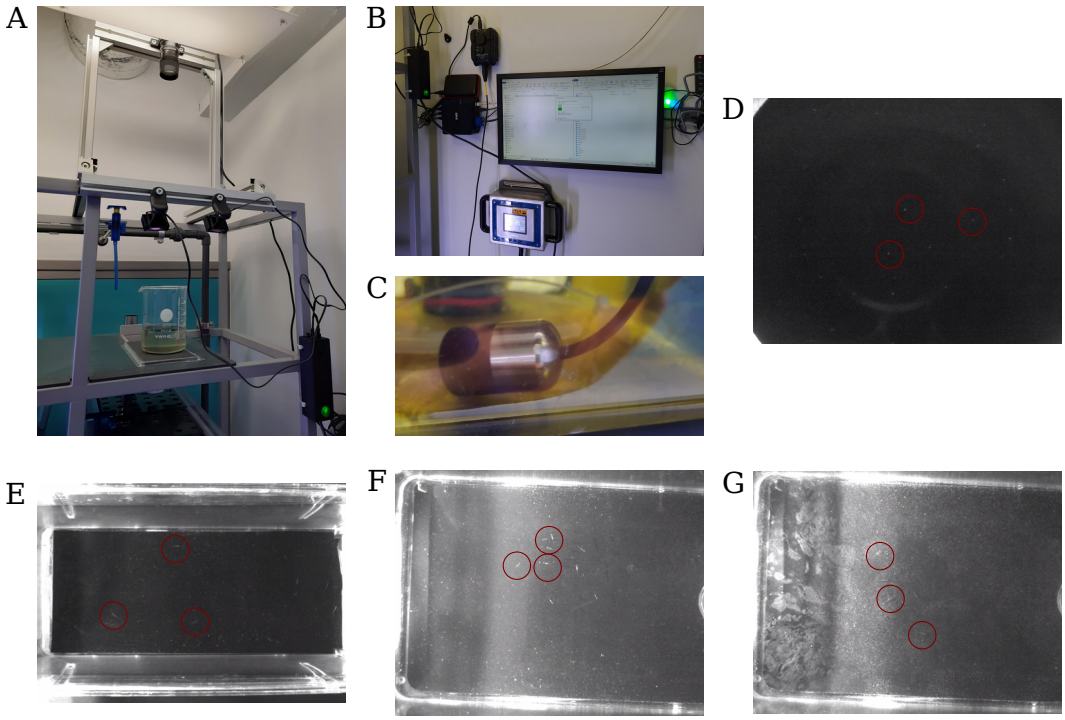

Fig. 3.5 ***MonitoRack setup.*** ***A*** *Photography of MonitoRack in the DC facility, with the camera, IR light and a beaker for larvae.* ***B*** *Computer controlling MonitoRack.* ***C*** *Hydrophone.* ***D*** *Frame showing larvae DC (7 dpf) in a 1 L beaker. Red circles indicate the position of some fish.* ***E*** *Frame showing juveniles DC (31 dpf) in a 3 L tank.* ***F*** *Frame showing young adults DC (54 dpf) in a 16 L tank.* ***G*** *Frame showing difficult conditions to track fish.*

MonitoRack analysis. The recordings performed with MonitoRack form a huge database for studying different behavioral aspects. Movies have to be pre-processed first in order to extract relevant features such as positions and orientations of the fishes on the movies and frequencies and patterns for auditory data.

Raphaël Candelier had started to work on the image processing workflow which consists of object detection, then object tracking. The first part, detection, is full of difficulties: indeed, at the larvae stage, the objects are very small (few pixels, fig.3.5.D) and are hardly detected. Another pitfall of MonitoRack is that it operates in real conditions, meaning that the recording conditions are not optimal for a good detection. Indeed, the fish are fed with powder and rotifers that can create shadow patches and oily surfaces, making the detection harder. Bubbles, dust and waves are other elements that can alter the detection process (see movie *Bad_Conditions.mp4* [1], fig.3.5.G)). For all these reasons, each movie is different and the overall detection process requires a long working phase.

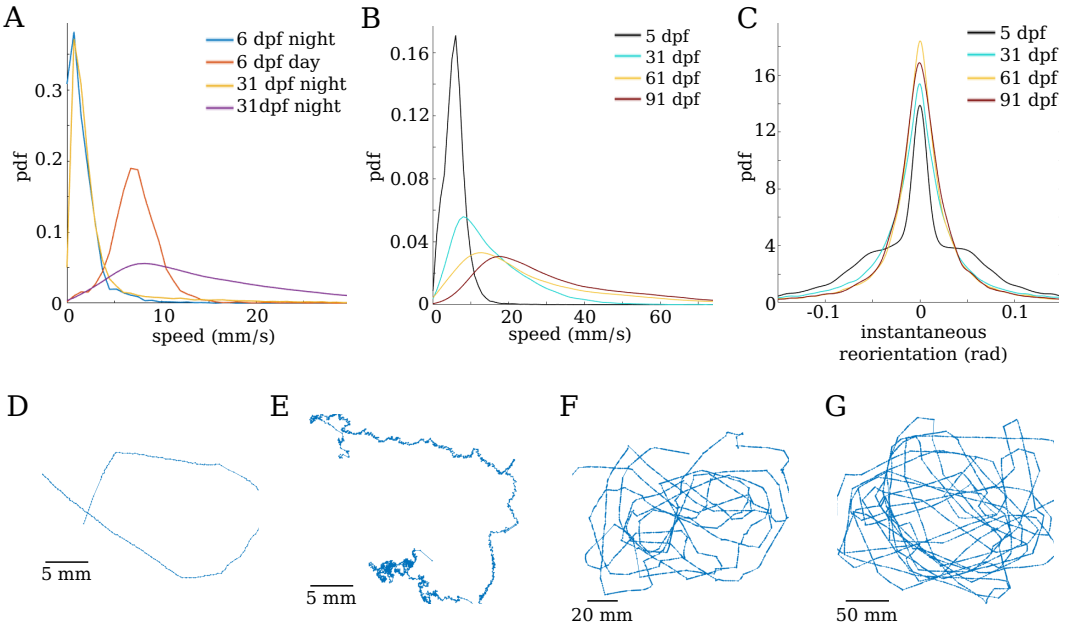

Fig. 3.6 ***MonitoRack first analysis.*** ***A*** *Speed pdf comparison between day and night for 6 and 31 dpf DC fish.* ***B*** *Speed pdf comparison between 5, 31, 61 and 91 dpf DC fish (daylight conditions).* ***C*** *Instantaneous reorientation pdf for 5, 31, 61 and 91 dpf DC fish.* ***D*** *Trajectory example of DC at 6 dpf (larva).* ***E*** *Trajectory example of DC at 31 dpf (juvenile).* ***F*** *Trajectory example of DC at 61 dpf (young adult).* ***G*** *Trajectory example of DC at 91 dpf (adult).*

First qualitative results. Even if all movies are not yet tracked, it is possible to report some qualitative results by simple observation and simple graphics.

With Raphaël Candelier, we observed movies at 7 dpf (1 L beaker, larvae, *2021-10-07 12h.mp4* [1]), 31 dpf (3 L tank, juveniles, *2021-11-01 12h.mp4* [1]) and 54 dpf (16 L tank, juvenile to adult transition, young adult, *2020-11-23 13h.mp4* [1]) acquired at 12 pm or 1 pm, between two feedings (usually around 9 am and 3 pm). Some fish movies were also analyzed to extract trajectories at 5, 6, 31, 61, 91 dpf. We noticed that swimming patterns between larvae (5-7 dpf) and juveniles/adults (31, 54, 61 and 91 dpf) evolved. While the locomotion of *DC* larvae can be considered continuous and smooth (see section 4.1.2, fig.3.6.D), *DC* juveniles and young adults have a more intermittent swimming pattern, with motion that resembles the burst and glide pattern found in almost all fish species (fig.3.6.F, G). Velocity distribution also changed over development with an increase in velocity and a higher variance (fig.3.6.B, annex.B.1). A switch in locomotor pattern is also known in ZF, but in this case, the burst and glide motion of larvae evolves into a more continuous swimming [86].

Moreover, it is clearly visible that at 54 dpf, *DC* young adults had developed a collective behavior of shoaling and schooling (fig.3.5.F). It seems that this behavior is not yet developed

for *DC* juveniles (31 dpf) but it is not possible to conclude on collective behavior acquisition. It is not present at larval stage (7 dpf). In ZF, collective behavior appears around 3 weeks-old [14], and does not feature body alignment.

We also examined movies acquired at 10 dpf (larvae), 30 dpf (juveniles) and 58 dpf (young adults) during daylight (10 am) and during nighttime (12 am) (*day_night.mp4* [1]). A difference in activity is visible between day and night for juvenile and young adults fish but less noticeable for larvae. However, by looking at the speed pdf at 6 and 31 dpf during day and night (fig.3.6.A), it is clear that light conditions and time have a strong influence on swimming pattern, leading to think that *DC* acquire at larval stage a circadian rhythm. To compare with ZF, circadian changes in locomotor activity are found at 5 dpf [87].

3.4 Discussion and perspective

***DC* facility.** After two years of the fish facility establishment dedicated to *Danionella cerebrum*, the global result is quite positive. The fish colony is stable, with healthy adults that are renewed every six to eight months, without major difficulties. Fishes are reproducing, which is a sign of good health. Moreover, fish facility member are now taking care of a certain number of technical tasks such as feeding, checking mechanical filters, changing them and controlling environmental parameters. PhD students and researcher working with *DC* still deal with eggs collection, fish transfers (to new containers, or pulling tank) and tank cleaning.

We succeeded to develop this fish facility in only two years, without major issues. We faced and handled some problems, such as a broken heater which made the pH increased a lot, water pressure difficulty, broken conductivity and temperature probes and inexplicable salinity increase. Overall, the fish facility creation went well. We obtained our fish from Filippo Del Bene who was installed at Institut Curie. His team moved to Institut de la Vision, where, with the help of Karine Duroure, they developed a new fish facility which will welcome both ZF and *DC* . This is the opportunity to have a backup of the *DC* lines.

The creation of the *DC* facility was a lot of responsibility and confidence from my supervisors. I defined some specific protocol for fish feeding and growing, that are working but might not be optimal. Establishing good protocols to raise fish on ideal conditions, would require more time and specific knowledge in fish husbandry.

Nevertheless, some drawbacks have to be mentioned. For further studies, it will be necessary to increase the number of *DC* transgenic lines available. To favor this project, a better control and knowledge on eggs production is suitable. Over the last couples of years, we observed huge eggs quantity fluctuation over weeks and months, without finding a good explanation. We noticed that after environmental parameter deviations, *DC* were spawning less, but decrease in clutch number also occurred randomly. Moreover, transgenesis has to

[1] https://drive.google.com/drive/folders/1hARZHqd5BPS165vCHm2xbigBzoakyst6?usp=sharing

be done during the first cell stage, which last for 45 min after the egg fertilization [84]. As *DC* are communal breeder, female lay eggs continuously and parameters triggering precisely the spawning are still unknown. We tend to collect more clutches after the first feeding, suggesting that *DC* lay more during the morning after eating, but this is not enough to ensure a good control of the fertilization time. Thus, creating new *DC* lines will need a constant vigilance of spawning.

Another point worth discussing is the consanguinity problem, or the genetic admixture problem. Indeed, our fish came from FDB team, which obtained them from Benjamin Judkewitz team (Berlin, Germany), which is using *DC* from the ichthyologist Ralf Britz (Dresden, Germany) who collected them in the field in Myanmar. Thus, our fish had been incrossed for many generations, without renewing their genetic background. For now, we do not observe any phenotypic modification and fertility decline. We can keep incrossing them, but at some point, renewing the genetic background of our colony could become necessary.

MonitoRack experiment. MonitoRack offers the possibility to record fish and their behaviors directly in the fish facility with no experimental condition constraints. Indeed, behavioral experiments developed in laboratory requires to remove fish from their regular environment to place them on setup with different characteristics. Even if fish are habituated for some time, their normal behaviors are more visible in the fish facility. MonitoRack provides an insight on the fish "intimacy" and allows characterizing swimming features (speed, distance, pattern), appearance of social behavior, sexual maturation and other yet undescribed behaviors, as they develop in time.

What is a great advantage to observe fish in non-perturbed environment, is also one disadvantage for recording quality. Indeed, fish swimming in their usual tank are not perturbed by any experimental conditions, but image recording is sensitive to fish facility environment such as dust particles, food which leaves oily sheets at water surface, technical maintenance and other activities needed for the fish well-being. Thus, fish tracking necessitates a lot of complex image processing steps that have to be adapted for each frame, recordings. Moreover, MonitoRack produces a lot of data, which has to be analyzed, and is thus a time-consuming process. However, it is important to keep in mind that this setup is giving access to simple fish features that should be achieved with deeper analysis on specific conditions (especially if we are interested on behavior modulation, fine dynamics and kinematics).

If we assume that data analysis process is working well, we can then think about more experiments to perform with MonitoRack. First, it will be interested to do the same experiment, following *DC* growing from 3 dpf up to 3 months and sexual maturity, with more fish at the beginning in the objective to raise at least 20 adults to detect the first spawning. Number is also crucial for male vocalization as it is linked to male-male-aggressive behavior when they are at least 5 [30]. Repeating these experiment will increase the statistical signifi-

cance to better determine temporal window of swimming pattern switch, collective behavior appearance, sexual maturity and others. As it is a long term experiment, one possibility should be to install more MonitoRack in order to parallelize the data acquisition. Other possibilities are to do the same with other fish species, especially with ZF to improve our comparative study, to add perturbation such as mirror, illumination changes, introduction of congeners from another tank, or fish from another species... In the future, those experiments would be possible when the analysis pipeline will be optimized.

So MonitoRack is a useful opportunity to observe fish in their ordinary conditions, which can give access to more temporal evolution insight. It is generating a lot of data, that are partially exploitable due to fish facility feature incompatibilities with fine recording, that require complex pre-processing step in order to extract quantitative results. Nevertheless, it can be used as a behavioral observation tool to select the most interesting ones for future research.

Conclusion. *DC* fish facility allows now PhD students and researchers to work with this species. Based on MonitoRack observations and collaboration, I started to explore the spontaneous navigation pattern of *DC* larvae in order to compare its swimming program with the one of ZF larvae for an evolutionary comparison [34], but also with older *DC* locomotion, for following maturation of this behavior from an observation and model point of view, and from a neuronal circuit organization.

In the following chapters, I am presenting first locomotion strategy models used by *DC* and ZF larvae. This behavior comparison will be completed with the study of the light-seeking behavior (chapter 4). In chapter 5, I move to the neuronal scale. I am showing the interesting neuronal population involved in swimming and the benefits of using *DC* larvae. This chapter will also complete the comparative study between *DC* and ZF at a neuronal level.

Chapter 4

Spontaneous locomotion and phototaxis of fish larvae

Danionella cerebrum is an emerging model for neuroscience studies due to its small size and optical transparency from larva to adult stage. It also displays a rich behavioral repertoire which offer direct readout from the underlying neuronal circuits. Moreover, the phylogeny proximity, the similar living environment and morphological similarities at larval period of *DC* and ZF may facilitate a comparative study between those two species, providing a better understand of evolutionary divergence at behavioral and neuronal scales. In this chapter, I detail the difference between the spontaneous locomotion and exploration between *DC* and ZF larvae, as well as their light preference.

In a first section, I summarize what is known on ZF larval spontaneous locomotion and I emphasize a simple descriptive model of ZF trajectories developed in the laboratory (4.1.1). Then, I propose a short overview of what has been characterized in the *DC* larval navigation, mostly from a collaborative study (4.1.2). To complete, I explain how I analyzed *DC* trajectories with the objective of defining a simple model of *DC* swimming pattern (4.1.2). I describe first observations I made on *DC* exploratory behavior at different developmental stage, to insist on the *DC* advantage to perform behavioral ontogeny research (4.1.4).

In a second time, I present how visual stimulation interferes with the ZF model, in order to provide a better understanding of the sensorimotor program of ZF, mostly with light-seeking behavior (4.2.1). This study will be applied to *DC* larvae to complete the evolutionary comparative study (4.2.2).

Personal contribution In this chapter, I introduce results that are from two published collaborations. For ZF spontaneous swimming and phototaxis, I worked in collaboration with Sophia Karpenko [35]. For this work, I developed and performed all the behavioral experiments for spontaneous, tropotaxis and klinotaxis behaviors. We discussed together on

the results of those experiments. She developed the two Markov-chain model. For studying *DC* phototaxis, I adapted the experimental protocols on tropotaxis and klinotaxis that I developed.

The second collaboration was for the comparative study on *DC* and ZF larvae done with Gokul Rajan [34]. On the behavioral part, my PhD supervisor Georges Debrégeas wrote the analysis codes for the long-term exploration analysis, that we discussed together. I detail in chapter 5 what I did for the calcium imaging data.

Unless explicitly stated, all the data I used in this chapter to establish the *DC* spontaneous swimming model, the swimming maturation process in *DC* and phototactic behavior, are data that I collected with different experimental setups and protocols than the one from [34].

I performed the analysis on the Poisson process. Trajectory smoothing, turn detection with the naive approach and linear regression were done in discussion with Monica Coraggioso, a PhD student who joined our laboratory in October 2021, on data that I collected and which are different from the data used in [34] for long-term exploration analysis.

4.1 Spontaneous locomotion

Behaviors are the visible outcome of neuronal circuit processing environmental information and inner states. They can be used as proxy to determine impacts of neuronal circuit perturbations such as neuronal ablation (swimming speed of ZF larvae in response to moving pattern was reduced when nucleus of the medial longitudinal fasciculus (nMLF) cells were ablated [62]) or neuronal activation (optogenetic activation of some V2a neurons on medulla leads to locomotor stops [88]) to only cite those two examples. Behavior description and model are important to precisely understand the effect of underlying motor neuronal system, but also to better identify neuronal population implication on processing information. Therefore, I am first describing what is known on ZF larval spontaneous locomotion before comparing it to what we reported with our collaborators on *DC* larval swimming. To go further, I am trying to propose a model depicting *DC* swimming pattern at 6 dpf. This model will benefit both locomotor neuronal circuit identification and swimming maturation through *DC* development.

4.1.1 Spontaneous locomotion of ZF larvae

ZF larvae at a few days post-fertilization (dpf) already display a rich behavioral repertoire (2.1.1, [16, 17]). At 5 dpf, they are able to swim, to hunt, and also to orient themselves according to environmental information such as light [89, 35], temperature [43, 5] and water-flow [90, 45]. All those behaviors require locomotion ability from the larval fish.

ZF larvae are swimming in "burst and glide" motions that are called bouts. They consist of short burst of tail beating alternating with passive periods named interbout intervals. Tail

active periods last ≈ 200 ms and happen every 0.5 to 1 second. Bouts can be identified as discrete locomotion units and categorized into specific types [17].

This classification into two kinds of movement, allows one building models which represent exploratory strategies used by larval ZF. A simple model was proposed by Karpenko et al. [35] in a collaborative study. We used a two Markov-chains model to describe ZF larval spontaneous locomotion. Only one input was defined for this model which is the fish reorientation between two consecutive bouts, leading to two bout categories: forward bout (reorientation angle < 0.22 rad $\approx 12°$) and turning bout (reorientation angle $> 12°$). The first Markov-chain controls the ZF larva choice between performing either a forward bout, or a turning event. The second Markov-chain defines the left and right orientation of turn bout and accounts for the directional persistence of successive bouts (fig.4.1).

ZF bouts can be categorized into more than two types. In 2018, Marques et al. employed an unsupervised clustering method to identify 13 basic patterns within the locomotor repertoire of ZF larvae [40]. They showed that those basic motor units can be associated into various combination to depict more complex behaviors such as hunting. Johnson et al. identified more bout types during hunting process [91]. Those new types allowed them to define new models that are able to predict and to generate fish trajectories in complex environments.

Simple and more complex description algorithms are determined and then used to address different questions. While complete and detailed characterization of swimming patterns provide a more realistic description of the diversity of motor patterns used by fish larvae, simpler models attempt to group those refined motor pattern into global movements that are sufficient for catching the main navigational strategy. In our laboratory, we decided to use this last approach for *DC* .

4.1.2 Spontaneous locomotion of *DC* larvae

All the results described in this section are from the collaborative work that results on a publication [34].

At 5 dpf, *DC* and ZF larvae body length are in the same size range, between 4.1 - 4.9 mm (fig.4.2.A). Hydrodynamic forces exerted on larvae are expected to control the locomotion and to depend on body length, swimming speed but also environmental features [92]. As those characteristic are similar for *DC* and ZF larvae, one may have expected to find burst and glide pattern on *DC* larval swimming behavior. Surprisingly, *DC* larvae swim in a continuous manner with continuous tail beating period that can last for several minutes (fig.4.2.B). In a more careful examination of the swimming kinematics with half-tail beat analysis, we showed that *DC* larvae move at a slower speed than ZF larvae, with a lower tail beating frequency. Acoustic stimulation triggers for both species a C-bend escape response but still with a smaller

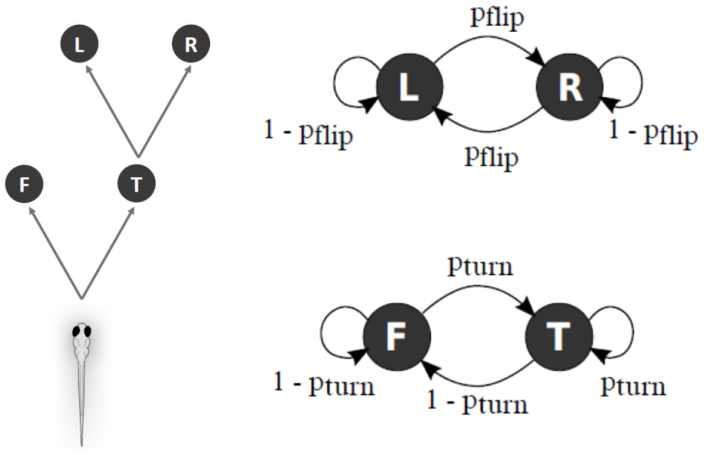

Fig. 4.1 ***Spontaneous locomotion of ZF larvae model.*** *2 Markov-chain model describing ZF swimming pattern. F: forward, T: turn. Adapted from [35].*

maximum speed and distance for *DC* . Nevertheless, the continuous swimming pattern of *DC* larvae is sustained in head-embedded larvae which is encouraging for using tail movement as a proxy for behavior in imaging studies.

Long-term exploration. We decided to explore how those two distinct swimming patterns impact the long-term exploration strategy of each species. For this, we computed the mean square displacement (MSD) which provides an observation of the relative area explored by a motile object. Despite their different short timescale behaviors, *DC* and ZF larvae long-term exploration kinematics are similar (fig.4.2.C). To understand this result, we identified the MSD ballistic contribution for each species as :

$$MSD_{bal}(t) =< [\int_{t_0}^{t_0+t} v * R(t'-t_0).dt']^2 > t_0$$

where v is the mean instantaneous velocity, and R the heading orientation correlation function.

For a purely ballistic process, R = 1 so $MSD_{bal} = (vt)^2$. By adding this MSD ballistic contribution to the graphic, it is showing that *DC* larvae have an initial ballistic component that last for 7 s, whereas the MSD of ZF is diverging from its ballistic model around 1 s, so after one or two bouts. Thus, even if *DC* are slower than ZF, they are less dispersive at the beginning.

To confirm this result, we looked more in details at the heading orientation correlation R(t), which enables to visualize the orientation persistency over a given period, for which R = 1 means a perfect maintenance of the orientation, whereas R = 0 represents a total randomization of those. R is dropping rapidly for ZF, in $\approx$ 1 s, which supports the rapid loss

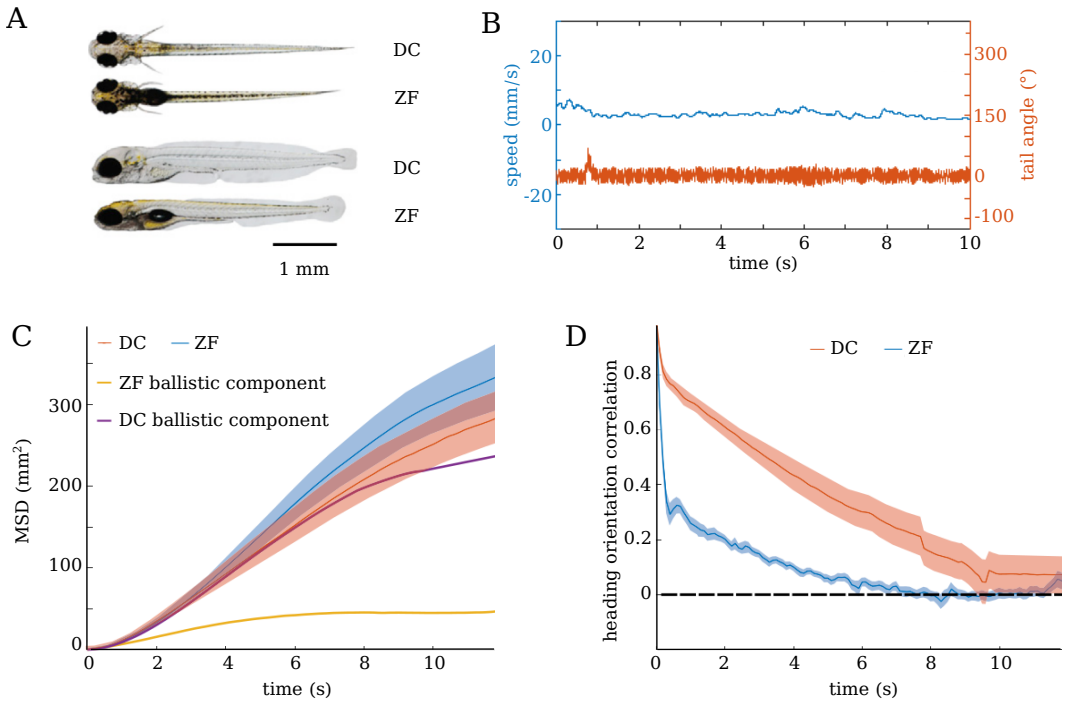

Fig. 4.2 ***Spontaneous locomotion of DC larvae.*** ***A*** *Top and side view of DC and ZF larvae (5 dpf).* ***B*** *Speed and tail angle at 5 dpf.* ***C*** *Mean square displacement for DC and ZF larvae trajectories.* ***D*** *Heading reorientation correlation. All figures are adapted from [34].*

of the ballistic contribution. For *DC* , the heading orientation correlation is slowly decreasing which is in accord with a longer ballistic contribution. This orientation persistency can be explained by the long straight swimming periods that separate reorientation events, which is a process well described for motile bacteria, called the run-and-tumble process [93]. By looking at *DC* trajectories (fig.4.2.D), it is possible to distinguish straight periods and turning events (fig.4.3.A).

With the objective of building a simple model describing spontaneous locomotion of *DC* larvae, I took inspiration from the run-and-tumble process described in bacteria to attempt defining two states on *DC* trajectories: straight period and turning events. I based my analysis on this two-state model, with the idea to model it with a two Markov-chains model similar to the one proposed by Karpenko et al. [35].

4.1.3 Determining *DC* larva spontaneous swimming model

4.1.3.1 Method

Experimental setup. To study the spontaneous exploratory behavior of *DC* larvae, I used 5 to 7 dpf WT *DC* . All the experiments were performed between 10 am and 8 pm.

Larvae were fed with rotifers 1 hour before the beginning of the experiments and at the end of the day. The experimental setup was installed in a light-tight box. The temperature inside was maintained between 26 and 28 °C using "The Cube" (Life Imaging Service). The arena consisted of a crystallizer of 14 cm diameter containing 1.5 cm in depth water (≈ 250 mL) from the *DC* facility. It was placed on a screen illuminated from below by a projector (ViewSonic M1). A camera (FLIR Chameleon3 CM3-U3-13Y3M-CS) with an adjustable macro lens (Navitar, Zoom 700) equipped with an IR filter recorded the fish behavior from above the tank, which was also illuminated by an IR LED panel (fig.4.3.A). Only one fish was used per experiment. The fish was adapted for 30 min then recorded for 30 min. The camera trigger was controlled with a custom-written software in Matlab (The MathWorks). The projector displayed a uniform white background at high intensity using the PsychToolBox (PTB) version 3.0.14 add-on. The behavior was recorded with the FlyCapture software, using the trigger mode 15, with parameter set at 0, trigger high, with a camera shutter time set at 14 ms (≈ 71 fps). The frames were recorded as AVI movie with a jpeg compression at 75 % (≈ 128 000 frames).

I also used this setup to record spontaneous behavior of few 1 month-old *DC* .

Tracking. It was not possible to use FastTrack for those experiments (see 2.2.2). Between 5 and 10 dpf, only *DC* eyes are visible and trackable but their size and gray color make them visually similar to certain dust particles and detection mistakes were thus too numerous.

The tracking was performed offline using a custom-written program in Matlab wrote by Raphaël Candelier. First, a background image is created by taking for each pixel the median value over 100 images randomly selected over the movie. Each frame is then processed following those steps: the background is subtracted, then the frames are filtered to remove noise (two filters are applied: a median filter with a 5*5 pixel size, then a Gaussian filter with 1 pixel standard deviation size), and finally, they are binarized with a threshold defined as 1/5 of the filtered image maximum intensity. This allows one to determine an approximate position of the objects. To refine fish eyes positions, a parabolic fit of the intensity peak near the detected objects is used to obtain sub-pixel coordinates. Finally, an algorithm based on the Kuhn-Munkres algorithm enables relating objects from frame to frame and to define trajectories.

After fish coordinates determination, only data within an 8 cm diameter area (ROI) centered on the arena center, were kept in order to avoid border effects (thigmotaxis behavior, which corresponds to a fish swimming along the arena border, and visual reflections or bias created by glass edges). For any given fish, multiple trajectories lying within the ROI with different duration, were defined (fig.4.3.A). All trajectories from every fish were analyzed together.

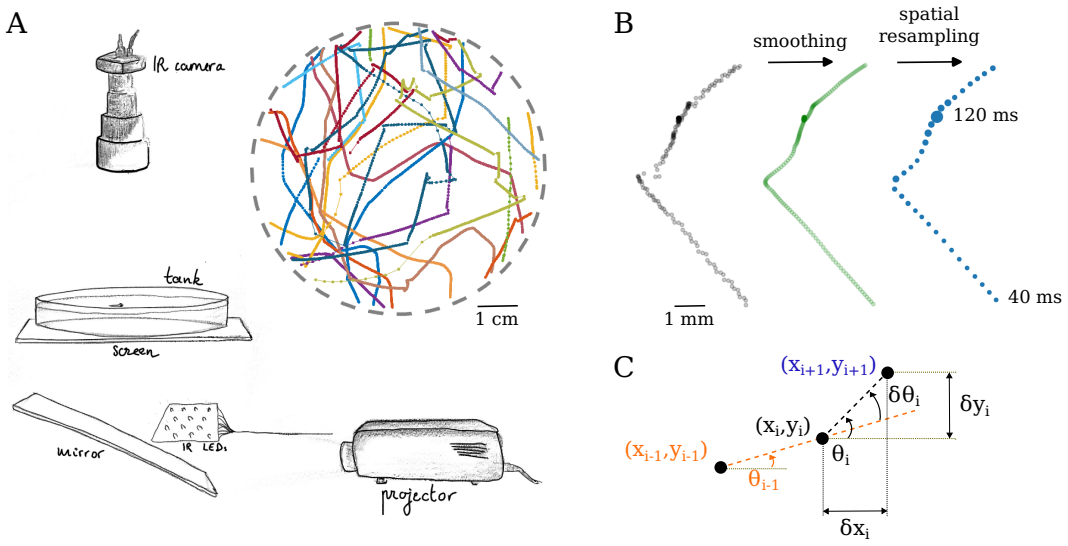

Fig. 4.3 ***Experimental setup and trajectory smoothing for DC larvae swimming.*** ***A*** *Experimental setup and DC larvae trajectories. Setup drawing by Sophia Karpenko [19].* ***B*** *Left trajectory (black): raw data, head oscillations are visible. Middle trajectory (green): raw data smoothed with the Savitzky-Golay filter. Right trajectory (blue): spatially resampled positions. Dot size is proportional to the time between two resampled positions.* ***C*** *Schema defining kinematic parameters for resampled positions:* $\delta x_i, \delta y_i, \theta_i, \delta\theta_i$

4.1.3.2 Trajectory smoothing

The recorded trajectories show rapid oscillation movements which reflect the larva head alternating motion that accompany the continuous tail beating (fig.4.3.B black). To eliminate these modulations, we decided to smooth the trajectories and to decrease the sampling rate. We applied a Savitzky-Golay filter which minimizes the least-squares error by fitting a second order polynomial with 25 points of the raw data (fig.4.3.B green). Even if most of the time *DC* larvae are swimming in a continuous manner, they also halt. Those stops create noisy positions where they happen, that hamper a correct angle determination (based on consecutive positions). To address this problem, we resampled the smoothed position with a constant space step *dl* that we fixed at 0.3 mm. It was not possible to use a time constant step in this case because of the halt duration variability, and to avoid an excessive smoothing that might alter trajectory shape. We kept track of the number of frame between each new position df_n. By keeping positions that were at least at *dl* distance from the previous data point, we managed to remove noise from non swimming period and to keep enough information on each trajectory (fig.4.3.B blue).

We used resampled positions to extract orientation sequence $\theta_i = \arctan(\delta x_i, \delta y_i)$ with $\delta x_i = x_{i+1} - x_i$ and $\delta y_i = y_{i+1} - y_i$ for each trajectory. Since we were interested in orientational

dynamics to identify straight periods and turning events, we also calculated the angular reorientation vector as $\delta\theta_i = \theta_i - \theta_{i-1}$ (fig.4.3.C). We also computed the mean speed between each resampled position $v_i = \sqrt{dx_i^2 + dy_i^2}/df_i$.

4.1.3.3 Identification of a Poisson process

Before starting to identify short dynamic involved in the long-term exploration process, I tested the hypothesis to compare *DC* exploration to the run-and-tumble process described from bacteria [93]. This process has a Poisson statistics, meaning that the probability to initiate a turn event in a fixed interval of time is constant and independent of the time delay since the last event.

To highlight this statistic, I computed the probability to have straight periods of a certain duration in function of time (fig.4.4.A). For this, I determined the turn events by using the angular acceleration in the resample coordinates. I defined a turn as a period of 0.4 seconds centered on an angular acceleration peak. I did not take into consideration events shorter than 1 second (not well-defined with this definition) and longer than 30 seconds (too rare).

I obtained a probability that is exponentially decreasing (fig.4.4.A, red curve: exponential fitting), which is characteristic of a Poisson process. Thus, it is reasonable to base the analysis and model of *DC* trajectories on the run-and-tumble process, and to find a proper way to determine two steps: straight periods and turn events.

4.1.3.4 Turning event detection: naive approach

We first decided to apply the same analysis as in Karpenko et al. [35] by examining the probability density function (pdf) of $\delta\theta$ (fig.4.4.B). As expected in *DC* , the reorientational distribution does not show the characteristic bimodal shape that was observed for ZF larvae. This is due to the relative sparsity of turning events in *DC* continuous swimming behavior, which is mainly composed of straight periods. This is visible on the pdf($\delta\theta$) which is highly concentrated around small angular values. It is thus difficult to define an angular threshold value to identify turns.

By watching *DC* larvae swimming, we noticed that their speed is not constant all along their trajectories (fig.4.4.C). By plotting on a same graphic the reorientation $\delta\theta$ and the speed v, we observed that some turns are followed by acceleration (fig.4.4.D). This is especially true for turns with a high reorientation value. Therefore, we decided to define turn event as a point for which a peak in $\delta\theta$ is followed by an increase in speed. Adding a parameter reduces errors in turn detection, but it requires defining two thresholds. It was possible to choose a common reorientation threshold for all trajectories, that we set at $\delta\theta_{th} = 20°$ (after different trial and error cycles), however, the speed threshold v_{th} must be determined for each trajectory, due to the individual variability in mean speed and random escape behaviors. To limit escape

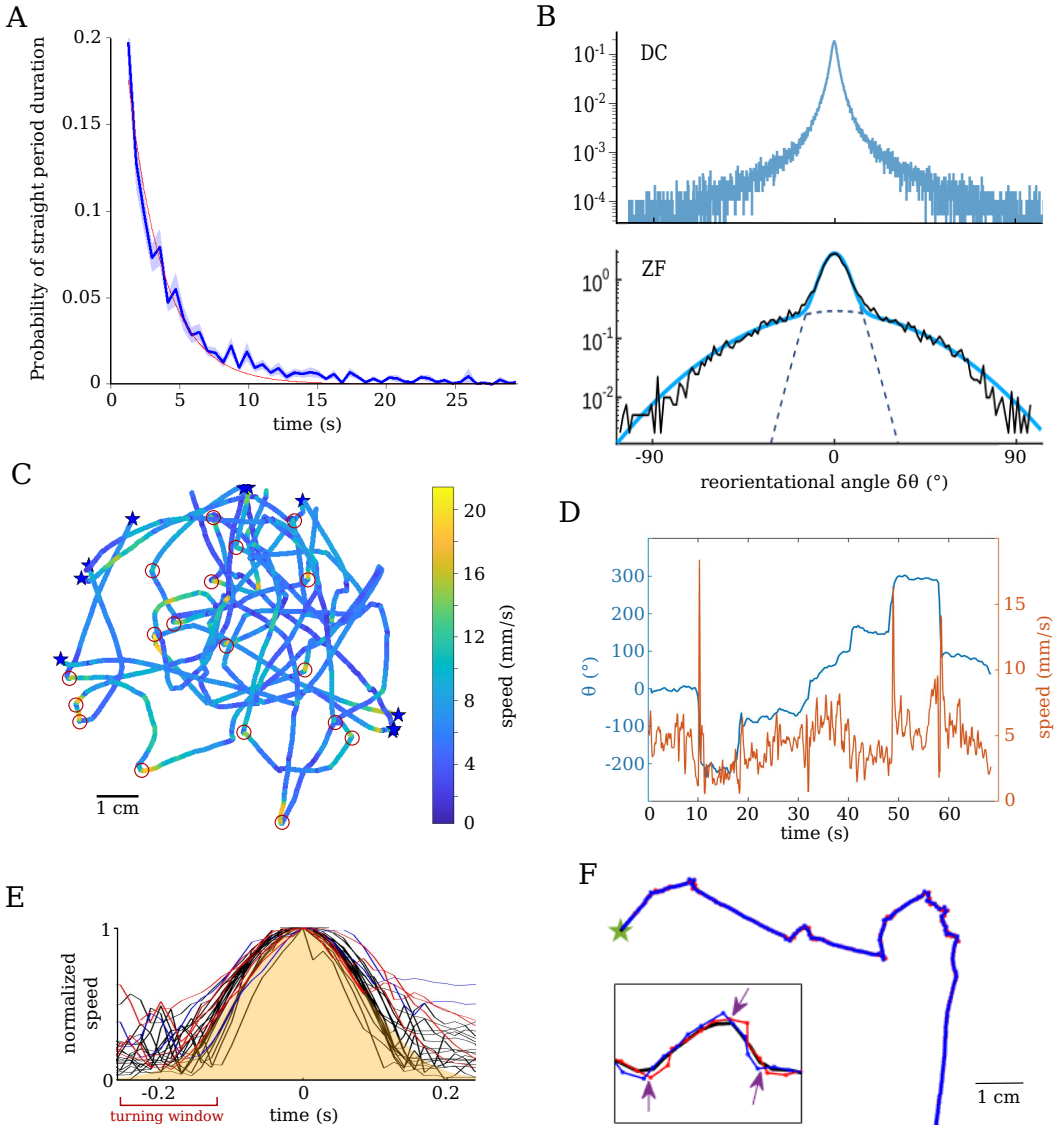

Fig. 4.4 ***Analysis of DC larval spontaneous swimming trajectories.*** *25 fish, 21 756 trajectories analyzed.* ***A*** *Probability of straight period duration in function of time. Red line: exponential fit.* ***B*** *Probability density function of reorientational angle ($\delta\theta_n$) for DC larvae (top) and ZF larvae (bottom, adapted from [35]).* ***C*** *Example of trajectories whose velocity is encoded by a color (see colorbar on the left). Red circle : turn events followed by speed acceleration.* ***D*** *Orientation θ and speed in function of time. Some turns are followed by acceleration.* ***E*** *Normalized speed peak after a turning event.* ***F*** *Linear regression model with forward (red), backward (blue) predicted trajectories and real one (black). Green star: starting position of the real trajectory. Arrow: detected turns.*

speed bias into speed distribution, we decided to restrain them at a maximum speed of 15 mm/s. We then fit them with a gaussian function (μ_s, σ_s) and we defined the speed threshold as $v_{th} = \mu_s + 3 * \sigma_s$.

These techniques only capture few turn as they are not all followed by an increase in speed. Nevertheless, we went deeper on the analysis of those turns. Each peak in speed were aligned with their maxima on the x-axis and normalized (fig.4.4.E). Interestingly, we found an intrinsic time constant of $\approx 0.4s$ which seems to be conserved across fish. We attempted to use this time constant to better determine turning events. We averaged the normalized speed peaks and correlated it with the speed time-series. We found that correlation not only increases after some turn, but also during the straight period, which suggest that *DC* modulate their speed all along their exploration and not only for reorientation.

4.1.3.5 Linear regression

As turn event detection was not successful with simple approaches, we decided to use a linear regression model for inferring fish position at a given position k (on the resampled space) knowing them at previous step. As we are working with space resampled positions, x and y coordinates are not independent of each other because of dl (indeed, we have $dl^2 = \delta x^2 + \delta y^2$). Therefore, we used $\delta\theta$, defined on resampled space, as independent parameters for the linear regression.

A linear regression model assumes that given a discrete data set $\{\delta\theta_{i,k}, \delta\theta_{i,k-1}, ..., \delta\theta_{i,k-p}\}_{i=1}^{N}$ of N trajectories containing k points, the variable $\delta\theta_{i,k}$ is linearly related to the p previous variables of the date set, such as:

$$\delta\theta_{i,t} = \beta_0 + \beta_1\delta\theta_{i,t-1} + \beta_2\delta\theta_{i,t-2} + ... + \beta_p\delta\theta_{i,t-p}$$

where $\{\beta_0, \beta_1, ..., \beta_p\}$ is a (p+1)-dimensional parameters vector whose values are optimized by minimizing the sum of the mean square loss function over the N trajectories. We forced β_0 being equal at 0 to avoid bias in any direction.

Taking the previous inferred coordinates (x_{k-1}, y_{k-1}), it is then possible to reconstruct the position (x_k, y_k) with the inferred reorientation angle $\delta\theta_k$ with these formulae:

$$\begin{aligned} x_k &= x_{k-1} + dl * cos(\theta_{k-1} + \delta\theta_k), \\ y_t &= y_{k-1} + dl * sin(\theta_{k-1} + \delta\theta_k), \\ \theta_k &= \theta_{k-1} + \delta\theta_k, \end{aligned}$$

with dl the distance value defined for the resampling (0.3 mm).

To train the linear regression model, we used all the trajectories. Thus, the forecast coordinates at step k should be aligned with the previous p positions. To detect turns, we evaluated the distance between the predicted point and the true position on the trajectory.

	β_1	β_2	β_3	β_4
Forward	0.125	-0.054	-0.037	-0.002
Backward	0.094	-0.046	-0.026	-0.025

Table 4.1: Linear regression coefficients β from 4.1.3.5 with $p = 4$

If this distance is lower than a certain threshold, the fish is on a straight period, otherwise, if the distance is over the threshold, it means that the fish is in a turning state, or accelerating as we fixed *dl*. To strengthen the turn detection, the linear regression model was also trained on the reverse trajectory direction. Turning positions were then determined at the position where the forward and backward predicted trajectories were diverging from the recorded one (fig.4.4.F).

The number of previous position to take into account in the model p is an important parameter. We tried with different p value but in all trials, we found that only β_1 has a significant contribution (table:4.1). This result can be interpreted as the fact that only the previous position has a significant predicting power of the upcoming position, and so the turning detection. The use of the linear regression model is thus similar to the naive approach, with the same issues in $\delta\theta$ peak identification.

From those two approaches, the naive one and the linear regression model, we learned that a single parameter is sufficient to predict the upcoming position. This strengthened our beliefs in modeling *DC* larval spontaneous swimming trajectories with a Markov process, which is a memoryless process meaning that the next state position (straight or turn) does not depend on the previous states. This idea will be explored by Monica Coraggioso during her PhD.

4.1.4 Switch in navigation program between larvae and juvenile *DC*

Most motile animals have different locomotor patterns at different developmental stages. For example, human babies are crawling and develop to bipedal walking around one-year-old. Another example comes from amphibians, which starts as tadpoles to swim with lateral undulations and with metamorphosis, acquire limbs and lose their tail and learn to swim and walk with their limbs.

In addition to our interest in understanding evolutionary process involved in the swimming pattern divergence between *DC* and ZF larvae, *DC* also offer a unique opportunity to study behavioral ontogeny not only at behavioral scale, but also at neuronal scale. It is challenging to closely follow behavior modification and its underlying neuronal circuit changes over various developmental stages in most vertebrate organisms. With its optical transparency and small size, the *DC* brain is accessible at every life stage which makes it suitable for monitoring neuronal circuit maturation.

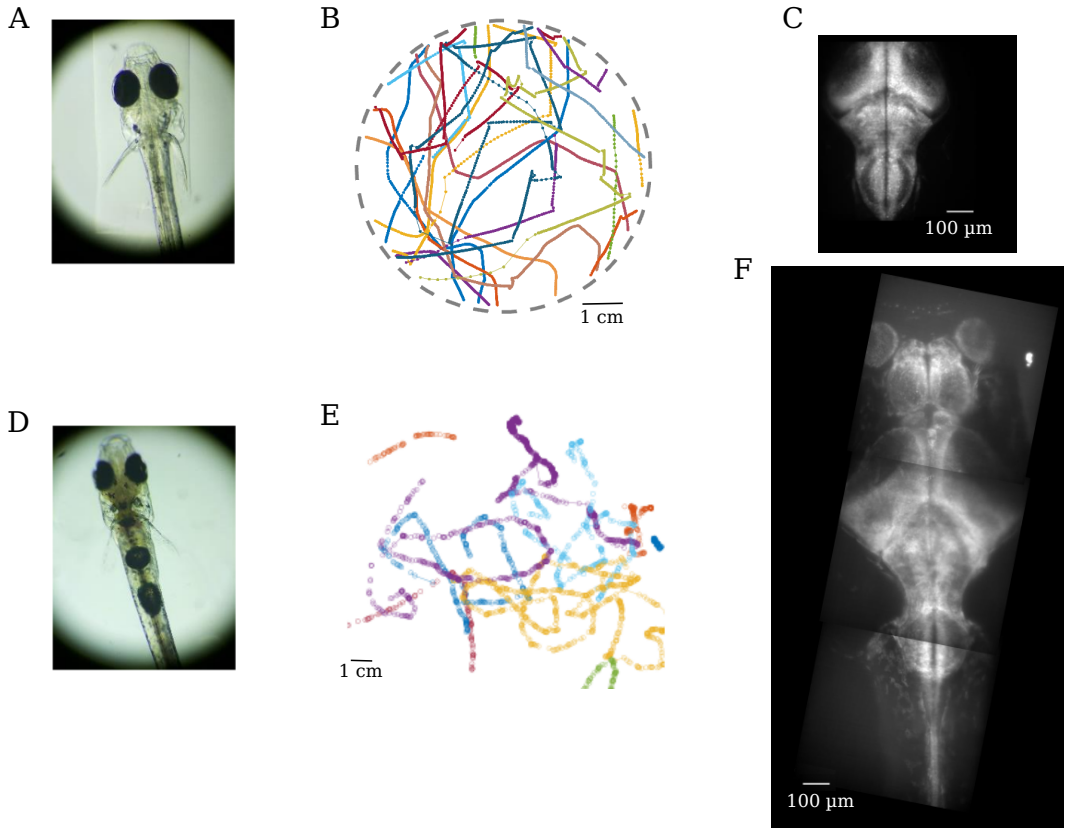

Fig. 4.5 ***DC at 6 dpf and 28 dpf comparison.*** *DC at 6 dpf:* ***A*** *Top view.* ***B*** *Continuous trajectories.* ***C*** *Z-projection of calcium imaging of Tg(elavl3:H2B-GCaMP6s) larva. DC at 28 dpf:* ***D*** *Top view.* ***E*** *Discrete motion trajectories.* ***F*** *Z-projection of calcium imaging of Tg(elavl3:H2B-GCaMP6s) juvenile.*

With this project, it is first important to characterize *DC* swimming pattern changes during development. With MonitoRack (3.3.4), we could observe a transition in their locomotion from larvae to adult stage. Indeed, as shown in a previous section (4.1), *DC* larvae swim with continuous tail motion. On the contrary, *DC* adults perform discrete motions which confirm that *DC* locomotor behavior and circuit are maturing. This change is already visible in juvenile fish at 28 dpf (fig.4.5.E). At 1 month-old, *DC* have started their first metamorphosis and adult traits begin to appear. They are longer and wider than larvae, but they stay in a size range that is compatible with the experimental and microscope imaging setups developed for ZF larvae [30].

Before deciphering neuronal circuits, we want to characterize this swimming pattern shift by modeling spontaneous swimming trajectories with simple models. It will be then possible to compare the switching dynamics between straight period and turning events, for example, and to quantify relevant parameters that can be used for determining neuronal circuit. This work is ongoing by Monica Corragioso (behavior and model) and Leonardo Demarchi (neu-

ronal circuit). In chapter 5 (5), I am presenting how we are identifying locomotor neuronal circuit on 6 dpf *DC* larvae.

4.2 Phototaxis

Exploring an environment is an essential behavior for motile animals. The ability to navigate allows them to inspect their milieu in research of food, but also to find mates, to explore a new habitat and to escape predators. During exploration, they are constantly exposed to multiple sensory information. They need to perceive and integrate this information in order to navigate toward the most adequate regions of their environment. Those sensory-motor mechanisms are essential for animal survival.

In ZF, the visual system is already functional around 3 dpf [49] and supports visually-guided behavior like prey capture, predator avoidance and countercurrent swimming. This early maturation drives our research toward understanding how light modulates locomotor system in larval fish.

4.2.1 Phototaxis in ZF larvae

Some research has been dedicated to study the response of ZF larvae to a luminous stimulus. ZF larvae display diverse reaction to light stimulation such as opto-kinetic response (eyes position responding to a moving pattern [49]), OMR (see 2), escape to looming stimulus [47] or their preference for bright regions. Some studies focused on the former behavior, also called ligh-seeking behavior or phototaxis, showing that after a habituation period under a uniform and constant illumination, ZF larvae tend to swim toward regions with the higher light intensities, which is qualified as positive phototaxis [94, 89, 42]. Nevertheless, few research explored the constant impact of light on the sensorimotor program of ZF larvae.

In the study "From behavior to circuit modeling of light-seeking navigation in zebrafish larvae" by S. Karpenko et al. [35], we explored the contribution and influence of tropophototaxis and klinophototaxis strategies on the spontaneous swimming model they developed (two Markov-chains model, fig.4.1.C). While tropo-taxis reflects the capacity of an animal having two sensory receptors to spatially compare environmental information, klino-taxis requires a temporal sampling of the stimulus intensity to allow the comparison and then the reorientation and navigation toward the preferred conditions. For this collaboration, I built and developed two closed-loop experiments with which we studied the tropophototaxis and klinophototaxis strategies and their impact on the spontaneous locomotor program established.

Closed-loop principle. Both closed-loop experiments are using the same experimental setup which is similar to the setup used for recording the *DC* larval spontaneous swimming

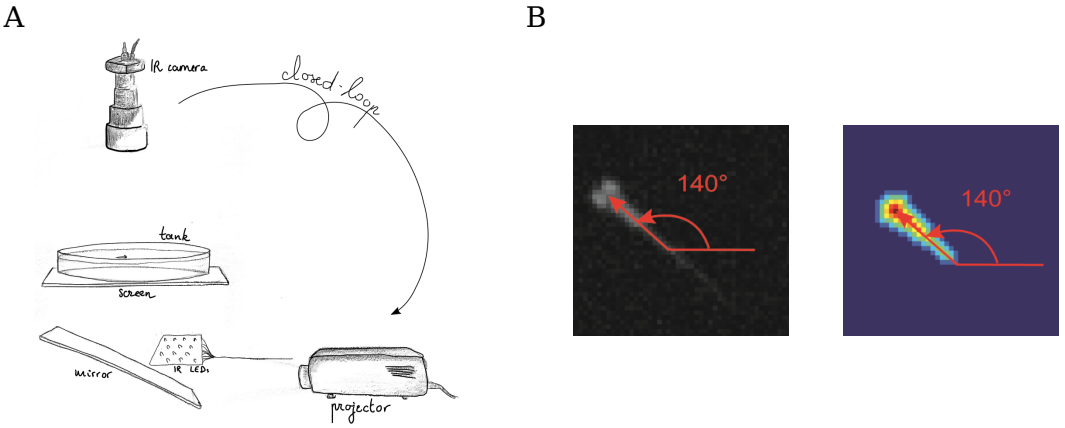

Fig. 4.6 ***ZF larvae phototaxis setup.*** ***A*** *Closed-loop experimental setup. From [19].* ***B*** *Binarization and orientation extraction.*

(fig.4.6.A). The only difference lies in the program controlling the visual stimulation displayed by the projector which depends on the fish orientation. For both strategies, only one fish were used at a time, with a habituation period of at least 8 minutes. The fish orientation corresponds to its angle from a fictive light source.

Positions and orientations of the ZF larva were extracted online, with a custom image processing which consists of a background subtraction, followed by a binarization and by a removing of noisy binarized object. We obtained a single object with coincides with fish eyes and swim bladder. From this elongated object, I extracted two points corresponding to the head position and the swim bladder (fig.4.6.B), and I could determine the fish orientation and modify the visual stimulation accordingly.

Fish behavior was tracked inside a restrained circular central ROI of 8 cm. When outside the ROI, a concentrically moving circular pattern (radial OMR) was displayed to trigger a fish OMR response to actively bring back the fish int the ROI. After re-entering the ROI, a new recording sequence started.

Tropophototaxis: spatial gradient. To depict the strategy used by ZF larvae when they receive different light intensity on each receptor (eye), we used a visual contrast pattern for which the sum of the intensities is constant (fig.4.7.A). When facing the virtual light source (fish angle equals 0), the contrast was null. We found that contrast does not alter the first Markov-chain, meaning that the probability of switching from the forward state to the turning state, is not impacted (fig.4.7.B). It is at the second Markov-chain level that light spatial gradient is acting. Indeed, we showed that the probability to execute a turn in the opposite direction of the previous turn, is affected by the contrast (fig.4.7.C,D). The next turn has more probability to drive the fish on the opposite direction to the last turn if it was pulling the fish away from the bright side (fig.4.8.E). Thus, ZF larvae are swimming toward

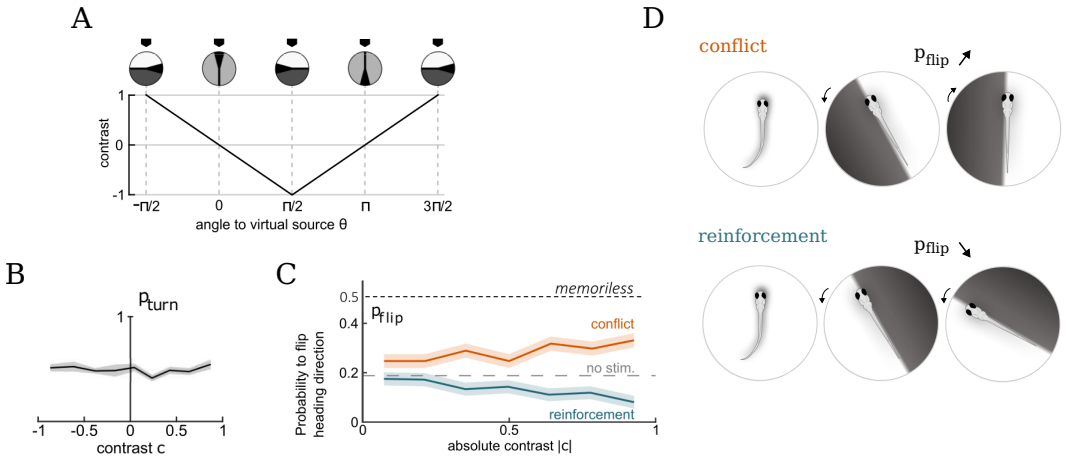

Fig. 4.7 ***Tropotakis strategy.*** ***A*** *Tropotaxis visual pattern.* ***B*** *Probability to flip in turning direction (p_{flip}) in function of contrast.* ***C*** *Probability to change state (forward or turn, p_{turn}) in function of contrast.* ***D*** *Impact of conflict or reinforcement bout on p_{flip}. All figures are adapted from [35, 19].*

bright regions, but they are avoiding dimmed areas.

Klinophototaxis: temporal gradient. In a second experiment, we investigated the strategy employed by ZF larvae when spatial clues are missing, meaning that eyes are receiving the same information (fig.4.8.A). Despite the absence of any directional indication, most of ZF larvae succeeded to orient themselves toward the virtual light source. In this case, we found that reorientation bouts were not biased toward the virtual source. Instead, it is the relative illumination gradient that influences the probability of turning (first Markov-chain),

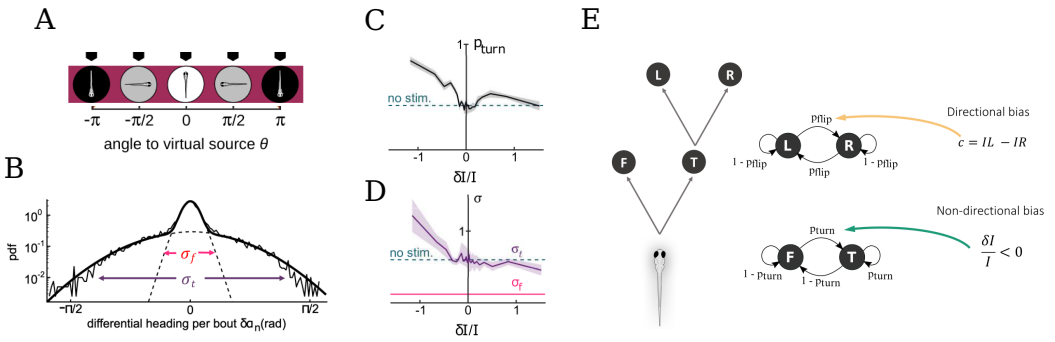

Fig. 4.8 ***Klinotaxis strategy.*** ***A*** *Klinotaxis visual pattern.* ***B*** *Definition of turning bout amplitude.* ***C*** *p_{turn} in function of light-gradient.* ***D*** *Turning bout amplitude (pink) in function of light gradient.* ***E*** *Influence of contrast and light-gradient on the 2 Markov-chain model of ZF larval spontaneous swimming. All figures are adapted from [35].*

which increases with a negative light gradient (fig.4.8.C) and amplifies the turn amplitude (fig.4.8.B,D). Again, ZF larvae are not orientating toward the virtual light source, but they are escaping from darker regions.

We showed the impact of contrast and light gradient stimulation on the spontaneous locomotor program of ZF larvae (fig.4.8.E) by using virtual reality experiments. Phototaxis is a robust behavior which is ecologically relevant for larvae. In order to strengthen our evolutionary comparison between ZF and *DC* , and also our behavioral maturation through development, we decided to explore this light-seeking behavior on *DC* .

4.2.2 Phototaxis in *DC* larvae

As *DC* is a relatively new vertebrate model in the laboratory, little is known about its behavioral responses to light stimulation. At 21 dpf, *DC* fish show a preference for dimmed environments [95]. I performed simple experiments to test *DC* larvae and adults light preference. As *DC* larvae have similar morphology to ZF larvae, we decided to adapt the previous closed-loop experiment to explore phototactic strategies used by *DC* .

4.2.2.1 Context

Before adapting our klinotaxis and tropotaxis experiment on *DC* larvae, I wanted to test the light preference of 6 dpf *DC* larvae. Using the experimental setup used for spontaneous swimming, I displayed on the screen a contrast pattern with one side of the screen illuminated with the projector maximum intensity, and on the other side, no intensity (almost black). I recorded for few minutes single *DC* larva exploration trajectories and I observed that *DC* larvae have a negative phototaxis (fig.4.9.A left), at the opposite of ZF larvae behavior. This preference toward the dimmed area can be explained by the fact that *DC* in their natural environment may prefer as well darker regions. In fact, they were first collected hidden among plant roots at the bottom of the stream.

In ZF, larvae tend to avoid dimmed environments, and thus favor the light regions, whereas adults are photophobic [96]. To verify if a similar behavioral switch in light preference occurs in *DC* , and to check the possibility to observe this switch at a neuronal scale, I reproduced the same contrast experiment mentioned before with *DC* adult. I found that they spent more time in the dimmer side, showing that even at adulthood, *DC* express a negative phototaxis (fig.4.9.A right). Thus, no switch in light preference is observable between *DC* larvae and adults. Thus, I focused my research on *DC* larvae phototaxis.

4.2.2.2 Adaptation of the closed-loop setup

The most challenging part of this adaptation was to detect correctly the fish position and orientation. Even if *DC* and ZF larvae size are in a same range, internal anatomies differ.

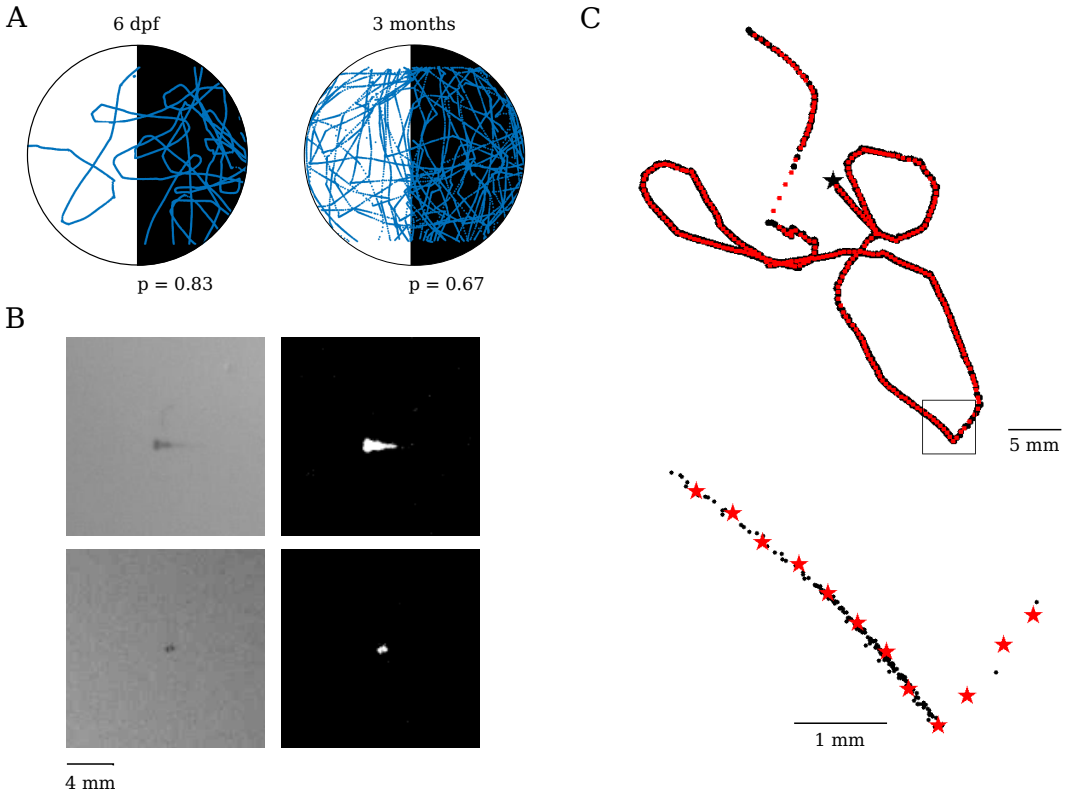

Fig. 4.9 ***DC larvae negative phototaxis.*** ***A*** *DC larvae and adults negative phototaxis. p are percentage of time spend by the fish on the dark area.* ***B*** *Binarization of ZF larva (top) and DC larva (bottom).* ***C*** *Example of a raw trajectory (black) recorded with the closed-loop program and its corresponding coordinates obtained with the exponential mean (red). Bottom : zoom on a trajectory part.*

Indeed, as it can be observed on fig.4.2.A, at 5 dpf, ZF larvae have a first swim bladder inflated whereas it is still missing for *DC* larvae. Both species possess two swim bladders at adult stages, which inflate sooner on ZF fish. The *DC* first swim bladder swelling occurs between 10 and 12 dpf [34]. To record fish behavior without visual stimulation conflict, fish are illuminated with an IR light panel and an IR filter is added to the camera. Fish eyes and swim bladders are covered with pigments that absorb IR light and thus appear black on the recorded frame. Moreover, WT ZF larvae are pigmented all along their spinal cord, which facilitates their detection after the image processing (fig.4.9.B top). This is not the case with *DC* larvae (fig.4.9.A bottom) and their optical transparency, coupled with a late inflation of their swim bladder, become here challenging issues.

Determining *DC* larva orientation. The closed-loop experiment acquisition frequency is limited by the camera shutter time as well as by the image processing and tracking time. I decided to not modify the shutter time of the camera. Image processing is a time-consuming

process that we have to limit to basic operations in order to keep a reasonable frame-rate. *DC* larvae swim slower than ZF larvae, with an average mean speed of around 4 mm/s [34]. As seen on section 4.1.3.2, *DC* larvae head is oscillating which can impact the determination of the fish orientation. To avoid this on the spontaneous swimming model section (4.1.3)), we applied a spatial threshold to resample the data. We fixed this threshold at $dl = 0.3mm$, which corresponds to a travelled time of $dt = dl/speed = 0.3/4 \approx 0.075\ s$, so a frame-rate of 13 Hz. I did not choose to decrease the recording framerate because it is essential to continuously monitor the fish orientation in order to adapt the visual pattern, not too abruptly, especially in case of acceleration or escape behavior (with 30 mm/s average speed, [34]).

With those limitations in mind, I worked on finding a solution to detect fish orientation with only its eye detectable. I supervised a L3 intern for 1 month, Samantha Fournier, who helped me with making the image processing more efficient and to develop another way to smooth *DC* larva trajectory.

For the image processing, with the ZF program, I was first binarizing and removing binarized and detected objects that were not the fish, on the whole frame (1024*1280 pixels). We changed this by first finding the darker pixel of the image (which should be above a certain value which corresponds to fish eyes), reducing the image around this pixel (60*60 pixels) and then performing the binarization and removing the non-fish binarized object. It is, after thinking, a good option to gain time.

As only the eyes are detected, it is not possible to infer the body fish orientation from the corresponding binarized object. Only fish trajectory direction can be extracted from a previous position and the actual. We implemented a code that record for 10 frames the fish position, without visual stimulation, in order to determine the trajectory orientation.

To smooth the trajectory, we computed another set of coordinates (x', y') in parallel to the raw coordinates (x,y), that are determined as:

$$x'(t) = \sum_{i=0}^{5} w_i * x(t-i)$$

where w_i are exponential decreasing weight.

To limit noise on the orientation angle, we added another condition to only consider exponential positions which are separated to a minimal distance of 8 pixels ($\approx$ 0.6 mm, which corresponds to the eye size, characteristic binarized object length) (fig.4.9.C), inspired from the smoothing done on spontaneous trajectories (see section 4.1.3.2). Every time a new sequence begins, 10 frames are used to determine the first trajectory orientation.

I incorporated those modifications to the already existing experimental programs. I am still checking that tropotakis and klinotaxis experiments are correctly adapted for *DC* larvae. Those experiments will be led by Monica Coraggioso.

4.3 Discussion

4.3.1 Spontaneous locomotion description

Evolution behavior divergences are part of the species diversification and can occur for diverse reasons: environmental pressure, gain or loss of a phenotypic or genotypic trait and others. At first, when we compared *DC* and ZF larvae morphological and environmental similarities, we expected to find similar swimming behavior due to similar hydrodynamic constraints. This hypothesis proved wrong, and we observed that the larval swimming behavior of those two species have diverged. We took this opportunity to perform a comparative study on morphological similar larvae with distinct locomotor programs [34].

Comparing two species at similar developmental step is a complex program. Diverse criteria can be applied to define when the development is at the same stage on different species such as anatomical (maturity of an internal or external organ), morphological (same body size criteria), age and molecular (gene expression) or hormonal (detection of some hormonal peaks) data, just to mention few examples. As *DC* constitutes a new model, little is known about its hormonal development. From an anatomical point of view, ZF first swim bladder is inflated about 4 dpf whereas the same happens at 10-12 dpf for *DC* . We decided not to base our study on similar anatomical and morphological, and we use instead the age of the larvae. This choice is supported by the fact that at these stage, fish larvae survival behaviors are already mature enough and tend to be stable over few days, before the appearance of more complex actions such as collective behavior [14]. Thus, we decided to work with *DC* and ZF larvae between 5 and 7 dpf [34].

One of the argument in favor of minimal behavioral models is to facilitate the neuronal population function identification and the modeling of neuronal circuit subunits involved in specific sensorimotor tasks. Simple models also have the advantage to only use few or only one inputs to characterize simplified but still complex results. This also eases the comparison of model specific parameters in order to follow variation of this model with development, in our case. Change in *DC* locomotor pattern between larval stage and juvenile stages, allows one to also perform a comparative study but with a developmental axis. Nevertheless, developing minimal model requires reducing behavior complexity. Those models are not reflecting the diverse contribution of environmental information, but highlight the small contribution of one specific stimulation on the sensorimotor program.

For the evolutionary comparison between *DC* and ZF, we plan to compare the simple models which describe their distinct swimming pattern. However, the model developed for ZF are based on bout unit and not on time unit, whereas for *DC* , this latest approach will be necessary.

4.3.2 Phototaxis

DC is as an interesting vertebrate model for neuroscience because of its natural optical transparency. However, this trait makes it trickier to track on wide field recording. Indeed, *DC* pigments are mainly located on their eyes, on their swim bladders and on the ventral surface of the abdomen. Few melanophores are localized on the head, on the top of the brain on adults. Thus, in larvae, only eyes are detectable with IR illumination. This was an issue to extract fish body orientation for the closed-loop programs developed from ZF WT pigmented larvae. We decided to maintain our illumination and to find a solution on the fish detection process. Even at juvenile and adult stages, each eye and swim bladders are separated with skin without pigments, which makes more difficult the binarization to only one object. For juvenile, we decided to implement a code which could detect three objects (both eyes and swim bladders) and determine fish position and orientation, to have both measured. Like this, it is possible to compare trajectory orientation of *DC* at all stage and thus, used the same model to follow swimming maturation.

It has been shown that ZF larvae have a negative phototaxis to light at 860 nm (near IR) [97]. When larvae were recorded to determine the model without visual bias, we did not notice a bias of the trajectory toward the opposite side of our IR panel light, probably because it is not visible to the fish and that IR light is diffused by the screen used for displaying visual stimulation. By watching habituation phase for *DC* experiments, larva trajectories were not biased toward one side. We could conclude that our IR illumination does not interfere with our visual stimulation.

DC larvae showed a negative phototaxis. The question is to determine if they prefer to navigate toward dimmed area, or if they avoid bright area, in the similar way ZF larvae are moving away from low light intensity. This preference for *DC* in dark environment can be understood as they tend to swim at the bottom of the water column, and to hide among plant roots. As for spontaneous swimming without visual bias, it is important to keep in mind that our experiments are not reflecting the complexity of sensory stimulation perceived by the fish.

4.3.3 Perspectives

Those results are part of two parallel studies. The first one is focusing on determining the evolution processes that lead to distinct locomotor behaviors on larvae fish that share similar morphologies. To determine part of those mechanics, I started to investigate the different environmental exploration strategies used by ZF and *DC* larvae. The underlying objective is to model with few dynamic parameters the spontaneous trajectories of those larvae. Simple models will then allow to decipher the neuronal circuits involved in swimming. They will also be part of the analytic strategy defined for the second study. *DC* fish, thanks to their optical

transparency at every life step, are offering a unique opportunity to follow the maturation of their behavior, both behaviorally and at neuronal circuit scale. For behavior, *DC* swimming is changing from larvae to juvenile stage. With the simple model developed for larvae, it will be possible to follow this evolution in dynamics and then to translate those observations to calcium imaging to decipher the neuronal circuit arrangements.

As *DC* larvae are swimming continuously, the arena of 14 cm is restraining their long straight phases. To bypass this constraint, a new experimental setup with an arena of 30 * 30 cm with a camera and a projector that can track online fish trajectory is developing, on the same basis as the beast [91]. This setup allows following larvae and other stage on longer period and distance, and also to neglect border effect. Spontaneous locomotion, phototaxis and other visual triggered behavior will be explored with less space constraints.

Defining and working with simple behavioral models ease the identification process of neuronal population function on the correspondent behavior. On the next chapter, I will present the light-sheet microscope setup I used to reveal distinct neuronal populations involved in spontaneous locomotion.

Chapter 5

DC locomotor neuronal circuit

With their natural optical transparency and small size at larval stage, transgenic lines have been developed for both *DC* and ZF species in order to record their whole-brain activity at neuronal scale. Thus, it is possible to complete the behavioral comparative study with the identification of the neuronal circuits involved in their different swimming patterns. It is also the opportunity to explore how those neuronal circuits have diverged.

I start with a short review on calcium imaging and light-sheet microscopy, the main tools I used to record whole brain neuronal activity, and also on what it is known about locomotor circuits. Then, I describe experiments and results obtained on the locomotor neuronal circuit in *DC* larvae.

Personal contribution Part of the work I present in this chapter was published in [34].

For this study, I developed and performed the analysis of calcium imaging data collected by Gokul Rajan with one of the light-sheet microscope developed at Laboratory Jean-Perrin. I had four *DC* brains to analyze. In order to confirm the published results, I recorded more calcium data on another light-sheet microscope setup, that I adapted for *DC* . Thus, the average brain results I show in this chapter were done with data from the 4 brains acquired by Gokul Rajan on one setup, and 7 others brains that I recorded on a microscope at Laboratoire Jean Perrin. Maintenance neurons and transient neurons (onset, offset) are already published in the collaborative study. I confirm those preliminary results with more data that I acquired and analyzed.

Even if the analysis protocols for calcium data are already published, I explain the analysis principle in more detail in section 5.2.2.

The behavior extraction protocol differs from the one performed in the published study, but has the same objective to binarize the fish behavior into swimming and non-swimming periods.

5.1 Recording neuron activity

5.1.1 Measuring action potential

Neuroscience is a recent research field that emerged during the 20^{th} century, although the interest for understanding how animals move and think is more ancient. Galen, a Greek physician from the 2^{nd} century, was one of the first to describe the central nervous system with "hard" and "soft nerves controlling sensation and motion. But it is only with the development of the microscopy and new staining techniques (Camillo Golgi and Santiago Ramón y Cajal, Nobel Prize in Physiology in 1906) that neuron was defined as the basic component of the nervous system.

A neuron is an excitable cell that can send electric information through its axon. Indeed, excitable cell membranes process ionic channels that can be opened or closed allowing for transient membrane depolarization called an action potential. This electrical signal can then be transmitted to other cells through synapses. First recordings of electricity in cells were done in the second half of the 19^{th} century by Carlo Matteucci and then by Emil du Bois-Reymond who are considered as the pioneers for electrophysiology. This branch of physiology aims at studying electrical properties of cells by measuring the electric current or voltage changes at the cell membrane. Those techniques require positioning electrodes directly at a neuron surface and allow recording neuron electric activity at sub-millisecond scale, enabling to measure single action potential that lasts for 3-5 ms [98].

Evolution of techniques toward large scale recording have led to a switch from the neuronal doctrine, in which individual neuron is a precise functional unit (theory defended by Golgi and Cajal) toward the actual vision, the network doctrine, that promotes neuron assembly as behavior generator [99]. It is then needed to develop methods that record neuron activity at a large scale, but with a neuronal scale spatial resolution. Fluorescence imaging is one of these methods.

5.1.2 Fluorescence calcium imaging

Many efforts were put together in order to achieve the simultaneous recording of thousands of neuron activity individually. A new approach has emerged from the combination of optical imaging techniques and fluorescent sensors that can target and follow specific chemical species involved in action potential or signaling pathway. A focus was given to the calcium ion Ca^{2+} which is an essential intracellular messenger in most eukaryotic cells. It is involved in the transmission of depolarizing signals and in synaptic activity [100]. In neurons, Ca^{2+} is involved in different cellular processes acting with different timescales. Among these, gene transcription can be mentioned as one of the longest event in which calcium is involved (can last for minutes to hours) whereas neurotransmitter released requires short calcium responses

(few milliseconds) [101]. At rest, calcium levels are of the order of 50-100 nM in the cytosol. But a depolarizing signal, such as an action potential, triggers an opening of the voltage-gated calcium channels, creating a massive Ca^{2+} influx, leading to a calcium level increase of the order of 10 to 100-fold [101]. It is this transient changes of calcium concentration in the cytosol elicited by neuronal electrical activity that is detected with fluorescent sensors.

Calcium fluorescent reporters are designed to have a fluorescence signal that increase with the calcium concentration. In neuroscience, the most widely used calcium fluorescent probe is the GCaMP family [102]. GCaMP is a Genetically Encoded Calcium Indicator (GECI) that associates a calcium sensor calmodulin (calcium-modulated protein, CaM) and a modified version of the Green Fluorescent Protein (GFP). GFP was discovered in jellyfish and emits light peak at about 515 nm when it is excited around 480 nm. When GCaMP binds to calcium, there is a conformational change that increases its quantum fluorescence efficiency. The measured fluorescence signals depend on multiple factor such as the expression level of the calcium reporter, its type, the excitation power, the detection methods. Thus, absolute value of fluorescence is not the optimal quantity to use. Therefore, the relative fluorescent variation ($\Delta F/F$) is commonly used to evaluate the neuron activity, defined by:

$$\frac{\Delta F}{F}(t) = \frac{F(t) - F_{baseline}(t)}{F_{baseline}(t) - F_{background}}$$

where $F(t)$ is the absolute fluorescence, $F_{baseline}(t)$ is the fluorescence baseline and $F_{background}$ is the background image value.

By definition, the fluorescence baseline is the fluorescence measured for a neuron at rest. As each neuron expresses a specific amount of fluorophore, they also have a proper fluorescence baseline. For larvae ZF, it is generally calculated by a running an average time window of a low percentile of the raw data. In our laboratory, the time window is set at 50 sec and the percentile at 10^{th} of the raw intensity [51]. This baseline allows removing long-term fluorescence modulation (as photobleaching which is unrelated to neuronal activity) without interfering with the calcium transient (it is also hypothesized that the studied behaviors do not involve long-term neuronal circuit activation).

The fluorescence response function of most GCaMP sensor can be approximated by:

$$K(t) \propto \exp\left(-\frac{t}{\tau_{decay}}\right)$$

where τ_{decay} the fluorescence decay time. By assuming a linear response, the measured fluorescence for each neuron is then the action potential train convolved with *K(t)* (plus noise). Based on the blind deconvolution technique to infer spike from fluorescence data developed in the lab [103], we determine the decay time constant for zebrafish transgenic lines *Tg(elavl3:H2B-GCaMP6s)* [51] and *Tg(elavl3:H2B-GCaMP6f)*, that are summarized in

τ_{decay} (s)	*In vitro*	*In vivo*
GCaMP6s	0.45 ± 0.04	3.5 ± 0.7
GCaMP6f	0.14 ± 0.02	1.6

Table 5.1: Fluorescence decay time constant for GCaMP6s and GCaMP6f calcium reporters *in vitro* [104] and *in vivo* [51].

table 5.1. The constants found by the blind deconvolution technique *in vivo* are 10 times higher than the ones found *in vitro* [104].

Thus, GCaMP reporters allow inferring an approximate spike train for each neuron. Coupled with whole-brain imaging such as light-sheet microscopy, it offers unique opportunity to have an insight on global neuronal circuits.

5.1.3 Light-sheet microscopy

Fluorescence imaging setup are composed of two optical units: a first one to trigger fluorophore excitation, and a second one to collect the photons emitted by the fluorescent reporters. In a 3D sample, fluorescent signals are coming from all the molecules that are under the excitation light, and that can be on and out of the focus plane of the recording pathway. In order to obtain only signal from a single layer, it is necessary to use optical sectioning techniques. Confocal and 2-photon microscopy are two point-scanning techniques widely used. For the first one, a pinhole positioned at the object focal point of the lens confine the photon collection to the ones emitted on the focal point and thus eliminates out-of-focus signals. The second method is based on the 2 photon effect [105]. To emit light, a fluorophore has to absorb a certain amount of energy to reach an excited state, from which it can relax by emitting a photon to go back to its ground state. This transition energy can either come from a single photon absorption ($E = \lambda h$, E: energy, λ: wavelength, h: Planck constant, $\lambda = 488nm$ for GCaMP), either from two photons whose sum of energies corresponds to the energy necessary to excite the molecule ($E_{excited} = 2 * E = 2 * \lambda h$, $\lambda = 930nm$ fog GCaMP). As the 2-photon effect is a non-linear process and requires a high photon density, it is only effective on the lens focal point. Both these point scanning methods are limited by their acquisition frequency which is inversely proportional to the number of scanning point and linked to the shutter time of the acquisition camera.

To overcome this limitation, light-sheet microscopy, also called selective-plane illumination microscopy, decouples the excitation and recording units by stimulating a whole layer of the sample perpendicularly to the observation plane. Thus, the optical sectioning is created by the illumination technique. The illumination plane can be obtained by different approaches: cylindrical-lens [106], lattice light-sheet [107] or digital scanning. Thomas Panier, in our team, built the first 1 photon light-sheet microscope in the laboratory by using the digital

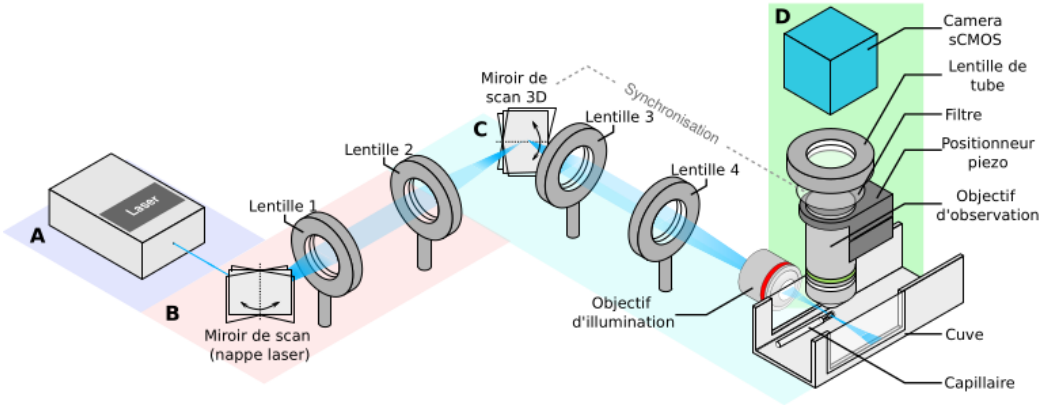

Fig. 5.1 ***1 photon light-sheet microscope.*** ***A*** *Laser.* ***B*** *Horizontal scanning to create the light-sheet.* ***C*** *Vertical scanning for volume imaging.* ***D*** *Recording part.*

scanning method (fig.5.1). He recorded whole brain of larval zebrafish the same year as M. Ahrens group in 2013 [20, 21]. To create the light-sheet, a laser beam is rapidly scanned with a mirror, in the horizontal plane. The frequency uses is set at 200 Hz (which should be higher than the acquisition rate, defined by the camera shutter). The light-sheet is focused on the object plane of a telescope to allow a two dimensions scanning. Another mirror and telescope enable to move the light-sheet in the third dimension, leading to a 3D imaging. The light-sheet width is defined by the oscillation amplitude of the scanning mirror and can go up to 2 mm which is enough to record larva ZF brain in its entirety. The important feature of the light-sheet is its thickness, or *waist* ω_0, which determines the vertical resolution and the optical sectioning efficiency. The laser is a gaussian beam, for which gaussian optical rules predict the laser thickness with this equation:

$$\omega(x) = \omega_0 \sqrt{1 + (\frac{x\lambda}{\pi\omega_0^2})^2}$$

where λ is the wavelength, which is at 488 nm. The smaller the *waist* ω_0 is, the more the beam is diverging. A compromise has to be found between the beam thickness which has to be smaller than a neuron size ($\approx$ 8 µm in average) and the total distance to image the whole brain width, around 500 µm for ZF at 6 dpf. The light-sheet profile of our microscope has been characterized and we obtained a waist of 4 µm and a thickness of 16 µm at a distance of $\pm$100 µm from the waist, which allow recording most of the neurons of a ZF larva.

5.2 Determine neuronal circuits in larval fish

5.2.1 Methods

This section only concerns the recordings I performed to confirm the results published in [34].

5.2.1.1 Calcium activity and tail recordings

Spontaneous swimming. Based on this published work [34], I used transgenic *Tg(elavl3:H2B-GCaMP6s)* at 6 dpf to confirm and determine the locomotor neuronal circuits of larval *DC*. The fish were embedded with low melting point agar (Sigma-Aldrich) at 2% in mass then drawn in a 1 mm diameter capillary, tail first. The tail was freed by cutting the agar around the anus. The fish inside the capillary was then held in a support filled with water from the *DC* facility for 20 min at least. After this habituation time, the fish was introduced in the microscope tank filled with *DC* facility water at room temperature. The fish was carefully pushed out of the capillary to position the brain out of the glass tube and was rotated along its rostro-caudal axis with the capillary to be dorsal-up. A 3D translation stage allowed to align the fish brain with the camera recording objective and the light-sheet. Before every experiment, the fish were adapted to the laser excitation light for some minutes.

The calcium activity acquisition rate was set at 1 brain volume per second, between 20 and 25 brain sections with 8 μm interlayer (each image were exposed for 20 ms or 25 ms). Images were binned, leaded to a pixel size of 0.8 x 0.8 μm^2.

The tail movements were recorded with an IR-sensitive FLIR Chameleon3 CM3-U3-13Y3M-CS camera at 100 fps, from below, via a mirror reflection. The tail was illuminated with an infrared LED. The acquisition was triggered with the same trigger used for neuronal activity recording. The acquisitions lasted between 20 and 30 min.

High-resolution stack. To ease the comparison across fish, all the brains recorded for the spontaneous swimming experiment were registered on a reference brain. To create this reference brain, five *Tg(elavl3:H2B-GCaMP6s)* fish at 6 dpf were immobilized, as described in the previous paragraph, into a capillary with 2% agar gel. The tails were not freed.

To create the high-resolution stack, the calcium camera shutter was set at 200ms. The whole brain volume was recorded four times with 1 μm interlayer and between 300 and 390 brain slices. The acquisition started above the brain and ended as deep as possible into the *DC* brain.

ANTS registration. All the brain stacks were mapped on a reference brain created for this operation. I used a program wrote in python by Matteo Dommanget-Kott (a PhD student from the LJP lab) which uses ANTs registration tools (Advances Normalization Tools [108]).

This program can be used to perform either a high-precision mapping (to create a high-resolution reference brain), or a low-precision registration (to map low resolution stack on high-resolution stack).

5.2.1.2 Calcium data analysis pipeline

The images acquired with the light-sheet microscope were processed offline using MATLAB, through a pipeline developed by the lab and previously described ([20], [51]).

Drift correction. First, the routine corrects the motion artifacts induced by the fish movements. XY drifts were corrected by registering each frame of the recording with respect to the first frame by determining the displacement vector that provided the maximum correlation. A corrected stack without motion artifact is produced and used for the rest of the processing and analysis.

Neuron segmentation and raw fluorescence extraction. The program automatically identifies the regions of interest (ROIs) corresponding to individual neuron nuclei. The brain contour is manually defined for each layers on a mean stack (average per layer of 1 over 70 frames) to increase the image contrast. A gaussian regressor is created with the size of a neuron (set at 6 μm). Two successive linear regressions and convolutions are done with this gaussian regressor. From the last regression, only the regression coefficients higher than a certain threshold are kept and each pixel with a value higher than all its neighbors is considered as neuron center and defined the coordinates. Every center is then assigned with a round shape of 6 μm. Every pixel inside this ROI in considered to be part of the neuron ROI. This algorithm allows identifying neurons finely, but if some neurons are very close to each other (less than 6 μm), it detects only one neuron. Finally, the raw fluorescence time signal $F(t)$ for each neuron is extracted by averaging the pixel intensities within each ROI.

Creating the reference brain. The reference brain used for my work were developed for 6 dpf *Tg(elavl3:H2B-GCaMP6s) DC* larvae fish brains recorded with 1 photon light-sheet microscopy. Among the high-resolution stacks made, one was selected as a first reference to register the others high-resolution brains on. This registration was done with the high-resolution programs, using the parameters from this study [109]. To generate the final reference brain, all the mapped brains and the first reference one were averaged (5.2).

Registration. All the mapping from the spontaneous swimming experiment brains to the reference brain were done with the low-precision registration program, using the parameters from https://github.com/nvladimus/ZebrafishBrainRegistration_Zbrain_ANTs/blob/master/registration_ZBrain-ANTs_nMLF_ablations.ipynb. The transformation matrix determined by the program is then applied to the neuron coordinates to allow comparison on the same brain referential.

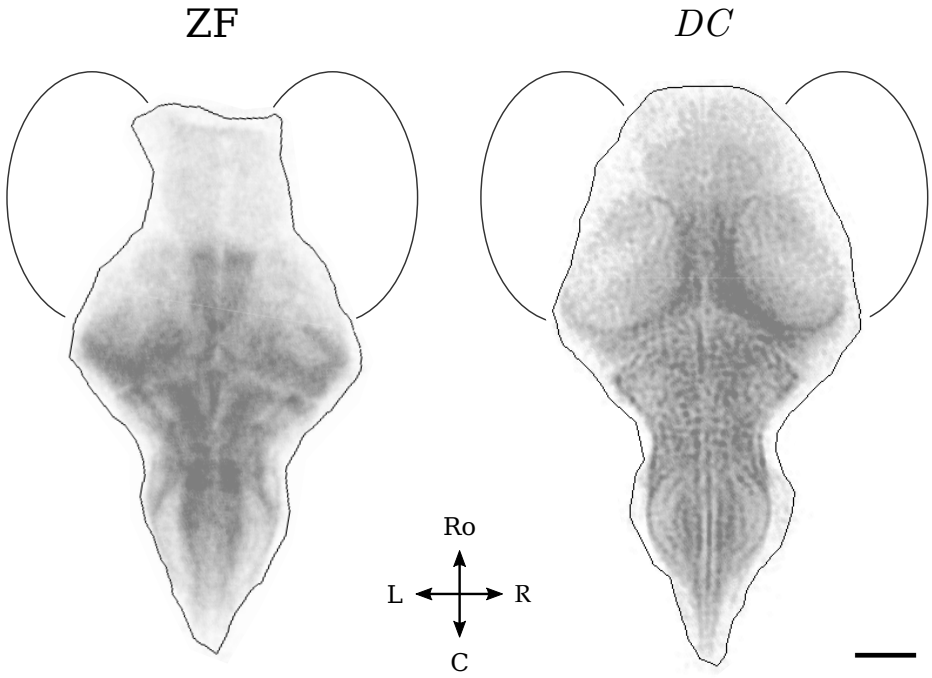

Fig. 5.2 *To compare brain size and anatomy of ZF larvae and DC larvae at 6 dpf. Neuron segmentation. Scale bar : 100 nm. ZF: segmentation and registration of six brains ($n_{neurons}$ = 178 300). DC: segmentation and registration of six brains ($n_{neurons}$ = 163 097)*

5.2.1.3 Behavior extraction

In parallel to the calcium data acquisition, the larva tail movement is recorded. The video is first cropped around the tail of the fish to minimize the size of the frames. A background is created by outlining and removing the tail, and then by applying a gaussian filter. This background is subtracted to each frame to create a new denoised movie. The tail is segmented into 10 sections. The amplitude movement for each segment is calculated by extracting the maximum correlation between each frame and a resting reference frame.

The tail behavior is then binarized into swimming and resting periods. To do this, only the displacement differential of the last segment of the tail is considered (the highest amplitude, symmetric). To reduce noise, a low-pass filter is used on the data. To determine the cut frequency, an interval of 5 Hz around the frequency with the maximum amplitude of the signal Fourier transform, which represents the mean tail beat frequency of the embedded fish, is fitted with a gaussian model. The cuttof frequency is defined as :

$$f_{cut} = \mu_{fit} + 3 * \sigma_{fit}$$

The distribution of the filtered signal is then fitted with the sum of two gaussian functions to depict both amplitude distributions from swimming and resting phases. Finally, the

amplitude threshold for behavior binarization is defined as:

$$Amp_{threshold} = \mu_{resting} \pm 4 * \sigma_{resting}$$

where $\mu_{resting}$ and $\sigma_{resting}$ are from the gaussian fit of the resting phases (with the smallest standard deviation). Swimming and resting periods smaller than 200 ms were removed.

5.2.2 Analysis

This section describes in more details the analysis I developed and performed for [34]. I used the analysis for the already published results as well as for the data I acquired to confirm the existing results.

5.2.2.1 Fluorescence baseline

Most of the pipeline analysis to extract $\Delta F/F$ from the calcium data were similar to the one already used and described for ZF larvae (5.2.1.2). However, *DC* and ZF larvae active swimming duration are not of the same order of magnitude: whereas ZF larvae perform short bouts of 200 ms, *DC* larvae swim continuously and their active periods can last from few seconds up to tens of minutes (4.1.2). This large variance in time raises a problem for the $F_{baseline}$ definition.

As explained in a previous section (5.1.2), it is the $\Delta F/F$ which is the common measure used to compare the calcium activity. For ZF larvae, the baseline fluorescence is determining with a sliding time window of tens of seconds. This duration was chosen to follow the long term fluorescence variations with the hypothesis that ZF larvae neuronal activity might not be sustained for so long. This assumption is valid if we consider the short and sparse bouts of ZF larvae, but it is rejected in the case of *DC* larvae which can swim continuously for few minutes.

As we are interested in active and inactive periods of locomotion on *DC* larvae, we decided to define two fluorescence baselines (ON and OFF) respectively based on those two phases. We calculated both baselines for each neuron as the 10^{th} percentile of the raw fluorescence within either active (ON), or inactive (OFF) period. A window of 10 seconds centered on every transition (from active to passive and passive to active) was removed. The baseline values were then interpolated between each inactive phases for the ON baseline, and between the active phases for the OFF baseline. We could then compute the $\Delta F/F$ based on both baseline as:

$$\frac{\Delta F}{F}(t)_{ON} = \frac{F(t) - F_{ONbaseline}(t)}{F_{ONbaseline}(t) - F_{background}}$$

and

$$\frac{\Delta F}{F}(t)_{OFF} = \frac{F(t) - F_{OFFbaseline}(t)}{F_{OFFbaseline}(t) - F_{background}}$$

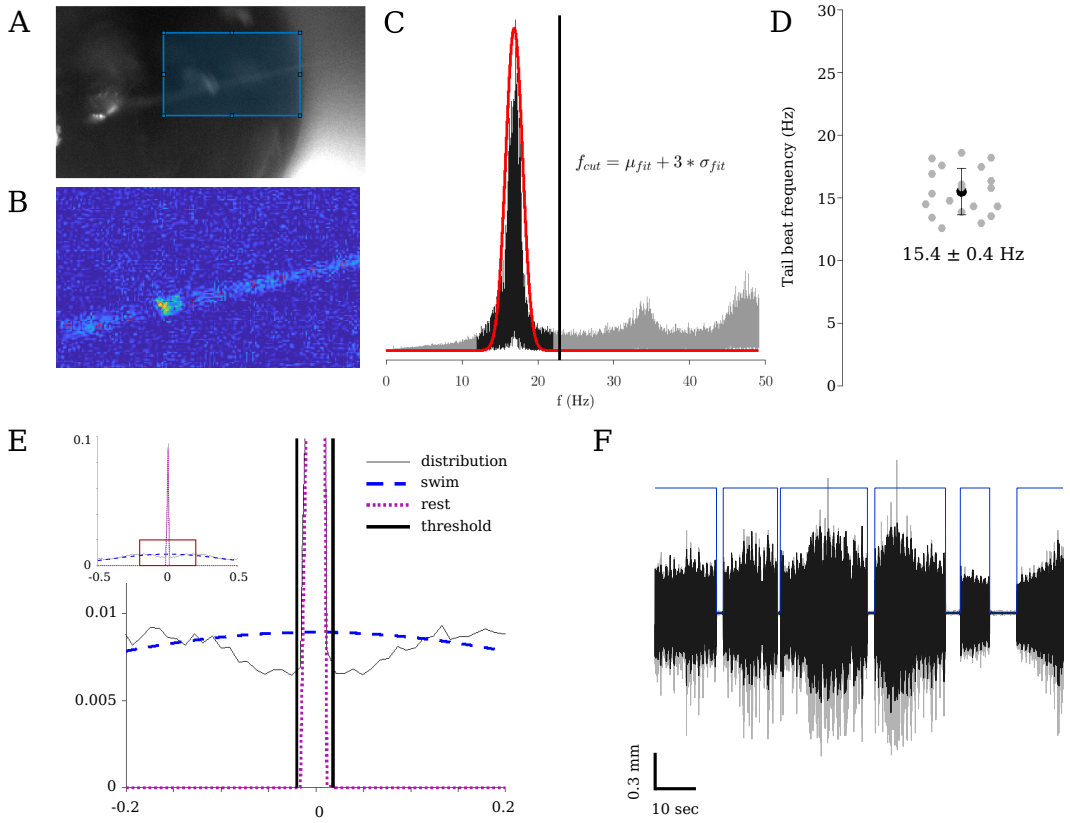

Fig. 5.3 ***Tail behavior binarization.*** ***A*** *Raw frame of tail recording during calcium activity recording.* ***B*** *Tail image after denoizing. In red are the segment centers.* ***C*** *FFT applied to the tail amplitude differential. Light gray: FFT amplitude. Dark: amplitude fitted by a gaussian. Red: gaussian fit. Vertical bar: cut frequency for the low-pass filter.* ***D*** *Mean tail beat frequency of embedded DC larvae (n = 20, mean ± sem).* ***E*** *Two gaussian fits (blue: swimming amplitude, purple: resting amplitude) of the low-pass filtered signal. Vertical lines: amplitude threshold applied for binarization.* ***F*** *Tail amplitude binarization in swimming and resting phases. Light gray: raw tail amplitude differential. Dark gray: signal filtered (low-pass). Blue: signal binarized.*

5.2.2.2 Linear regression

To identify neurons that are responsive to spontaneous tail free behavior, I used a linear regression adapted from the method developed by Miri et al. [110] and used in the laboratory [51]. The idea is to describe the neuronal activity of each neuron as a linear combination of different regressors x_j such as:

$$y = \sum_j \beta_j x_j + \beta_0$$

where y is the fluorescence signal for one neuron, β_j is the regression coefficient for the regressor x_j and β_0 the noise. Neurons with high correlation with a regressor j will have a high regression coefficient β_j. Moreover, t-score values are computed for each coefficient to test if the neuron has a significant correlation to the regressor. Thus, a neuron is defined as relevant for a given regressor if it has both a high regression coefficient and a high t-score value. The regressors are established with the binarized tail behavior (5.2.1.3). Five regressors are defined: a *constant* one to remove potential offset on the fluorescence, *swimming* which is correlated to the active phases of the tail, *resting*, based on the non-active period behavior, *ONset*, which correspond to the transition from a resting to a swimming state (defined as the period 1 second before and 3 seconds after the transition) and finally *OFFset* which coincides with the end of an active phase and the beginning of a resting one (same definition as the *onset* regressor but with the negative switch). All regressors, except the *constant* one, are convolved with the calcium kernel *K(t)* (5.1.2) with a time constant of 3.5 s, which approximates the *elavl3:H2B-GCaMP6s* fluorescence response.

To identify the highly responsive neurons for a specific regressor, I developed another method than the one used in the laboratory [51]. I first fit both the regression coefficient and t-score distributions with a gaussian model to extract sub-distributions responsible for noise defined as the maximum of the original distribution ± the standard deviation found by the model (fig.5.4.A,B, brown). Those sub-distributions are then fitted with another gaussian model ($\mu_{noise}, \sigma_{noise}$) to obtain a better characterization of the gaussian noise. Then, I define threshold values for both regression coefficient and t-score as:

$$threshold_{coeff} = \mu_{noisecoeff} + 3\sigma_{noisecoeff}$$

$$threshold_{tscore} = \mu_{noisetscore} + 3\sigma_{noisetscore}$$

Neurons that have both a regression coefficient and a t-score value above these thresholds are considered highly correlated to the regressor.

I created a score to quantify the responsiveness of the highly correlated neurons for an individual brain. The score for neuron j is calculated as:

$$score_j = \beta_j / threshold_{coeff} + tscore_j / threshold_{tscore}$$

The higher the score is, the more responsive is the neuron (fig.5.4.C,E).

5.2.2.3 ONset and OFFset regressors

As *DC* swim with long period of activity intersected with inactive periods of few seconds up to minutes, it is possible to look for neurons that are actives at those state transitions. I used two regressors, the ONset which characterizes the positive transition, triggering a swim, and the OFFset, which depicts the negative transition, ending an active period. To build those, I used the initiation and termination of swim events (based on the tail acquisition data) with a time window -3 s to +1 s around the initiation/termination event.

5.2.2.4 Average neuronal population across fish

To average the results from the linear regression over all brains, I used a function which estimates the response density probability on a 3D grid. It based on the *Kernel density estimation* methods, for which the kernel is a gaussian function with a standard deviation of 12.9 μm. I kept only grid elements that had a probability larger than 0.2.

5.2.3 Neuronal circuit

5.2.3.1 Maintenance neurons

To identify neurons that were recruited during spontaneous swimming periods of *DC* larvae, I performed a linear regression on the $\Delta F/F_{OFF}$ with one regressor reflecting those swim events (called *swim regressor*). By selecting only neurons that had a **positive** and high value for both their regression coefficient and their t-score, three neuronal clusters emerged (average on 11 *DC* brains). A first one is mainly localized in the medial hindbrain, where most of the neurons are projecting to the spinal cord and sending information to the motorneurons (fig.5.4,F region 1). They are forming a stripe that can comprise both glutamatergic neurons and a glycinergic stripe that has been reported as active during zebrafish larvae motion [111]. Two lateral symmetric nuclei are found in the mid-brain (fig.5.4,F region 2). Those nuclei could correspond to the mesencephalic locomotor region (MLR) which has recently been identified in ZF larvae [112].

The last main neuronal group is located on the medial mid-brain which we identified as the mesencephalic locomotion maintenance neurons (MLMNs, fig.5.4,F region 3). Those neurons are active during the long swimming periods, as it is showed in the fig.5.4.D. This correlation between the neuronal activity and the length of the active periods suggests that those neuronal nuclei are involved in the maintenance of the swimming duration, in particular the MLMNs which are more downstream in the locomotor control circuit.

Comparison with ZF larvae. Similar experiments were performed with 6 dpf ZF larvae, with the same linear regression analysis, with the only difference that fluorescence baseline

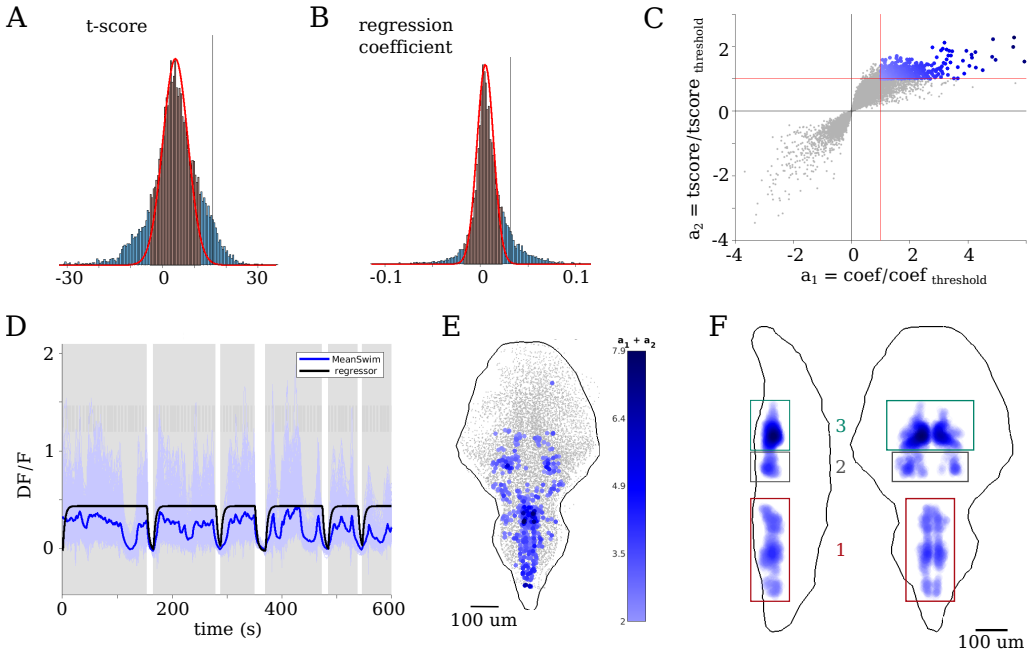

Fig. 5.4 ***Active neurons determination and maintenance neurons.*** ***A*** *t-score distribution for one brain, with in brown, the sub-distribution fitted with a gaussian model (red) and the threshold (vertical line).* ***B*** *Regression coefficient distribution for the same brain, with in brown, the sub-distribution fitted with a gaussian model (red) and the threshold (vertical line).* ***C*** *Visualization of the responsiveness score definition for maintenance neurons. Corresponding maintenance neurons localization on DC brain.* ***D*** $\Delta F/F$ *of all maintenance neurons found. Dark line: swimming regressor. Blue line: average of maintenance neuron* $\Delta F/F$*. Gray area: swim.* ***E*** *Maintenance neurons color coded with their responsiveness score.* ***F*** *Average of all maintenance neurons from 11 brains. Region 1: hindbrain. Region 2: midbrain lateral nuclei. Region 3: MLMN.*

was defined as the 10th percentile of a 50 s moving window (definition used in our laboratory). As ZF larvae performed short bout motion, I only carried out the linear regression with the corresponding swimming regressor. Results showed that similar regions than the ones found on *DC* larvae are also selected from the analysis. We found a similar cluster than the MLMNs. To strengthen the hypothesis according which MLMNs could control the length of a swim, Rajan et al. [34] activated optogenetically the MLMNs in ZF larvae. They observed an increase in the bout mean duration and frequency reinforcing the important role of the MLMNs on the swim duration maintenance.

5.2.3.2 Resting neurons

Those results are unpublished.

The first time I performed the linear regression analysis with the swim regressor, I picked the higher **absolute** value for regression coefficient and t-score, removing sign interpretation. When I plotted all the fluorescence signals selected, I could clearly identify two patterns: one in which the fluorescence signals were correlated with the swim events (the maintenance neurons described in the previous paragraph) and a second group of neurons whose calcium activity were anti-correlated with the swim regressor. This second group coincided with neurons with negative regression coefficient and t-score values. These result suggested that during inactive periods for which the *DC* larvae is not swimming, some neurons are continuously firing. I am referring to those neurons as resting neurons.

To highlight better those resting neurons, I decided to use the ON baseline (5.2.2) to consider swimming events as non-firing period for the resting neurons, and on the opposite, to consider resting events as firing period. With this baseline, the fluorescence signal of these neurons will increase with their activation (non swimming periods) and decrease at rest (swimming period). I performed another linear regression with the $\Delta F/F_{ON}$ and a regressor built on the non-swimming events of the larvae (fig.5.5,A,B).

I found different neuronal populations. A first one is located in the hindbrain of *DC* larvae (fig.5.5,C region 1). They have a different pattern than the ones found as active during swimming periods: they are more lateral and dorsal in the brain, which might match with the inhibitory GABA-ergic and glycinergic neurons pattern found in both *DC* and ZF larvae. Other wide neuronal populations are localized at the boundary between hindbrain and midbrain, that I could not identify (fig.5.5,C region 2). The most puzzling population is the top medial one in the midbrain, that seems to correspond to the raphe nucleus (fig.5.5,C region 3). This nucleus produces serotonin (5-HT), a neurotransmitter involved in numerous behaviors, and which in larval zebrafish, has been reported to increase bout frequency and to decrease resting periods [113], and that it is used in mammals to enhance locomotion ([88] used 5-HT to trigger mouse locomotion). I am discussing this result in the next section (5.3).

I plotted on a same graph the average $\Delta F/F$of maintenance and resting neurons. It is clearly visible that those two populations are anti-correlated. Even during swimming events, it is possible to observe a switch in neuronal activity (fig.5.5,D before 200 s). It might be possible to identify swimming periods directly with the activity of these neurons.

5.2.3.3 Transition events

As the active and inactive swimming periods of *DC* larvae are long compare to the fluorescence decay time of the GCaMP6s sensor, it is possible to further dissect the locomotor neuronal circuit, at the event transition. In lamprey and mice, the existence of neurons that fire to

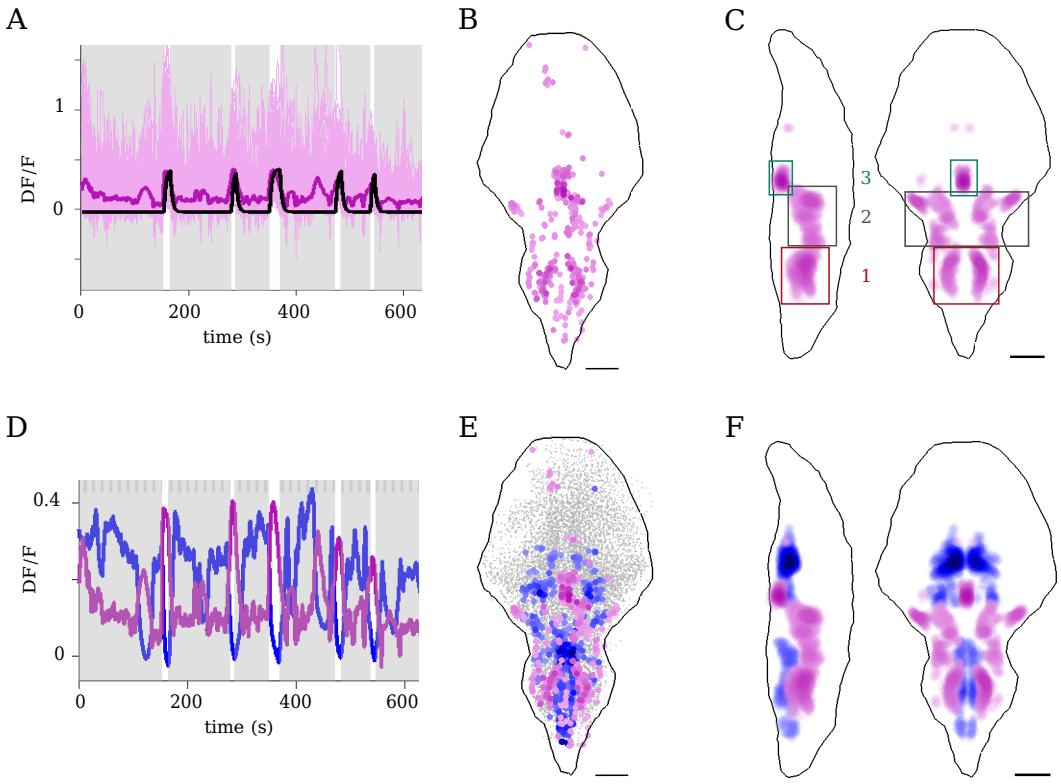

Fig. 5.5 ***Resting neurons and comparison between maintenance and resting neurons.*** ***A*** *$\Delta F/F$ of all resting neurons found (same brain than fig.5.4.E). Dark line: resting regressor. Purple line: average of resting neuron $\Delta F/F$. Gray area: swim.* ***B*** *Corresponding resting neuron localization on DC brain.* ***C*** *Average of all resting neurons from 11 brains. Region 1: hindbrain, GABA-ergic neurons. Region 2: midbrain. Region 3: raphe.* ***D*** *$\Delta F/F$ average of maintenance (blue) and resting neurons (purple). They are anti-correlated. Gray area: swim.* ***E*** *Corresponding maintenance and resting neuron localization on DC brain.* ***F*** *Superposition of maintenance and resting neuron localization on DC brain.*

favor a swim halt has been reported ([114], [88]). In fish, those neurons are not yet identified. One possible explanation is the lack of time resolution due to a similar order of magnitude between the ZF bout event ($\approx$ 200 ms), the fluorescence decay time of the calcium sensor ($\approx$ ms to s).

To do this, I defined two new regressors, each one correlated either with the rest to swim transition, the *ONset* regressor, or with the end of a swim event, the *OFFset* regressor (5.2.2.3). I used a multilinear regression with four regressors: constant, *swimming*, *ONset* and *OFFset* regressors, that I implemented on $\Delta F/F_{ON}$, $\Delta F/F_{OFF}$ and raw data.

ONset neurons. To underline neurons involved in eliciting an active period, I looked for neurons with high regression coefficients and t-score values for the ONset regressor. I plotted all the $\Delta F/F_{ON}$ of those neurons, as well as their mean activity to present positive $\Delta F/F$ values (fig.5.6.A). It appeared that most of the ONset neurons are located in the same regions as maintenance neurons. This is strongly visible when comparing the average brain for maintenance neurons (fig.5.4.F) and for ONset neurons (fig.5.6.C, annex.C.2.A). Even the mean $\Delta F/F$ of the ONset neurons is similar to the mean $\Delta F/F$ of maintenance neurons, meaning that after their excepted activity peak to start a swim event, the fluorescence signal of the ONset neurons does not go back to the baseline level but rather decays slowly.

OFFset neurons. Neurons that can trigger the end of an active period had already been identified in lamprey [114], *Xenopus* [115] and mice [88]. It is the first time that in fish, this kind of neurons is detected. I plotted all the $\Delta F/F_{OFF}$ of those neurons, as well as their mean activity to present positive $\Delta F/F$ values (fig.5.6.A). Peaks at the end of a swim period are narrower than the one for ONset neurons. OFFset neurons are also partially found in the same regions as resting neurons (fig.5.6.F and annex.C.2.C): they are part of the inhibitory GABAergic neurons in the hindbrain, located at the boundary between hindbrain and midbrain, and in the raphe nucleus. Some of those OFFset neurons are also found in the same region of the MLMNs but more dorsally.

5.2.4 Other trials

As *Danionella cerebrum* is a new emerging model, I took the opportunity to test the limit of this model and I tried diverse experiments.

5.2.4.1 Image juvenile fish from 6 to 28 dpf

I was involved in establishing preliminary results for an ANR grant application including two PhD supervisors and other collaborators. One part of this proposal consists in following the maturation of the neuronal locomotor circuit during development. This project was motivated

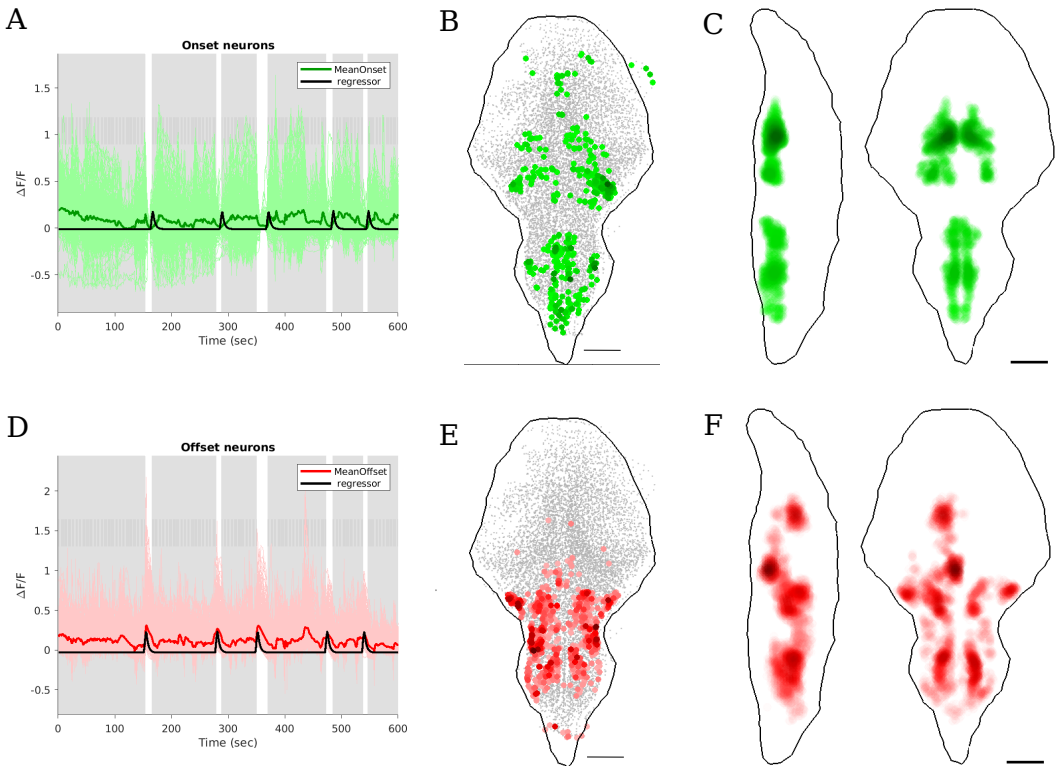

Fig. 5.6 ***ONset, OFFset neurons*** ***A*** *$\Delta F/F$ of all ONset neurons found (same brain than fig.5.4.E). Dark line: ONset regressor. Green line: average of resting neuron $\Delta F/F$. ($\Delta F/F$ off baseline). Gray area: swim.* ***B*** *Corresponding ONset neuron localization on DC brain.* ***C*** *Average of all ONset neurons from 11 brains.* ***D*** *$\Delta F/F$ of all OFFset neurons found (same brain than fig.5.4.E). Dark line: OFFset regressor. Red line: average of resting neuron $\Delta F/F$. ($\Delta F/F$ on baseline). Gray area: swim.* ***B*** *Corresponding OFFset neuron localization on DC brain.* ***C*** *Average of all OFFset neurons from 11 brains. All scale bars are measuring 100 µm.*

by the fact that *DC* are transparent at every stage of their life and that *DC* undergo a switch in their swimming pattern between the larval and the juvenile stages.

My work consisted in proving that the brain of *DC* can be easily and fully imaged from 6 dpf to 28 dpf with the 1 photon light-sheet microscope of the laboratory. The main challenges were the size of *DC* juvenile and the way they breathe. Indeed, at 6 dpf, *DC* larvae are breathing trough oxygen diffusion by the skin, but it is unknown how 28 dpf *DC* juveniles are breathing. Moreover, the holder for the larvae in the microscope was designed for capillary of 1.5 mm external diameter (0.9 mm inner diameter). At 28 dpf, the *DC* juveniles are taller and bigger (3.3).

To overcome the size problem, I designed new holders in which bigger capillaries with 2.0 mm external diameter and 1.5 mm inner diameter, that are wide enough to contain juvenile

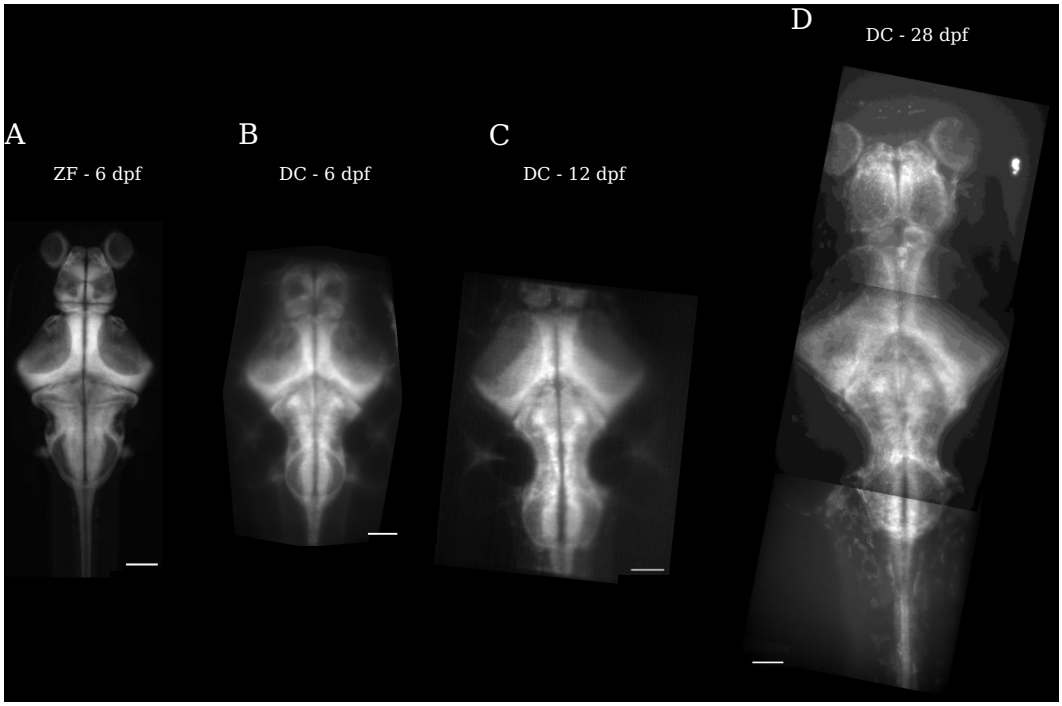

Fig. 5.7 ***Vertical projection of calcium imaging data of ZF and DC brains at different age.*** ***A*** *6 dpf ZF brain.* ***B*** *6 dpf DC brain.* ***C*** *12 dpf DC brain. Ears are taking more space.* ***D*** *28 dpf DC brain after stitching. At juvenile stage, DC brain is bigger and it is not possible to acquire the whole brain activity with our camera field of view. All scale bar measure 100 µm.*

DC. With this configuration, I succeeded to image *DC* fish at 6 dpf, 12 dpf and 28 dpf, as it is presenting on 5.7B,C,D. I did one trial with the juvenile *DC* that I kept 3 hours in 2% agar gel. I freed the fish and after one hour in a beaker at rest, it was swimming as usual. At 1 month-old, *DC* juveniles are bigger and their brain have evolved: ears develop a lot and push the hindbrain which get thicker, and the whole brain elongates. With our recording configuration, it is not possible to image *DC* 1 month-old brain in is entirety. Nevertheless, a wide brain area is still accessible.

Those preliminary results are proof of concept for the possibility to image easily *DC* from 6 to 28 dpf, and let the door open to diverse studies.

5.2.4.2 2P light sheet microscopy on *DC* larva at 6 dpf

In 2015, the laboratory published a paper presenting a new light-sheet microscope with a 2 photon laser stimulation ($\lambda = 930$ nm) [116]. This setup was developed mainly to investigate the neuronal circuit involved in processing visual stimulation without bias created by the 1 photon laser, set at 488 nm. Indeed, the most sensitive region of the fish visible spectrum is

around 500 nm ([117]), whereas, the larvae ZF are not receptive to IR light (above 900 nm, [97]). The 2 photon stimulation has other advantages as a higher penetration distance into the brain and a smaller photobleaching effect.

Even if *DC* larvae are almost fully transparent, they have some pigments located on the top of their skull (fig.3.4.B) that absorb IR light, which can be lethal for the larvae. To perform whole brain imaging with the 2 photon laser, I used *DC Tg(elavl3:H2B-GCaMP6s)* at 5 dpf without pigments (those larvae are described on the 3.2.4). I did different trials with 70 to 80 % laser power and between 30 and 40 ms camera shutter. I could image the brain of those larvae without any noticeable problem.

I also tried to image *DC* larvae that had pigments but as expected, the pigments are not suitable for this kind of imaging. In other words, if we want to perform functional imaging with a 2 photon laser, we will need to have a *DC* line without any pigments.

5.3 Discussion

As those experiments were done for preliminary results to initiate new studies. Most of the results I presented here, need to be confirmed with others techniques. In the following, I will propose speculative hypotheses regarding the brain regions where are localized the neuronal population I found on *DC* larvae. Moreover, I discuss the advantages of the techniques and analysis I used, as well as what it is more questionable and what should be done to strengthen the results.

5.3.1 Experimental setup and analysis

Baseline definition. One essential parameter I had to redefine for *DC* calcium data was the fluorescence baseline for each neuron. As explained in a previous section (5.1.2), most of the researcher are working with the $\Delta F/F$, which allows comparing relative variation on fluorescence. The methods used to calculate $\Delta F/F$and especially the fluorescence baseline are as multiple as the number of researcher (10^{th} percentiles of a 50s moving window [51], median fluorescence value selected on a 3 s-long period of inactivity [112], the average fluorescence for the whole ROI across frames when the static grating was presented [111]). That could explain why $\Delta F/F$ numerical value can be so different. Defining a good baseline is complex due to the diversity of features that can perturb it. The main issue is that the baseline value modifies the data and can totally change the result.

To assess my result, I here explain the choice I made to define my baselines. For *DC* larvae, I interpreted the fluorescence baseline as the fluorescence when a neuron is not active. As I was interested in neurons that are recruited during swim phases, I first defined the OFF baseline which corresponds to the 10^{th} percentile of the inactive periods of the larva. I also removed a few seconds around each transition step not to take into account fluorescence

increases or decays. I found the maintenance neurons, with positive $\Delta F/F$, and the resting neurons with negative $\Delta F/F$. Therefore, I also defined the ON baseline, with which I could prove that resting neurons are recruited for non-swimming periods.

For the ONset and OFFset, I performed the multilinear regression with both the OFF and ON baseline. By comparing ONset and OFFset neuronal population found with the both baselines, I did not notice huge difference, which is visible on the average brain put in annex (annex.C.1). In order to plot positive $\Delta F/F$, I favored the ONset neurons found with the OFF baseline, and the OFFset neurons with the ON baseline.

I also performed the multilinear regression on the raw data, in order to confirm by observation the neuronal population found.

Experimental setup. Thanks to morphological similarities between *DC* and ZF, we could use the light-sheet microscope without any modification. As for older fish, at 1 month-old, they are longer and bigger than the larvae, but the use of larger microcapillary allowed us to perform imaging by simply redesigning the capillary holder. However, it is still unknown when *DC* are using their gills for breathing. At 12 dpf, it seems that oxygen diffusion through the skin is still operating. It is less clear for 28 dpf fish, for which short embedded time should be found.

It is important to mention here, that *DC* larvae are more fragile than ZF and they have to be handled with care. Moreover, I observed really different spontaneous swimming behaviors: some larvae could swim for 20 to 30 min in a row, while others did not swim at all, some others were alternating between short swimming periods (less than 10 s) and similar breaks, some were swimming for long period with short resting phases, still not suitable to determine neuronal circuit dynamics. An idea to trigger swim and rest periods in *DC* could be to add a visual stimulation, such as OMR pattern moving and stopping. This technique already implemented for ZF seems to work well. The only problem is that it is not anymore a spontaneous behavior, but a visually driving swimming, which is adding complexity to the neuronal circuit as visual stimulation integration and processing has to be taken into account. Another possibility could be to introduce a water flow in the fish body direction. As its tail is free, fish can perceive mechanical forces which triggers a swimming against the flow.

To have a behavior readout, the fishtail is freed of the agarose, around the anus. Tail motion can create motion artifacts on the calcium activity data. To minimize those, larvae should be put on the microcapillary center, with homogenous agarose around it, which is complicated to control. Another solution can be to increase the percentage of mass of agarose used, with the risk to suffocate the fish and to distort the light-sheet. Using bigger capillary can also work, but with the risk to increase the distance travelled by the laser into agarose. Those motion issues are mitigated with the drift correction, but big movements are difficult to correct. This has to be thought when older *DC* will be used, as they have more strength.

Behavior extraction. Having a precise description and characterization of the tail motions in the embedded and imaged larvae is important to facilitate the identification of the underlying neuronal circuit. Calcium activity data is recorded at 1 brain volume per second, with 25 to 30 layers, i.e. one layer every 30-40 ms. It is also necessary to take into account the larva tail beat frequency, in order to have enough sample point to correctly capture the whole tail motion. In *DC* embedded larvae, the average tail beat frequency is 15 Hz (fig.5.3.D), so using an acquisition framerate of 100 Hz, allows 6 sampled point for each cycle. Moreover, the fluorescence decay of GCaMP6s is of the order of a few seconds, so with the corresponding calcium data, it is not possible to find neurons with an activity that would be modulated at the tail beat frequency. For all those reasons, I chose to record tail motion at 100 Hz.

The was to propose a first level description of neuronal populations involved in swimming pattern. Therefore, the tail motion data was only exploited at a first level, to determine when the fish was swimming or not. This restrained description allowed me to highlight four different groups of neurons. A more precise analysis on both tail data and calcium activity could lead to determine neurons that control the fish state either toward a straight swim, either toward a turning state, as it is proposed in the spontaneous swimming model (4.1.3). One difficulty will be to find on the tail motion data when the fish is turning. With the microcapillary technique, the larva can be twisted during the embedded procedure. Even if the head is aligned horizontally for the calcium activity recording, the rest of the body can be distorted and thus, the larva can have tail motions biased toward one direction or another.

Recently, Böhm et al. [118] used voltage imaging in ZF larval spinal cord and identified three groups of neurons, one of which is oscillating and is most likely constituted of V0v and V2a neurons, which have been described as the major excitatory source that drives the CPG [119]. An idea could be to combine both calcium activity recording on the brain and voltage imaging on the spinal cord, on fully embedded fish, the second data giving access to a precise left-right pattern. This dual imaging requires more development on voltage sensor and recording capacity. Electrophysiology can also work for defining tail activity with a better precision, but it is an invasive technique that interferes with spontaneous behavior.

5.3.2 Neuronal circuit

No precise brain atlas on labelling different brain region on *DC* larvae are available to date. I thus relied on the high brain anatomical and physiological similarities between *DC* and ZF larvae to identify the brain regions of interest.

Maintenance neurons. With the data I acquired and aggregated with the one used in [34], I was able to confirm the identity of the three main regions highly correlated with swimming periods. The first one is located in the hindbrain, forming two straight stripes on each side of the rostro-caudal axis (fig.5.4.F). Most of the neurons in the hindbrain send

projection to motorneurons and other kind of neurons in the spinal cord, and are known for their implication in locomotor control [111], specially the reticulo-spinal (RS) neurons [112, 120]. By comparing with the in situ hybridization and immunohistochemistry done by Rajan et al. [34], region 1 might contain both excitatory (glutamatergic) and inhibitory (glycinergic) neurons, that can act on speed modulation [121]. Again, by comparison with data from Carbo et al. [112], those maintenance neurons from region 1 might be part of the V2a RS neurons from the retropontine and medulla regions.

In vertebrates, most of the higher brain controls on locomotion are converging onto the mesencephalic locomotor region (MLR). This region has been located in numerous species such as cats [122], lamprey [123] and mice [124], etc. However, it has not been located in fish yet. In a recent study, Carbo et al. [112] proposed a putative localization for this MLR which seems to be compatible with our maintenance neurons found in region 2 (fig.5.4.F region 2). Moreover, they showed that by stimulating the MLR, some V2a RS neurons are recruited along the retropontine and medulla regions, which might correspond to the maintenance neurons from region 1. This strengthens the hypothesis that the region 2 is most likely the MLR on *DC* brain [112].

The neurons from the third region where maintenance neurons were identified, were called mesencephalic locomotor maintenance neurons (MLMNs) by Rajan et al. [34]. This region might incorporate the nMLFn (nucleus of the medial longitudinal fasiculus) which is known to send projections in the hindbrain and spinal cord [62]. In this study, we assumed that this region could modulate the activity of downstream RS neurons and thus control swimming phase duration. This region was also found on ZF larvae, for which a continuous stimulation of this area was efficient to elicit longer swim events. More experiments need to be performed to confirm this hypothesis and to understand the MLMNs' role in both species.

Resting neurons. To my knowledge, it is the first time that sustained active neurons during non-active periods, different from sleep state, are identified in fish, and in vertebrates. In mice, some V2a neuron activation favors halt in locomotion and maintains non-active period [88], but it is unclear if this neuron activation is always correlated with non-active period, as no direct recording of this cell activity has been done in parallel of VNR or in-vivo locomotion recording. It is not possible to detect them with calcium imaging in ZF larvae as the temporal resolution allowed by calcium sensors is not enough to observe a fluorescence decay during the short bouts.

A first resting neuronal population found in *DC* hindbrain: two medial stripes with circle arc shapes (fig.5.5C region 1), different from the maintenance neurons found in this region (fig.5.4.F region 1). Those resting neurons could be inhibitory GABA-ergic neurons, as suggested by comparison with the in situ hybridization and immunohistochemistry done in [34].

The second region (fig.5.5C region 2) gathers a lot of different and symmetrical populations. More investigation should be done to identify precisely the localization as well as the inhibitory or excitatory classes of those neurons.

The third and last region is the more intriguing one. Neurons seem to localize at the same area as the raphe nucleus (fig.5.5C region 3). The raphe nucleus produces serotonin neurotransmitter, which is involved in a lot of different behaviors such as locomotion [113, 125], aggression (high level of 5-HT, low aggressivity), fear, anxiety [126] and sleep initiation and maintenance [127], for example.

Surprisingly, 5-HT acts in an opposite manner in ZF larvae and adults. In the former, it has been demonstrated that after a water-flow stimulation, the calcium activity increases in serotonergic neurons of the dorsal raphe, favoring arousal [128]. Moreover, a 5-HT bath in larvae increases the bout frequency and reduces rest duration [113]. On the contrary, ZF adults exposed to 5-HT bath are less active [125].

From those published results, it is intriguing to find resting neurons on a similar area as the major source of 5-HT, the raphe nucleus. Before going any further on assumptions and questions, the precise identification of those neurons from region 3 must be checked. As no brain atlas with precise region identification is available for the *DC* brain, one possibility is to image with a high-resolution stack (see 5.2.1.2) then to perform an immunohistochemistry targeting serotonergic neurons, and to compare the two images. In the hypothesis of this comparison confirms the identification, a lot of questions arise. From an evolutionary point of view, homologous neurons and neurotransmitter can impact in different way behavior in closely related species [129]. It might be the case here as in ZF larva, 5-HT promotes swimming events whereas in *DC* , the raphe nucleus which produces 5-HT is correlated with non-active periods. Moreover, from a maturation viewpoint, 5-HT plays a different role in ZF adults, so we can wonder if it is also the case in *DC* .

To conclude on resting neurons, it is the first time that such neurons are found in fish, and more broadly in vertebrates. More experiments have to be done to correctly characterize their implications on the neuronal locomotor circuit. Precise identification of their localization, especially for the population found where the raphe nucleus is located in ZF larvae, and their type (excitatory, inhibitory). This is an interesting founding for a better understanding and description of brainstem locomotor circuit.

Transient neurons. With their long swim and resting phases, *DC* larvae allow exploring dynamics into locomotor circuits with the fluorescent calcium imaging time resolution. We tried to find neurons that can either activate swim event, the ONset neurons, either trigger a halt, the OFFset neurons. Those neurons were found respectively on the same regions as maintenance and resting neurons (fig.C.2).

I can give two hypotheses for this result. The first one is to view the maintenance/ONset

neurons, and resting/OFFset neurons as a continuous and smooth categorization. It is tempting to label every neuronal population involved in a circuit as to define specific components in an electrical circuit, for the analogy. Reality is much more complex and boundaries between transient and sustaining neuronal population might be more flexible than expected.

The second idea concerns the circuit itself. It is conceivable that triggering event neurons exist. However, among the maintenance/ONset neurons, and resting/OFFset neurons, they are a mix of inhibitory and excitatory neurons. We can hypothesize that during swimming, inhibitory maintenance neurons silence the resting neurons that inhibit the CPG generation, whereas the excitatory maintenance neurons activate this generator. In the opposite for resting neurons. In that case, switching from active to inactive is mediated by another population, more downstream from the MLR, that can come from sensory information acquisition and processing. Those latter centers might be located in the forebrain of the fish, between the eyes, a region that is difficult to access with light-sheet imaging.

5.3.3 Perspectives

Locomotor circuit identification. These results are preliminary. It will be necessary to confirm the identity of the associated brain regions. I tried to map the *DC* reference brain onto the ZF reference brain from the Zbrain atlas, but it did not work with the actual parameters used in ANTs. Even if they look really similar, the brain morphology is different. More investigations have to be done to better understand the contribution of each neuronal population to the locomotor neuronal circuit.

Locomotor circuit maturation. One of the main project supported by those results are the study of the ontogeny of the locomotor circuit. A PhD student has already started to image older fish, at 12 dpf. It appeared that at this age, embedded larvae are swimming less, pushing him to think of a way to stimulate their locomotion. We thought about adding a visual stimulation, an OMR pattern, under the fish as it is already working for ZF larvae.

Regarding older fish, as shown in a previous figure (fig.5.7.F), one month-old *DC* brain is bigger. With our recording camera field of view, it is not possible to image the whole brain, but the hindbrain and midbrain should still be accessible in their entirety. One of my concern is the fish immobilization and breathing. In ZF, gills start to be necessary for breathing between 14 and 21 dpf [130], even if oxygen diffusion through the skin is still slightly effective at adulthood in some fish species (10 to 30 %, [131]). For *DC* , I did a first test with a one month-old fish embedded for 3 hours. I observed the heart beating rate before and after the immobilization and I noticed a decrease. I freed the tail and after few hours, it was freely-swimming as before. So it seems possible to image 1-month old *DC* , for which the fluorescence intensity is similar than in larvae, and immobilization in agarose is possible. One option to solve both the few swimming events and breathing issues could be

to implement a water flow parallel to the fish body. This water flow should be slight to avoid agarose motion.

To summarize this part, I confirmed preliminary published results [34]. I showed that it is possible to define the locomotor neuronal circuit on *Danionella cerebrum* and to follow its modulation all along its development. I found at least two groups of neurons involved in this circuit: the maintenance and the resting neurons. Among the maintenance neurons, three main regions can be identified : neurons in the hindbrain, the potential mesencephalic locomotor region and the mesencephalic locomotor maintenance neurons. As for the resting neurons, it is the first time that this kind of sustainable active neurons correlated with resting periods are shown. They are located on each medial side of the hindbrain, at the boundary between hindbrain and midbrain, and maybe in the raphe nucleus. Moreover, I showed that it is possible to image *DC* brain from 6 dpf up to 28 dpf, allowing ontogenic investigation on the locomotor circuit and others.

Chapter 6

Conclusions and perspectives

6.1 Evidence accumulation in zebrafish larvae

The first project I was involved in aimed at studying the mechanisms of evidence accumulation in ZF larvae. For this, I chose to combine two different sensory reflexes : the opto-motor response and the acoustic startle escape. A first challenge was to identify when the fish had accumulated enough information to act in consequence, so in case of OMR, to orient itself in the direction of the moving visual pattern. The current way is to consider the latency between the onset of the visual stimulation and the triggering of the first bout. I observed a delay in the first bout latency response, in line with previous studies [62]. However, this first bout does not always orient the fish along the visual pattern direction, suggesting that the initiation of this first bout might not reflect evidence accumulation.

A second problem was to probe the information accumulation, before the response threshold, to observe if it could nevertheless have an impact. I chose to trigger an escape response with an acoustic stimulation, while a visual pattern was presented to elicit an OMR reflex, and to observe the triggered escape direction. As acoustic stimulation can elicit two escape responses that recruit different neuronal pathways, I was expecting that the long-latency escapes would be more affected by the visual stimulation. For this specific type of escape, results are not conclusive, even when I selected fish that should respond more. When escapes are not differentiated, the escape tend to be biased in the direction oppposite to the moving pattern direction, for visual stimulation duration of the same order as the latency observed without acoustic stimulation. An escape direction opposite the visual stimulation orientation can be explained with an ecological interpretation of the OMR, which mimics the movement of the fish reference space by the water-current. Thus, escaping against the OMR direction corresponds to flight in the water-current, which increases the fish velocity. Long-latency escapes role are still intriguing because they do not recruit Mauthner cell pathway and they seem to integrate some sensory stimulation. Due to the design of my experiment, I did not

trigger a lot of those long latency escapes. By reducing the acoustic intensity, it could be possible to obtain more long latency escape, and then to either test if long latency escapes favor multisensory integration, or if other interpretation are possible.

With time, these experiments can be improved to extend evidence accumulation, to have a larger time for exploring this mechanism (with a lower OMR speed [62]), and to elicit more long latency escapes with a lower acoustic stimulation. It could be interesting to explore the contribution of spatial and temporal integration. For the spatial contribution, the grid size of the OMR pattern can be adapted to its velocity in order to have a constant number of stripe passing under the fish, and to record the first bout latency. For the temporal integration, a possibility could be to perturb the accumulation at a given time in embedded fish with eyes freed, to trigger the OKR reflex.

From the collaboration I did with Gokul Rajan, I became aware of the existence of *Danionella cerebrum* and I decided to stop the previous project to move on another one with a lot of possibilities to explore.

6.2 *Danionella cerebrum* : a promising model

Putting effort in developing a new organism model for research is done with the objective of broadening research possibilities and to stimulate new ideas. *Danionella cerebrum* possesses a lot of interesting characteristics: it is a miniature fish, almost fully transparent during its whole lifespan, it displays a wide behavioral repertoire which includes vocal communication, shoaling and schooling. It also lacks an ossified skull on the top of its head, and its close evolutionary relationship with *Danio rerio* allows one to benefit from the rich knowledge and available techniques developed for this species, and to perform cross-comparison between organism models. Thus, a lot of perspectives are open with *DC* .

***DC* and ZF comparative study.** During my PhD, I contributed to two complementary projects. The first one aims at highlighting the evolution differences at behavioral and neuronal scales, that led to two related species that have different locomotor pattern and opposite light preference. For this, I adapted and performed free-swimming experiments and analyses on ZF and *DC* larvae to characterize their swimming patterns under a uniform light environment and with visual stimulation. The goal was to propose a model with few parameters that should reproduce their respective spontaneous exploration. A simple model has already been proposed by Karpenko et al. [35], in which only the reorientation angle between two bouts is enough to reproduce the global trajectory of ZF larvae. With a similar ambition, I tried to model *DC* continuous swimming with a run and tumble process as in bacteria [93]. However, defining the straight and turning events is challenging. Those models are built on data from a small arena, that restrains larvae movements, especially for *DC* larvae. To

bypass this problem, a larger experimental setup will be soon ready to track larvae on 30 * 30 cm space.

For light-seeking behaviors, *DC* have a negative phototaxis, and due to their transparent body, are more difficult to track. Tropotaxis and klinotaxis experiments that I designed for ZF larvae, will allow us to explore the light bias on the spontaneous locomotor model of *DC* . Then, it will be possible to compare the light impact on exploration program between both species.

Those models will then ease the identification of the neuronal circuits associated to their respective behaviors. For this, I started to use calcium imaging and light-sheet microscopy to record at single-cell resolution the whole brain of those larvae. As *DC* swimming dynamics are different from ZF, I could highlight neurons that could have not been reported with ZF short bouts. Those neurons are recruited only when *DC* are not swimming and remain silent during the swimming periods. They are mostly located on the hindbrain, but also on a region that might correspond to the raphe nucleus. I made this hypothesis based on the localization of the raphe nucleus on the ZF brain. To confirm this, it will be necessary to design an atlas of *DC* larval brain. One option is to design it entirely, which would require a large effort. A second one is to find a transformation mapping making a correspondence between *DC* larval brain and ZF larval brain, so as to reuse the existing ZF annotated brain atlas.

From the collaborative work done on *DC* [34], we also found a neuronal population called the mesencephalic locomotion maintenance neurons that are activated during swimming events in both *DC* and ZF brains. We showed that a sustained activation of those neurons on ZF led to an increase in swimming activity suggesting that their activation is correlated with swimming duration. It was not possible to test this assumption in *DC* due to the lack of transgenic lines available for optogenetic stimulation.

Effect of development on neuronal circuits. The second project takes advantage of the optical transparency of *DC* during their whole life to explore how neuronal circuits mature with development. This project will benefit from the behavioral model developed for *DC* swimming at larval stage to compare the evolution of exploration dynamics at juvenile and adult stage. With the data from MonitoRack and the free-swimming experiment I performed on 1 month-old *DC* , I showed that the swimming pattern of *DC* evolves from larval to juvenile stages. This could be the result of a rearrangement of neuronal connection. This assumption will be explored with whole brain imaging at single cell resolution, from larvae to juvenile (1 month-old) fish with major modification of the microscope setup. We will focus on the locomotor neuronal circuit as well as the sensory-motor program involved in phototaxis.

With new GCaMP probes with shorter fluorescence decay time [132], it will be possible to have a better temporal resolution for investigating the role and dynamics of the transitive neurons. Moreover, development of optogenetic lines will also favor the dissection of the

locomotor neuronal circuit.

This opportunity to follow at different developmental stages a specific neuronal circuit is unique and allows exploring maturation processes as well as aging mechanism, at different scales and in a same organism model.

***DC* limitations.** Despite their numerous advantages that are suitable for research and neuroscience, it is important to take a step back and note some limitation to *DC* as an animal model. First, as for all animal models, it is important to keep in mind that general results found with *DC* might not generalize to other species. Thus, it is important to expand the range of animal models before generalizing results.

Regarding *DC* , I succeeded in developing a fish facility in one year and a half with a colony that is now stable and allows research works. However, those fish are not as easy to grow as ZF. Indeed, they do not produce the same amount of eggs and spawning is not temporally controlled yet. Moreover, they are communal breeders which is a limiting factor for crossing transgenic lines. They are also more sensitive to variations of environmental condition, that have a direct impact on the eggs number. Finally, larvae are more fragile and need more caution when they are handled.

Most of the limitations are coming from the lack of knowledge on technical maintenance and aquaculture knowledge on this species. Thus future research works should focus on a better knowledge on *DC* husbandry.

A promising model. *Danionella cerebrum* offers multiple opportunities thanks to its natural features and its close relationship to *Danio rerio*. We decided to exploit its small size, optical transparency and repertoire behavior to concentrate our research on the mechanisms involved in evolution process and maturation during development. In most vertebrates, it is not possible to record at both behavioral and neuronal scales the effect of maturation at different stages. Thus, *Danionella cerebrum* may open a new window into the understanding of aging processes from genes, to neuronal circuits and behaviors.

Appendix A

Chapter 2

Escape /OMR duration	0 ms	250 ms	500 ms	750 ms	1000 ms
SLC + LLC (all)	0.86 (461)	0.81 (434)	0.78 (399)	0.82 (429)	0.85 (435)
SLC + LLC (g q, no b)	0.50 (265)	0.38 (206)	0.34 (176)	0.32 (165)	0.20 (102)
SLC (all)	0.83 (443)	0.76 (411)	0.67 (343)	0.72 (378)	0.75 (387)
SLC (g q, no b)	0.47 (253)	0.36 (193)	0.29 (147)	0.29 (152)	0.17 (85)
LLC (all)	0.03 (18)	0.04 (23)	0.11 (56)	0.10 (51)	0.09 (48)
LLC (g q, no b)	0.02 (12)	0.02 (13)	0.06 (29)	0.02 (13)	0.03 (17)
total fish	535	539	512	523	514

Table A.1: Escape number for the OMR and acoustic experiments. (g q, no b): good quadrant, no bout during OMR.

Parameters	Value or explanations
Background	imported for each experimental date
Binary threshold	5
Dilatation	0
Kernel size	1
Kernel type	2
Light background	0
Maximal angle	90
Maximal length	100
Maximal occlusion	100
Maximal size	1000
Maximal time	10
Minimal size	35
Morphological operation	3
Number of images background	749: by default, number of frames
Object number	1
RIO top x	0
ROI bottom x	0
ROI bottom y	0
ROI top x	0
ROI top y	0
Registration	0
Spot to track	0
Weight	0.5
layout = 1	

Table A.2: FastTrack parameters used. From parameters.param file generated by FastTrack. The version used was anterior to version 5.2.1, it needs to be converted to be use on actual version (see https://www.fasttrack.sh/docs/setParam).

Appendix B

Chapter 3

Feeding protocol for *Danionella cerebrum* (2 times a day on weekdays, 1 time a day on weekends)

Larvae

Larvae are in **beakers on the bench**. There is a button on the front of the bench to turn on a light plate under the beakers to see them better.

Beakers in the "To Feed" area (more then 5 dpf)
Preparation of food for the larvae - use the summary table

- **Count the number of beakers** in the "To Feed" area.

- **Depending on the number of beakers**, take the **corresponding volume of rotifer culture** (see summary table, (at 15g salt /L)) and put it in the beaker at the entrance to the Danionella room.

- **Add the corresponding volume of osmosis water** (see summary table) and **wait 20 minutes** for dilution (the rotifers are now in water at 5g salt/L).

- **Pass the solution of rotifers + osmosed water through a fine filter** (the one with a black edge). (These first 2 steps correspond, in a simplified way, to the protocol used to feed the zebrafish larvae).

- Using a beaker, **take the volume of system water corresponding** (see summary table), either directly into a 16 L tank or via a water outlet of the rack.

- Using a pasteur pipette, **take the rotifers from the bottom of the filter** and **place them in the beaker** containing the system water.

- **Add the corresponding number of drops of alguae** (see summary table) to the beaker. **Shake.**

- Using a 100 mL beaker, **carefully add 30 mL of system water containing the rotifers per beaker**, running it down the wall of the beaker.
If any mixture remains, distribute it first to the 3 L (juvenile) and then to the 16 L (adult) beakers.

- Wash the beakers, filter and pipettes.

Beakers in the 'Do Not Feed' section (less than 5 days)
Adding system water to the beakers - use the summary table

To prevent spontaneous evaporation of water from the beakers, it is necessary to add water every day.

- **Count the number of beakers in the "Do Not Feed" section.**

- Using a beaker, **take the volume of system water corresponding** (see summary table), either directly into a 16 L tank or via a water outlet of the rack.

- Using a 100 mL beaker, **carefully add 30 mL of system water per beaker**, running it down the wall of the beaker.

- If any system water remains, discard it in the sink.

- Wash the used beakers

- **Turn off the light plate** (button on the front of the bench).

Feeding protocol for *Danionella cerebrum* (2 times a day on weekdays, *1 time a day on weekends)*

Juveniles and adults

J**uveniles and adults** are located in the **16 L and 3 L tanks respectively**. There is a power strip on the right hand side of the tanks which can be switched on for a better view of the fish.

Preparation of food for the juveniles and adults

MORNING

- Take **200 mL of rotifer culture**. **Add 400 mL of osmosis water** and **wait 20 min** for dilution.

- Pass the rotifers + osmosis water solution through a fine filter (the one with the black edge).

- In a **tube** (falcon), **add 1 spoon (large white plastic spoon, 0.5 mL) of GM 150**. The powder is in tube in the fridge door, it is labelled 150).

- Using a pasteur pipette, **take the rotifers from the bottom of the filter** and **put them in the tube containing the powder mixture. Add 2 drops of RG** (refrigerator).

- Add 40 mL of osmosis water to the tube. Close the tube and shake.

- Using a pasteur pipette, dispense 1 mL of the mixture per 10 fish (e.g. if the tank contains 38 fish, dispense 4 mL of the mixture).
If any mixture remains, discard it.

- Clean the falcon.

- Turn off the power strip (the light behind the tanks).

AFTERNOON

- In a **tube** (falcon), **add 1 spoon (large white plastic spoon, 0.5 mL) of GM 150**. he powder is in tube in the fridge door, it is labelled 150).

- Add 40 mL of osmosis water to the tube. Close the tube and shake.

- Using a pasteur pipette, dispense 1 mL of the mixture per 10 fish (e.g. if the tank contains 38 fish, dispense 4 mL of the mixture).
If any mixture remains, discard it.

- Clean the falcon.

- Turn off the power strip (the light behind the tanks).

Summary table of feeding *Danionella cerebrum* larvae

Beaker number	Volume of rotifer culture to take (mL)	Volume of osmosis water to add, for dilution (mL)	Number of algae to add	Volume of system water to take (mL)
1	10	20	1 drop	30
2	20	40	1 drop	60
3	30	60	2 drops	90
4	40	80	2 drops	120
5	50	100	3 drops	150
6	60	120	3 drops	180
7	70	140	4 drops	210
8	80	160	4 drops	240
9	90	180	5 drops	270
10	100	200	5 drops	300
11	110	220	6 drops	330
12	120	240	6 drops	360
13	130	260	7 drops	390
14	140	280	7 drops	420
15	150	300	8 drops	450

Monitoring of water physico-chemical parameters Danionella room

Parameterrs	Monday	Tuesday	Wednesday	Thursday	Friday	Saturday	Sunday	NH4, NO2, NO3, pH
Name								
Time 1st feeding								NH4 =
Time 2nd feeding						/	/	N02 =
T° Air (°C)								NO3 =
pH								pH
T° water (°C)								
Conductivity (us/cm)								

Parameterrs	Monday	Tuesday	Wednesday	Thursday	Friday	Saturday	Sunday	NH4, NO2, NO3, pH
Name								
Time 1st feeding								NH4 =
Time 2nd feeding						/	/	N02 =
T° Air (°C)								NO3 =
pH								pH
T° water (°C)								
Conductivity (us/cm)								

Parameterrs	Monday	Tuesday	Wednesday	Thursday	Friday	Saturday	Sunday	NH4, NO2, NO3, pH
Name								
Time 1st feeding								NH4 =
Time 2nd feeding						/	/	N02 =
T° Air (°C)								NO3 =
pH								pH
T° water (°C)								
Conductivity (us/cm)								

Parameterrs	Monday	Tuesday	Wednesday	Thursday	Friday	Saturday	Sunday	NH4, NO2, NO3, pH
Name								
Time 1st feeding								NH4 =
Time 2nd feeding						/	/	N02 =
T° Air (°C)								NO3 =
pH								pH
T° water (°C)								
Conductivity (us/cm)								

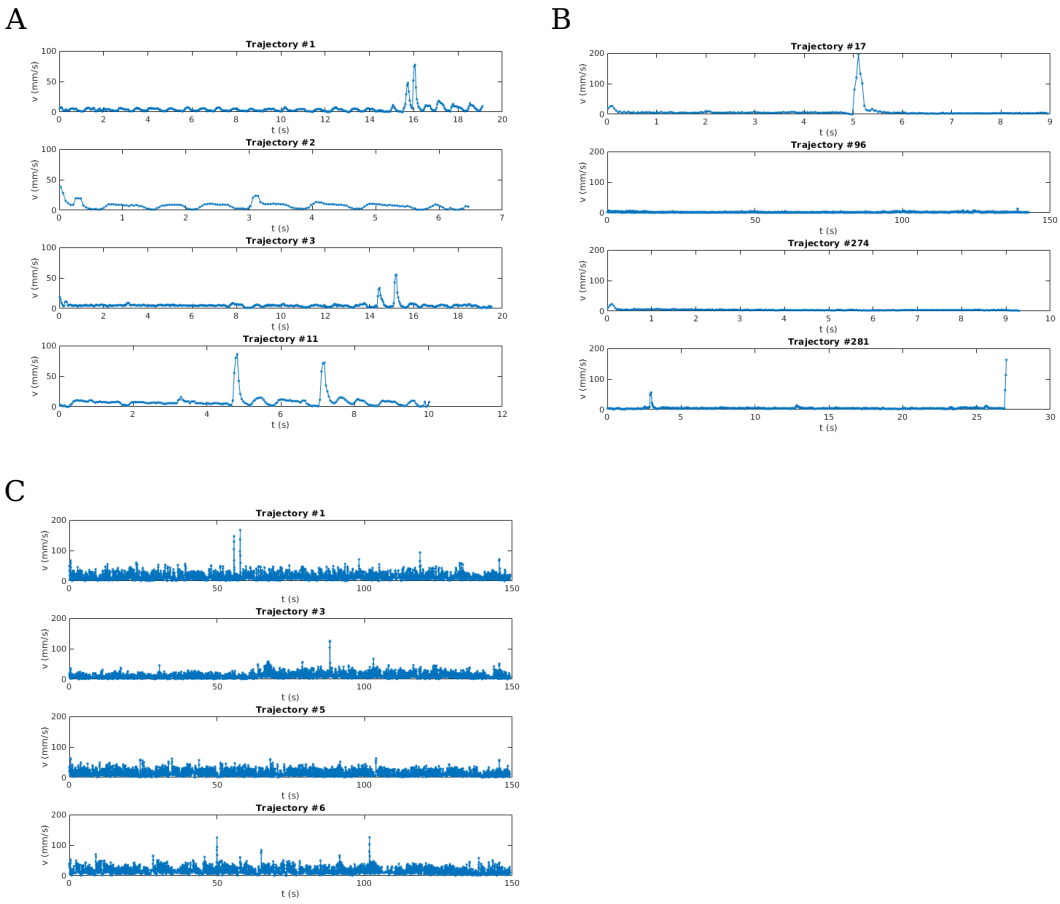

Fig. B.1 *DC fish facility parameters recording - chapter 3*

Appendix C

Chapter 5

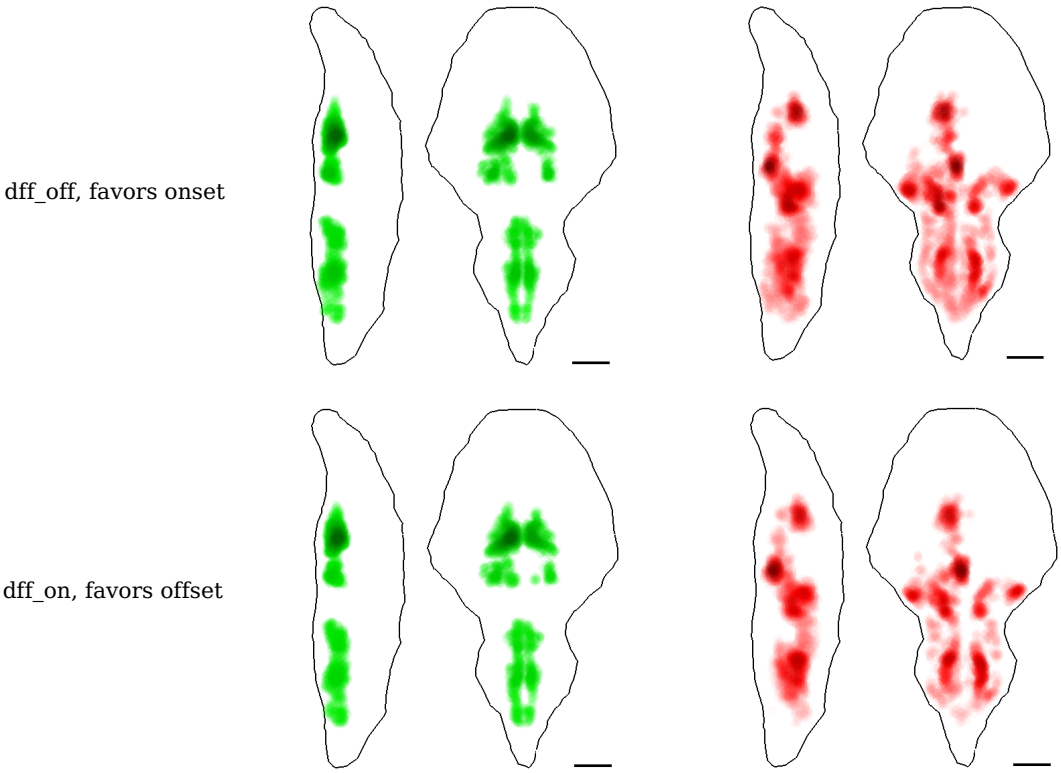

Fig. C.1 ***Comparison of the average brain for onset and offset neurons for $\Delta F/F$on and $\Delta F/F$off.*** *All scale bar measure 100 µm. - chapter 5*

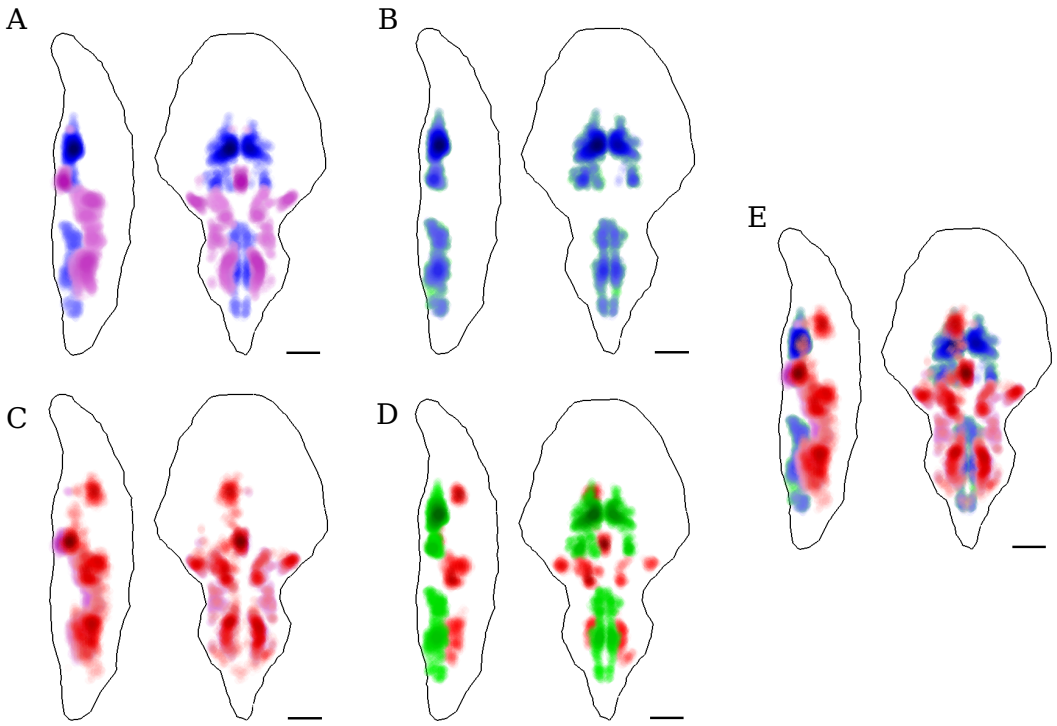

Fig. C.2 ***Comparison of the average brain.*** ***A*** *Superposition of maintenance and resting neurons.* ***B*** *Superposition of maintenance and ONset neurons.* ***C*** *Superposition of ONset and OFFset neurons.* ***D*** *Superposition of resting and OFFset neurons.* ***E*** *Superposition of maintenance, resting, ONset and OFFset neurons. All scale bar measure 100 µm. - chapter 5*

Bibliography

[1] W. M. Cowan, D. H. Harter & E. R. Kandel; "The emergence of modern neuroscience: some implications for neurology and psychiatry"; Annual review of neuroscience **23**, p. 343 (2000). 1

[2] J. S. Dittman & J. M. Kaplan; "Behavioral impact of neurotransmitter-activated G-protein-coupled receptors: muscarinic and GABAB receptors regulate Caenorhabditis elegans locomotion"; Journal of Neuroscience **28**, pp. 7104–7112 (2008). 2

[3] R. A. Jain, M. A. Wolman, K. C. Marsden, J. C. Nelson, H. Shoenhard, F. A. Echeverry, C. Szi, H. Bell, J. Skinner, E. N. Cobbs *et al.*; "A forward genetic screen in zebrafish identifies the G-protein-coupled receptor CaSR as a modulator of sensorimotor decision making"; Current Biology **28**, pp. 1357–1369 (2018). 2, 10, 11

[4] K. M. Studholme, H. S. Gompf & L. P. Morin; "Brief light stimulation during the mouse nocturnal activity phase simultaneously induces a decline in core temperature and locomotor activity followed by EEG-determined sleep"; American Journal of Physiology-Regulatory, Integrative and Comparative Physiology **304**, pp. R459–R471 (2013). 2

[5] G. Le Goc, J. Lafaye, S. Karpenko, V. Bormuth, R. Candelier & G. Debrégeas; "Thermal Modulation of Zebrafish Exploratory Statistics Reveals Constraints on Individual Behavioral Variability"; BMC Biology **19**, p. 208 (2021). 2, 10, 42

[6] S. Tümpel, L. M. Wiedemann & R. Krumlauf; "Hox genes and segmentation of the vertebrate hindbrain"; Current topics in developmental biology **88**, pp. 103–137 (2009). 3

[7] T. M. Jessell; "Neuronal specification in the spinal cord: inductive signals and transcriptional codes"; Nature Reviews Genetics **1**, pp. 20–29 (2000). 3

[8] P. S. Katz; "Neural mechanisms underlying the evolvability of behaviour"; Philosophical Transactions of the Royal Society B: Biological Sciences **366**, pp. 2086–2099 (2011). 3

[9] S. J. Cook, T. A. Jarrell, C. A. Brittin, Y. Wang, A. E. Bloniarz, M. A. Yakovlev, K. C. Nguyen, L. T.-H. Tang, E. A. Bayer, J. S. Duerr *et al.*; "Whole-animal connectomes of both Caenorhabditis elegans sexes"; Nature **571**, pp. 63–71 (2019). 3

[10] J. G. White, E. Southgate, J. N. Thomson, S. Brenner *et al.*; "The structure of the nervous system of the nematode Caenorhabditis elegans"; Philos Trans R Soc Lond B Biol Sci **314**, pp. 1–340 (1986). 3

[11] J. Keifer & C. H. Summers; "Putting the "biology" back into "neurobiology": the strength of diversity in animal model systems for neuroscience research"; Frontiers in Systems Neuroscience **10**, p. 69 (2016). 3

[12] J. S. Nelson, T. C. Grande & M. V. Wilson; *Fishes of the World* (John Wiley & Sons) (2016). 4

[13] G. Streisinger, C. Walker, N. Dower, D. Knauber & F. Singer; "Production of clones of homozygous diploid zebra fish (Brachydanio rerio)"; Nature **291**, pp. 293–296 (1981). 4

[14] E. Dreosti, G. Lopes, A. R. Kampff & S. W. Wilson; "Development of social behavior in young zebrafish"; Frontiers in neural circuits **9**, p. 39 (2015). 4, 24, 37, 59

[15] G. Sumbre & G. G. De Polavieja; "The world according to zebrafish: how neural circuits generate behavior"; (2014). 4

[16] S. A. Budick & D. M. O'Malley; "Locomotor repertoire of the larval zebrafish: swimming, turning and prey capture"; Journal of Experimental Biology **203**, pp. 2565–2579 (2000). 4, 9, 42

[17] K. Fero, T. Yokogawa & H. A. Burgess; "The behavioral repertoire of larval zebrafish"; in "Zebrafish models in neurobehavioral research," pp. 249–291 (Springer) (2011). 4, 9, 42, 43

[18] J. A. Lister, C. P. Robertson, T. Lepage, S. L. Johnson & D. W. Raible; "Nacre encodes a zebrafish microphthalmia-related protein that regulates neural-crest-derived pigment cell fate"; Development **126**, pp. 3757–3767 (1999). 4, 5

[19] S. Karpenko; *Naviguer avec la lumière: du comportement aux circuits neuronaux chez la larve de poisson zèbre*; Ph.D. thesis (2020). 5, 47, 54, 55

[20] T. Panier, S. A. Romano, R. Olive, T. Pietri, G. Sumbre, R. Candelier & G. Debrégeas; "Fast Functional Imaging of Multiple Brain Regions in Intact Zebrafish Larvae Using Selective Plane Illumination Microscopy"; Frontiers in Neural Circuits **7** (2013). ISSN 1662-5110. 5, 67, 69

[21] M. B. Ahrens, M. B. Orger, D. N. Robson, J. M. Li & P. J. Keller; "Whole-brain functional imaging at cellular resolution using light-sheet microscopy"; Nature methods **10**, pp. 413–420 (2013). 5, 67

[22] K. Naruse, M. Tanaka & H. Takeda; *Medaka: a model for organogenesis, human disease, and evolution* (Springer Science & Business Media) (2011). 6

[23] Y. Kim, H. G. Nam & D. R. Valenzano; "The short-lived African turquoise killifish: an emerging experimental model for ageing"; Disease models & mechanisms **9**, pp. 115–129 (2016). 6

[24] D. P. Baumann & A. Ingalls; "Mexican tetra (Astyanax mexicanus): biology, husbandry, and experimental protocols"; in "Laboratory Fish in Biomedical Research," pp. 311–347 (Elsevier) (2022). 6

[25] J. Kowalko; "Utilizing the blind cavefish Astyanax mexicanus to understand the genetic basis of behavioral evolution"; Journal of Experimental Biology **223**, p. jeb208835 (2020). 6

[26] Wikipédia; "Oryzias latipes — Wikipédia, l'encyclopédie libre"; (2020). http://fr.wikipedia.org/w/index.php?title=Oryzias_latipes&oldid=177721388; [En ligne; Page disponible le 17-décembre-2020]. 6

[27] H. Bilandžija, B. Hollifield, M. Steck, G. Meng, M. Ng, A. D. Koch, R. Gračan, H. Ćetković, M. L. Porter, K. J. Renner *et al.*; "Phenotypic plasticity as a mechanism of cave colonization and adaptation"; Elife **9**, p. e51830 (2020). 6

[28] E. N. Rittmeyer, A. Allison, M. C. Gründler, D. K. Thompson & C. C. Austin; "Ecological guild evolution and the discovery of the world's smallest vertebrate"; PLoS one **7**, p. e29797 (2012). 6, 7

[29] R. Britz & K. Conway; "Osteology of Paedocypris, a miniature and highly developmentally truncated fish (Teleostei: Ostariophysi: Cyprinidae)"; Journal of Morphology **270**, pp. 389–412 (2009). 6

[30] L. Schulze, J. Henninger, M. Kadobianskyi, T. Chaigne, A. I. Faustino, N. Hakiy, S. Albadri, M. Schuelke, L. Maler, F. Del Bene *et al.*; "Transparent Danionella translucida as a genetically tractable vertebrate brain model"; Nature methods **15**, pp. 977–983 (2018). 6, 24, 25, 33, 38, 52

[31] M. Kottelat, R. Britz, T. H. Hui & K.-E. Witte; "Paedocypris, a new genus of Southeast Asian cyprinid fish with a remarkable sexual dimorphism, comprises the world's smallest vertebrate"; Proceedings of the Royal Society B: Biological Sciences **273**, pp. 895–899 (2006). 7

[32] T. R. Roberts; "Danionella translucida, a new genus and species of cyprinid fish from Burma, one of the smallest living vertebrates"; Environmental Biology of Fishes **16**, pp. 231–241 (1986). 7, 23

[33] R. Britz, K. W. Conway & L. Rüber; "The emerging vertebrate model species for neurophysiological studies is Danionella cerebrum, new species (Teleostei: Cyprinidae)"; Scientific reports **11**, pp. 1–11 (2021). 7, 23, 24, 26

[34] G. Rajan, J. Lafaye, G. Faini, M. Carbo-Tano, K. Duroure, D. Tanese, T. Panier, R. Candelier, J. Henninger, R. Britz *et al.*; "Evolutionary divergence of locomotion in two related vertebrate species"; Cell Reports **38**, p. 110585 (2022). 7, 8, 24, 25, 30, 31, 39, 42, 43, 45, 57, 58, 59, 63, 68, 71, 75, 83, 84, 87, 91

[35] S. Karpenko, S. Wolf, J. Lafaye, G. Le Goc, T. Panier, V. Bormuth, R. Candelier & G. Debrégeas; "From behavior to circuit modeling of light-seeking navigation in zebrafish larvae"; Elife **9**, p. e52882 (2020). 9, 10, 15, 41, 42, 43, 44, 45, 48, 49, 53, 55, 90

[36] H. A. Burgess & M. Granato; "Modulation of locomotor activity in larval zebrafish during light adaptation"; Journal of Experimental Biology **210**, pp. 2526–2539 (2007). 9, 10, 11

[37] H. A. Burgess & M. Granato; "Modulation of locomotor activity in larval zebrafish during light adaptation"; Journal of Experimental Biology **210**, pp. 2526–2539 (2007). 9, 10, 11

[38] M. B. McElligott & D. M. O'Malley; "Prey tracking by larval zebrafish: axial kinematics and visual control"; Brain, behavior and evolution **66**, pp. 177–196 (2005). 9

[39] I. H. Bianco, A. R. Kampff & F. Engert; "Prey capture behavior evoked by simple visual stimuli in larval zebrafish"; Frontiers in systems neuroscience **5**, p. 101 (2011). 9, 10

[40] J. C. Marques, S. Lackner, R. Félix & M. B. Orger; "Structure of the Zebrafish Locomotor Repertoire Revealed with Unsupervised Behavioral Clustering"; Current Biology **28**, pp. 181–195.e5 (2018). ISSN 09609822. 9, 43

[41] T. W. Dunn, Y. Mu, S. Narayan, O. Randlett, E. A. Naumann, C.-T. Yang, A. F. Schier, J. Freeman, F. Engert & M. B. Ahrens; "Brain-wide mapping of neural activity controlling zebrafish exploratory locomotion"; Elife **5**, p. e12741 (2016). 10

[42] S. Wolf, A. M. Dubreuil, T. Bertoni, U. L. Böhm, V. Bormuth, R. Candelier, S. Karpenko, D. G. Hildebrand, I. H. Bianco, R. Monasson *et al.*; "Sensorimotor computation underlying phototaxis in zebrafish"; Nature communications **8**, pp. 1–12 (2017). 10, 53

[43] M. Haesemeyer, D. N. Robson, J. M. Li, A. F. Schier & F. Engert; "The structure and timescales of heat perception in larval zebrafish"; Cell systems **1**, pp. 338–348 (2015). 10, 42

[44] F. Kermen, L. Darnet, C. Wiest, F. Palumbo, J. Bechert, O. Uslu & E. Yaksi; "Stimulus-specific behavioral responses of zebrafish to a large range of odors exhibit individual variability"; Bmc Biology **18**, pp. 1–16 (2020). 10

[45] R. Olive, S. Wolf, A. Dubreuil, V. Bormuth, G. Debrégeas & R. Candelier; "Rheotaxis of larval zebrafish: behavioral study of a multi-sensory process"; Frontiers in systems neuroscience **10**, p. 14 (2016). 10, 42

[46] R. Eaton, R. Lee & M. Foreman; "The Mauthner cell and other identified neurons of the brainstem escape network of fish"; Progress in neurobiology **63**, pp. 467–485 (2001). 10, 11

[47] T. W. Dunn, C. Gebhardt, E. A. Naumann, C. Riegler, M. B. Ahrens, F. Engert & F. Del Bene; "Neural circuits underlying visually evoked escapes in larval zebrafish"; Neuron **89**, pp. 613–628 (2016). 10, 11, 53

[48] M. B. Orger, A. R. Kampff, K. E. Severi, J. H. Bollmann & F. Engert; "Control of visually guided behavior by distinct populations of spinal projection neurons"; Nature neuroscience **11**, pp. 327–333 (2008). 10, 11

[49] S. S. Easter Jr & G. N. Nicola; "The development of vision in the zebrafish (Danio rerio)"; Developmental biology **180**, pp. 646–663 (1996). 10, 53

[50] I. H. Bianco, L.-H. Ma, D. Schoppik, D. N. Robson, M. B. Orger, J. C. Beck, J. M. Li, A. F. Schier, F. Engert & R. Baker; "The tangential nucleus controls a gravito-inertial vestibulo-ocular reflex"; Current Biology **22**, pp. 1285–1295 (2012). 10

[51] G. Migault, T. L. van der Plas, H. Trentesaux, T. Panier, R. Candelier, R. Proville, B. Englitz, G. Debrégeas & V. Bormuth; "Whole-brain calcium

imaging during physiological vestibular stimulation in larval zebrafish"; Current Biology **28**, pp. 3723–3735 (2018). 10, 65, 66, 69, 73, 81

[52] V. Haikala, M. Joesch, A. Borst & A. S. Mauss; "Optogenetic control of fly optomotor responses"; Journal of Neuroscience **33**, pp. 13927–13934 (2013). 10

[53] G. D. McCann & G. MacGinitie; "Optomotor response studies of insect vision"; Proceedings of the Royal Society of London. Series B. Biological Sciences **163**, pp. 369–401 (1965). 10

[54] G. Arnold; "Rheotropism in fishes"; Biological reviews **49**, pp. 515–576 (1974). 10

[55] M. B. Orger & H. Baier; "Channeling of red and green cone inputs to the zebrafish optomotor response"; Visual neuroscience **22**, pp. 275–281 (2005). 10

[56] J. Abdeljalil, M. Hamid, O. Abdel-Mouttalib, R. Stéphane, R. Raymond, A. Johan, S. José, C. Pierre & P. Serge; "The optomotor response: a robust first-line visual screening method for mice"; Vision research **45**, pp. 1439–1446 (2005). 10

[57] M. B. Orger, E. Gahtan, A. Muto, P. Page-McCaw, M. C. Smear & H. Baier; "Behavioral screening assays in zebrafish"; in "Methods in cell biology," , volume 77pp. 53–68 (Elsevier) (2004). 10

[58] F. Richards, W. Alderton, G. Kimber, Z. Liu, I. Strang, W. Redfern, J.-P. Valentin, M. Winter & T. Hutchinson; "Validation of the use of zebrafish larvae in visual safety assessment"; Journal of pharmacological and toxicological methods **58**, pp. 50–58 (2008). 10

[59] E. A. Naumann, J. E. Fitzgerald, T. W. Dunn, J. Rihel, H. Sompolinsky & F. Engert; "From whole-brain data to functional circuit models: the zebrafish optomotor response"; Cell **167**, pp. 947–960 (2016). 10

[60] I. Rock & D. Smith; "The optomotor response and induced motion of the self"; Perception **15**, pp. 497–502 (1986). 10

[61] M. B. Orger, M. C. Smear, S. M. Anstis & H. Baier; "Perception of Fourier and non-Fourier motion by larval zebrafish"; Nature neuroscience **3**, pp. 1128–1133 (2000). 10

[62] K. E. Severi, R. Portugues, J. C. Marques, D. M. O'Malley, M. B. Orger & F. Engert; "Neural control and modulation of swimming speed in the larval zebrafish"; Neuron **83**, pp. 692–707 (2014). 11, 14, 20, 21, 42, 84, 89, 90

[63] E. Brustein, L. Saint-Amant, R. R. Buss, M. Chong, J. R. McDearmid & P. Drapeau; "Steps during the development of the zebrafish locomotor network"; Journal of Physiology-Paris **97**, pp. 77–86 (2003). 11

[64] S. DasGupta, C. H. Ferreira & G. Miesenböck; "FoxP influences the speed and accuracy of a perceptual decision in Drosophila"; Science **344**, pp. 901–904 (2014). 12

[65] O. Odoemene, S. Pisupati, H. Nguyen & A. K. Churchland; "Visual evidence accumulation guides decision-making in unrestrained mice"; Journal of Neuroscience **38**, pp. 10143–10155 (2018). 12

[66] J. D. Roitman & M. N. Shadlen; "Response of neurons in the lateral intraparietal area during a combined visual discrimination reaction time task"; Journal of neuroscience **22**, pp. 9475–9489 (2002). 12

[67] B. W. Brunton, M. M. Botvinick & C. D. Brody; "Rats and humans can optimally accumulate evidence for decision-making"; Science **340**, pp. 95–98 (2013). 12

[68] E. I. Dragomir, V. Štih & R. Portugues; "Evidence accumulation during a sensorimotor decision task revealed by whole-brain imaging"; Nature Neuroscience **23**, pp. 85–93 (2020). 12

[69] A. Bahl & F. Engert; "Neural circuits for evidence accumulation and decision making in larval zebrafish"; Nature neuroscience **23**, pp. 94–102 (2020). 12

[70] R. Olive; *Perception des écoulements et des vibrations chez la larve de poisson-zèbre: étude comportementale et imagerie*; Ph.D. thesis; Université Pierre et Marie Curie-Paris VI (2015). 13

[71] B. Gallois & R. Candelier; "FastTrack: an open-source software for tracking varying numbers of deformable objects"; PLoS computational biology **17**, p. e1008697 (2021). 15

[72] P. Berens; "CircStat: a MATLAB toolbox for circular statistics"; Journal of statistical software **31**, pp. 1–21 (2009). 16

[73] R. Britz; "Danionella mirifica, a new species of miniature fish from Upper Myanmar (Ostariophysi: Cyprinidae)"; Ichthyological Exploration of Freshwaters **14**, pp. 217–222 (2003). 23

[74] R. Britz, K. W. Conway & L. Rüber; "Spectacular morphological novelty in a miniature cyprinid fish, Danionella dracula n. sp." Proceedings of the Royal Society B: Biological Sciences **276**, pp. 2179–2186 (2009). 23, 26

[75] R. Britz; "Danionella priapus, a new species of miniature cyprinid fish from West Bengal, India (Teleostei: Cypriniformes: Cyprinidae)"; Zootaxa **2277**, pp. 53–60 (2009). 23

[76] Y. Hu, A. Mauri, J. Donahue, R. Singh, B. Acosta & S. McMenamin; "Thyroid hormone coordinates developmental trajectories but does not underlie developmental truncation in danionins"; Developmental Dynamics **248**, pp. 1144–1154 (2019). 24

[77] R. Britz & K. W. Conway; "Danionella dracula, an escape from the cypriniform Bauplan via developmental truncation?" Journal of morphology **277**, pp. 147–166 (2016). 24, 26

[78] R. L. Tatarsky, Z. Guo, S. C. Campbell, H. Kim, W. Fang, J. T. Perelmuter, E. R. Schuppe, H. K. Reeve & A. H. Bass; "Acoustic and postural displays in a miniature and transparent teleost fish, Danionella dracula"; bioRxiv (2021). 24, 25, 33

[79] A. Penalva, J. Bedke, E. S. Cook, J. P. Barrios, E. P. Bertram & A. D. Douglass; "Establishment of the miniature fish species Danionella translucida as a genetically and optically tractable neuroscience model"; bioRxiv p. 444026 (2018). 24, 25

[80] D. M. Chow, D. Sinefeld, K. E. Kolkman, D. G. Ouzounov, N. Akbari, R. Tatarsky, A. Bass, C. Xu & J. R. Fetcho; "Deep three-photon imaging of the brain in intact adult zebrafish"; Nature methods **17**, pp. 605–608 (2020). 24

[81] N. Akbari, R. L. Tatarsky, A. H. Bass & C. Xu; "Whole-brain optical access in small adult vertebrates with two-and three-photon microscopy"; bioRxiv (2021). 24

[82] M. Kadobianskyi, L. Schulze, M. Schuelke & B. Judkewitz; "Hybrid genome assembly and annotation of Danionella translucida"; Scientific data **6**, pp. 1–7 (2019). 24

[83] G. Rajan, K. Duroure & F. Del Bene; "Danionella translucida, a tankful of new opportunities"; in "Laboratory Fish in Biomedical Research," pp. 409–418 (Elsevier) (2022). 28

[84] C. B. Kimmel, W. W. Ballard, S. R. Kimmel, B. Ullmann & T. F. Schilling; "Stages of embryonic development of the zebrafish"; Developmental dynamics **203**, pp. 253–310 (1995). 31, 38

[85] S. K. McMenamin & D. M. Parichy; "Metamorphosis in teleosts"; Current topics in developmental biology **103**, pp. 127–165 (2013). 32

[86] L. A. Fuiman & P. W. Webb; "Ontogeny of routine swimming activity and performance in zebra danios (Teleostei: Cyprinidae)"; Animal Behaviour **36**, pp. 250–261 (1988). 36

[87] M. W. Hurd & G. M. Cahill; "Entraining signals initiate behavioral circadian rhythmicity in larval zebrafish"; Journal of biological rhythms **17**, pp. 307–314 (2002). 37

[88] J. Bouvier, V. Caggiano, R. Leiras, V. Caldeira, C. Bellardita, K. Balueva, A. Fuchs & O. Kiehn; "Descending command neurons in the brainstem that halt locomotion"; Cell **163**, pp. 1191–1203 (2015). 42, 76, 78, 84

[89] X. Chen & F. Engert; "Navigational strategies underlying phototaxis in larval zebrafish"; Frontiers in systems neuroscience **8**, p. 39 (2014). 42, 53

[90] J. Olszewski, M. Haehnel, M. Taguchi & J. C. Liao; "Zebrafish larvae exhibit rheotaxis and can escape a continuous suction source using their lateral line"; PloS one **7**, p. e36661 (2012). 42

[91] R. E. Johnson, S. Linderman, T. Panier, C. L. Wee, E. Song, K. J. Herrera, A. Miller & F. Engert; "Probabilistic models of larval zebrafish behavior reveal structure on many scales"; Current Biology **30**, pp. 70–82 (2020). 43, 61

[92] J. L. van Leeuwen, C. J. Voesenek & U. K. Müller; "How body torque and Strouhal number change with swimming speed and developmental stage in larval zebrafish"; Journal of The Royal Society Interface **12**, p. 20150479 (2015). 43

[93] H. C. Berg & D. A. Brown; "Chemotaxis in Escherichia coli analysed by three-dimensional tracking"; Nature **239**, pp. 500–504 (1972). 45, 48, 90

[94] H. A. Burgess, H. Schoch & M. Granato; "Distinct retinal pathways drive spatial orientation behaviors in zebrafish navigation"; Current biology **20**, pp. 381–386 (2010). 53

[95] G. Rajan; *Divergence of exploratory locomotion and the underlying neuronal circuitry in two closely related vertebrate species*; Ph.D. thesis; Université Paris sciences et lettres (2020). 56

[96] E. Serra, C. Medalha & R. Mattioli; "Natural preference of zebrafish (Danio rerio) for a dark environment"; Brazilian journal of medical and biological research **32**, pp. 1551–1553 (1999). 56

[97] S. Hartmann, R. Vogt, J. Kunze, A. Rauschert, K.-D. Kuhnert, J. Wanzenböck, D. K. Lamatsch & K. Witte; "Zebrafish larvae show negative phototaxis to near-infrared light"; PloS one **13**, p. e0207264 (2018). 60, 81

[98] M. Scanziani & M. Häusser; "Electrophysiology in the Age of Light"; Nature **461**, pp. 930–939 (2009). ISSN 0028-0836, 1476-4687. 64

[99] R. Yuste; "From the Neuron Doctrine to Neural Networks"; Nature Reviews Neuroscience **16**, pp. 487–497 (2015). ISSN 1471-003X, 1471-0048. 64

[100] M. Brini, T. Calì, D. Ottolini & E. Carafoli; "Neuronal calcium signaling: function and dysfunction"; Cellular and molecular life sciences **71**, pp. 2787–2814 (2014). 64

[101] C. Grienberger & A. Konnerth; "Imaging Calcium in Neurons"; Neuron **73**, pp. 862–885 (2012). ISSN 08966273. 65

[102] J. Nakai, M. Ohkura & K. Imoto; "A high signal-to-noise Ca2+ probe composed of a single green fluorescent protein"; Nature biotechnology **19**, pp. 137–141 (2001). 65

[103] J. Tubiana, S. Wolf, T. Panier & G. Debregeas; "Blind Deconvolution for Spike Inference from Fluorescence Recordings"; Journal of Neuroscience Methods **342**, p. 108763 (2020). ISSN 01650270. 65

[104] H. Dana, Y. Sun, B. Mohar, B. K. Hulse, A. M. Kerlin, J. P. Hasseman, G. Tsegaye, A. Tsang, A. Wong, R. Patel, J. J. Macklin, Y. Chen, A. Konnerth, V. Jayaraman, L. L. Looger, E. R. Schreiter, K. Svoboda & D. S. Kim; "High-Performance Calcium Sensors for Imaging Activity in Neuronal Populations and Microcompartments"; Nature Methods **16**, pp. 649–657 (2019). ISSN 1548-7091, 1548-7105. 66

[105] R. K. Benninger & D. W. Piston; "Two-photon excitation microscopy for the study of living cells and tissues"; Current protocols in cell biology **59**, pp. 4–11 (2013). 66

[106] J. Huisken, J. Swoger, F. Del Bene, J. Wittbrodt & E. H. Stelzer; "Optical sectioning deep inside live embryos by selective plane illumination microscopy"; Science **305**, pp. 1007–1009 (2004). 66

[107] B.-C. Chen, W. R. Legant, K. Wang, L. Shao, D. E. Milkie, M. W. Davidson, C. Janetopoulos, X. S. Wu, J. A. Hammer III, Z. Liu *et al.*; "Lattice light-sheet microscopy: imaging molecules to embryos at high spatiotemporal resolution"; Science **346**, p. 1257998 (2014). 66

[108] B. B. Avants, N. Tustison, G. Song *et al.*; "Advanced normalization tools (ANTS)"; Insight j **2**, pp. 1–35 (2009). 68

[109] G. Marquart, K. Tabor, E. Horstick, M. Brown, A. Geoca, N. Polys & H. Burgess; "High-precision registration between zebrafish brain atlases using symmetric diffeomorphic normalization. Gigascience, 6 (8)"; (2017). 69

[110] A. Miri, K. Daie, R. D. Burdine, E. Aksay & D. W. Tank; "Regression-based identification of behavior-encoding neurons during large-scale optical imaging of neural activity at cellular resolution"; Journal of neurophysiology **105**, pp. 964–980 (2011). 73

[111] K. E. Severi, U. L. Böhm & C. Wyart; "Investigation of hindbrain activity during active locomotion reveals inhibitory neurons involved in sensorimotor processing"; Scientific reports **8**, pp. 1–11 (2018). 74, 81, 84

[112] M. Carbo-Tano, M. Lapoix, X. Jia, F. Auclair, R. Dubuc & C. Wyart; "Functional coupling of the mesencephalic locomotor region and V2a reticulospinal neurons driving forward locomotion"; bioRxiv (2022). 74, 81, 84

[113] E. Brustein, M. Chong, B. Holmqvist & P. Drapeau; "Serotonin patterns locomotor network activity in the developing zebrafish by modulating quiescent periods"; Journal of neurobiology **57**, pp. 303–322 (2003). 76, 85

[114] S. Grätsch, F. Auclair, O. Demers, E. Auguste, A. Hanna, A. Büschges & R. Dubuc; "A brainstem neural substrate for stopping locomotion"; Journal of Neuroscience **39**, pp. 1044–1057 (2019). 78

[115] R. Perrins, A. Walford & A. Roberts; "Sensory activation and role of inhibitory reticulospinal neurons that stop swimming in hatchling frog tadpoles"; Journal of Neuroscience **22**, pp. 4229–4240 (2002). 78

[116] S. Wolf, W. Supatto, G. Debrégeas, P. Mahou, S. G. Kruglik, J.-M. Sintes, E. Beaurepaire & R. Candelier; "Whole-Brain Functional Imaging with Two-Photon Light-Sheet Microscopy"; Nature Methods **12**, pp. 379–380 (2015). ISSN 1548-7091, 1548-7105. 80

[117] M. L. Risner, E. Lemerise, E. V. Vukmanic & A. Moore; "Behavioral spectral sensitivity of the zebrafish (Danio rerio)"; Vision research **46**, pp. 2625–2635 (2006). 81

[118] U. L. Böhm, Y. Kimura, T. Kawashima, M. B. Ahrens, S.-i. Higashijima, F. Engert & A. E. Cohen; "Voltage imaging identifies spinal circuits that modulate locomotor adaptation in zebrafish"; Neuron **110**, pp. 1211–1222 (2022). 83

[119] E. E. Ljunggren, S. Haupt, J. Ausborn, K. Ampatzis & A. El Manira; "Optogenetic activation of excitatory premotor interneurons is sufficient to generate coordinated locomotor activity in larval zebrafish"; Journal of Neuroscience **34**, pp. 134–139 (2014). 83

[120] L. Ruder & S. Arber; "Brainstem circuits controlling action diversification"; Annual review of neuroscience **42**, pp. 485–504 (2019). 84

[121] P. Capelli, C. Pivetta, M. Soledad Esposito & S. Arber; "Locomotor speed control circuits in the caudal brainstem"; Nature **551**, pp. 373–377 (2017). 84

[122] M. L. Shik; "Control of walking and running by means of electrical stimulation of the midbrain"; Biophysics **11**, pp. 659–666 (1966). 84

[123] M. G. Sirota, G. V. Di Prisco & R. Dubuc; "Stimulation of the mesencephalic locomotor region elicits controlled swimming in semi-intact lampreys"; European Journal of Neuroscience **12**, pp. 4081–4092 (2000). 84

[124] A. M. Lee, J. L. Hoy, A. Bonci, L. Wilbrecht, M. P. Stryker & C. M. Niell; "Identification of a brainstem circuit regulating visual cortical state in parallel with locomotion"; Neuron **83**, pp. 455–466 (2014). 84

[125] J. P. Gabriel, R. Mahmood, A. Kyriakatos, I. Söll, G. Hauptmann, R. L. Calabrese & A. El Manira; "Serotonergic modulation of locomotion in zebrafish—endogenous release and synaptic mechanisms"; Journal of Neuroscience **29**, pp. 10387–10395 (2009). 85

[126] C. Lillesaar; "The serotonergic system in fish"; Journal of chemical neuroanatomy **41**, pp. 294–308 (2011). 85

[127] G. Oikonomou, M. Altermatt, R.-w. Zhang, G. M. Coughlin, C. Montz, V. Gradinaru & D. A. Prober; "The serotonergic raphe promote sleep in zebrafish and mice"; Neuron **103**, pp. 686–701 (2019). 85

[128] T. Yokogawa, M. C. Hannan & H. A. Burgess; "The dorsal raphe modulates sensory responsiveness during arousal in zebrafish"; Journal of Neuroscience **32**, pp. 15205–15215 (2012). 85

[129] P. S. Katz & J. L. Lillvis; "Reconciling the deep homology of neuromodulation with the evolution of behavior"; Current opinion in neurobiology **29**, pp. 39–47 (2014). 85

[130] P. Rombough; "Gills are needed for ionoregulation before they are needed for O2 uptake in developing zebrafish, Danio rerio"; Journal of Experimental Biology **205**, pp. 1787–1794 (2002). 86

[131] R. Kirsch & G. Nonnotte; "Cutaneous respiration in three freshwater teleosts"; Respiration physiology **29**, pp. 339–354 (1977). 86

[132] N. Helassa, B. Podor, A. Fine & K. Török; "Design and mechanistic insight into ultrafast calcium indicators for monitoring intracellular calcium dynamics"; Scientific reports **6**, pp. 1–14 (2016). 91